Tectonic evolution and global crustal architecture of the European Variscan belt constrained by geophysical data

Karel Schulmann, Jean-Bernard Edel, José R Martínez Catalán, Stanislaw Mazur, Alexandra Guy, Jean-Marc Lardeaux, Puy Ayarza, Imma Palomeras

Tectonic evolution and global crustal architecture of the European Variscan belt constrained by geophysical data

Karel Schulmann, Jean-Bernard Edel, José R. Martínez Catalán, Stanislaw Mazur, Alexandra Guy, Jean-Marc Lardeaux, Puy Ayarza, Imma Palomeras

PII: S0012-8252(22)00279-3

DOI: https://doi.org/10.1016/j.earscirev.2022.104195

Reference: EARTH 104195

To appear in: *Earth-Science Reviews*

Received date: 5 April 2022

Revised date: 9 June 2022

Accepted date: 21 September 2022

Please cite this article as: K. Schulmann, J.-B. Edel, J.R. Martínez Catalán, et al., Tectonic evolution and global crustal architecture of the European Variscan belt constrained by geophysical data, *Earth-Science Reviews* (2022), https://doi.org/10.1016/j.earscirev.2022.104195

Tectonic evolution and global crustal architecture of the European Variscan belt constrained by geophysical data

Karel Schulmann[a,b] , Jean-Bernard Edel[a], José R. Martínez Catalán[c], Stanislaw Mazur[d], Alexandra Guy[b], Jean-Marc Lardeaux[b,e], Puy Ayarza[c], Imma Palomeras[c]

[a] *Institut Terre et Environment de Strasbourg, Université de Strasbourg, UMR 7063, 1 Rue Blessig, 67084 Strasbourg, France*

[b] *Center for Lithospheric Research, Czech Geological Survey, Klárov 3, 11821, Prague 1, Czech Republic*

[c] *Departamento de Geología, Universidad de Salamanca, 37008 Salamanca, Spain*

[d] *Institute of Geological Sciences, Research Centre in Kraków, Senacka 1, 31-002 Kraków, Poland*

[e] *Géoazur - UMR 7329, Université Côte d'Azur, 250 Rue A. Einstein, Sophia-Antipolis, 06560 Valbonne, France*

Abstract: The European Variscan belt is a unique orogen that is covered by comprehensive sets of seismic and potential field data from the Iberian Peninsula in the west to the Polish Sudetes in the east. The combination of both allows for a new interpretation of the structure and evolution of the European Variscides at the continental scale. The European Variscan belt has been divided into three domains according to distinct geological and geophysical characteristics: 1) the North-eastern Variscan Domain (NVD) outcropping in the Bohemian Massif, Black Forest and Vosges Massifs, and the Rhenish Massif, 2) the Central Variscan Domain (CVD) represented by the French Massif Central, Armorican Massif and British Variscides, and 3) The South-western Variscan Domain (SVD) represented by the Iberian Massif. The gravity data show the presence of high amplitude, short-wavelength gravity anomalies that are mainly correlated with the outcrops of eclogites, ultramafic rocks and ophiolites. These anomalies locate the main body of the Mid-Variscan Allochthon in the SVD and CVD and the Devonian Mid-Variscan suture in the NVD. The gravity data also show medium amplitude elongated long-wavelength gravity highs aligned parallel to the structural grain of the Variscan belt, represented by the deformed Teplá-Barrandian-Kraichgau upper crustal rocks, a Devonian supra-subduction basin in the Mid-Variscan Allochthon, and the autochthonous rocks of the Central Iberian Zone in the SVD, the Armorican Massif in the CVD and the Saxothuringian Zone in the NVD. The short wavelength negative gravity anomalies are mainly developed in the central part of the belt and coincide with Carboniferous (330 – 310 Ma) per- to meta-aluminous magmatic bodies, pre-Variscan orthogneisses and Carboniferous felsic granulite bodies. Noticeably, Permian (300 – 290 Ma) granitoids do not reveal any gravity lows indicating that these bodies are not deeply rooted. The magnetic data show two belts correlated to Carboniferous Rhenohercynian and Devonian Mid-Variscan magmatic arc granitoids. The Rhenohercynian and Mid-Variscan subduction systems are well imaged by moderately SE dipping primary A-type reflectors in reflection seismic lines in the NVD and CVD, while in the SVD the reflectors related to the Rhenohercynian subduction are dipping to the NE and the seismic signature of the Mid-Variscan suture is weakly developed. In the NVD, a third belt of SE-dipping reflectors is attributed to the Carboniferous subduction of the Saxothuringian continental lithosphere beneath the Mid-Variscan Allochthon. Younger B-type moderately dipping reflectors in the upper-middle crust coincide with outcrops of Carboniferous detachments, sometimes limiting granite plutons and core complexes along-strike the core of the Variscan orogeny. C-type reflectors occur mainly in the deep crust and are considered as an expression of lower crustal flow resulting from extensional re-equilibration of the previously thickened Variscan crust. A

synthesis of P-wave velocity logs at the scale of the whole Variscan belt shows the existence of three different continental crusts: (i) cratonic crust marked by a thick, high velocity lower crust, (ii) transitional crust characterised by a relatively thin high velocity lower crust and intermediate velocity middle crust, and (iii) a thin Variscan orogenic crust defined by low velocity lower and middle crust. The latter crustal type coincides with regional outcrops of 330 – 310 Ma per- to meta- aluminous granitoids and associated gravity lows along-strike the belt. It is argued that the specific "Variscan" orogenic crust originated by Carboniferous extensional thinning and extensive melting of previously thickened "Tibetan" type crust and not from Permian tectogenesis, which is restricted to marginal parts of the orogen.

Key words: European Variscan Belt, seismic and potential field data, tectonics, crustal architecture

1. Introduction

The European Variscan belt is a classical collisional orogenic system characterised by Devonian to Carboniferous oceanic subductions and terrane accretion followed by a major Carboniferous collision between the Gondwana and Laurussia continental masses (Matte et al., 1986; Matte, 2001; Stampfli et al., 2013; Edel et al., 2018, Martínez Catalán et al., 2021). Concerning the oceans involved, published models contemplate between just one (Rheic; Kroner and Romer, 2013) and five (Rheic, Saxothuringian, Moldanubian, Rhenohercynian and Paleotethys; Franke et al., 2017). Even more have been recognized or can be hidden inside the Alpine domains (Neubauer et al., 2022).

Two main oceanic sutures are traditionally recognized resulting from Carboniferous closure of the Devonian Rhenohercynian basin in the NW and the Middle-Upper Devonian closure of a Cambro-Ordovician ocean pertaining to the Rheic realm further SE (e.g., Matte, 2001; Franke et al., 2017), although probably representing a marginal ocean instead of the true Rheic (Martínez Catalán et al., 2021). A Carboniferous subduction zone located between these two previously mentioned sutures was recently identified in the Saxothuringian Zone of the Bohemian Massif and northern Vosges (Franke and Żelaźniewicz 2000; Mazur and Aleksandrowski 2001; Edel and Schulmann 2009) and could represent the closure of another narrow ocean of the Rheic domain. Collisions involved three Gondwana-derived terranes: Avalonia, that was underthrust beneath a large Gondwana-derived block here referred to as the Autochthon, which in turn was overthrust by a large nappe stack formed by peri-Gondwanan oceanic and continental terranes (e.g., Faure et al., 2009; Lardeaux et al., 2014; Martínez Catalán et al., 1997, 2020). The latter will be referred to as the Mid-Variscan Allochthon following Martínez Catalán et al. (2021).

Altogether, the architecture of the whole orogenic belt is highly noncylindrical and varies from east to west according to the importance of the allochthonous domain relative to that of its autochthonous counterpart. In the east (Bohemian Massif) and part of the centre (French Massif Central), the Allochthon dominates, while in the west (Armorican and Iberian massifs), the outcropping domains are dominantly autochthonous, and the Allochthon in NW Iberia is only represented by five klippen underlain by a common parautochthonous thrust sheet. In all cases, the Allochthon has an important continental component of peri-Gondwana origin, while the oceanic component is irregularly distributed, but always separating two continental domains (e.g., Lardeaux et al., 2014; Martínez Catalán et al., 2021). The principal terrane boundaries are often concealed by Mesozoic – Cenozoic basins in Central Europe and sea water of the Atlantic Ocean and the English Channel in the west. The scattered exposures

of Variscan massifs in Europe thus preclude a full understanding of orogenic architecture including the position of oceanic sutures, magmatic arcs and the origin of the dominant orogenic fabric. Despite these shortcomings, it was recognized that the Variscan belt was formed by a succession of tectonic events related first to the closure of oceanic domains and associated amalgamation of peri-Gondwana blocks followed by reworking of the whole system due to relative movements of the Laurussia and Gondwana megablocks during the final formation of the Pangea supercontinent (Arthaud and Matte, 1977; Behr et al., 1984; Matte, 1991; Edel et al., 2018). The finite structural pattern of the orogen and the nature of the lower crust thus result from a number of events during which the accreted crust was magmatically recycled and tectonically reworked (e.g., Artemieva and Meissner, 2012).

Continental-scale geophysical studies have allowed geologists to define the main continental blocks (Pharaoh, 1999; Oncken et al., 1999; Grad et al., 2002; Mazur et al., 2015) and their mutual boundaries using mainly refraction and to a lesser scale reflection seismic profiles (Meissner, 1986, 1999; Córdoba et al., 1987, 1988; Pérez-Estaún et al., 1994; Álvarez-Marrón et al., 1996; Pulgar et al., 1996; Ayarza et al., 1998; Simancas et al., 2003; Edel and Schulmann, 2009; Guterch et al., 2010; Martínez Poyatos et al., 2012; Ehsan et al., 2015). Moreover, published gravity and aeromagnetic maps from various databases were mostly used to unravel the geometry of geological units at the local scale (Edel and Fluck, 1989; Edel and Weber, 1995; Ayarza and Martínez Catalán, 2007; Martínez Catalán et al., 2012, 2018; García-Lobón et al., 2014; Baptiste et al., 2016; Mikołajczak et al., 2019). Rarely, both seismic and potential field methods were combined to develop large-scale tectonic models at the scale of individual domains of the Variscan belt (e.g., Guy et al., 2011; Martinez Catalan et al., 2014; Mazur et al., 2020). Therefore, these studies result in models that may be mutually incompatible as they are valid only for part of orogenic system and do not take into consideration results and models developed elsewhere.

To fill the gap, we collected and synthesised the gravity and magnetic data as well as results of both reflection and refraction profiles gathered over the whole western and central part of the European continent. The potential field data are analysed using various filtering techniques to bring a coherent and homogeneous set of maps over the whole belt, which provides a tool to interpret both deep and shallow crustal anomalies. These datasets are used to build a map of gravity and magnetic lineaments that identify deep crustal heterogeneities often related to boundaries of individual terranes or shallow crustal structures related to the distribution of granitoids or tectonic units. In addition, the aeromagnetic data are synthesised to define highly magnetic magmatic arcs and sutures composed of mafic and ultramafic rocks.

Refraction seismic data combined with gravity surveys are further used to characterise variations of the thickness of lower and upper crust across the belt, while reflection seismic profiles with modelled gravity and magnetic profiles help to precise the boundaries of terranes and the deep crustal structure of individual deformed continental segments. Altogether, the existing set of geophysical data from the European Variscan belt is here analysed by a homogeneous set of techniques allowing characterization of the 3D crustal architecture of the whole belt. Finally, an innovative model of the amalgamation of one of the principal collisional systems on the Earth is proposed together with reworking of continental crust during a 110 m.y. long Palaeozoic history.

2. Geology of the European Variscan belt

The continental European Variscan basement crops out in seven main massifs which from the west to the east are the Iberian Massif in Spain and Portugal, the Pyrenean Axial Zone between Spain and France, the Armorican Massif and Massif Central in France, the Rhine-Ardennes or Rhenish Massif in Germany, France and Belgium, the Vosges-Schwarzwald massifs at the French-German border, and the Bohemian Massif, scattered between Germany, Austria, Czech Republic and Poland (**Fig. 1**). The general structure, lithologies and to a certain degree tectonic history are common for the Bohemian, Schwarzwald and Vosges Massifs but differences increase to the west, in the French and Iberian parts of the orogen (Ballèvre et al., 2014; Lardeaux et al., 2014). Most of geophysical studies such as expensive seismic sections cover parts of the individual massifs and only rarely transcend their boundaries.

Since pioneering work by Kossmat (1927), the geological structure of the Variscan orogen is represented by NE-SW tectonic zones formed by continental domains and mutually separated by oceanic sutures (Matte, 2001). Some of these tectonic zones are also described in the Alpine belt in which a significant part of the Variscan crust was reworked (Von Raumer et al., 1999, 2013). The Alpine Helvetic-Dauphinois and Penninic Zones show many witnesses of the Variscan Moldanubian Zone (Von Raumer et al., 2009, 2013: Spalla et al., 2014; Jouffray et al., 2020; Regorda et al., 2020). Moreover, in the last two decades, distinct Variscan oceanic sutures have been recognized within the Alpine Autroalpine and Southalpine domains (see Marotta and Spalla, 2007; Chang et al., 2021; Filippi et al., 2021; Neubauer et al., 2022 with references therein). Such a situation is also found in the Apennines, where pieces of the Variscan crust (i.e. the Calabria–Peloritani Terrane) are now well recognized (see Fornelli et al., 2020, with references therein). However, although the

lithological, petrological and geochronological Variscan markers are sometimes well preserved in the Alps, the Variscan geophysical signatures have been largely erased by alpine orogenesis. Consequently, the Varican structuration of the Alpine belt is beyond the scope of this paper.

The along-strike geometry of the European Variscan belt is non-cylindrical being disrupted by lithosphere-scale NW-SE trending transcurrent faults and modified in the west by the large Ibero-Armorican oroclinal bend. From that reason Edel et al. (2018) divided the belt into three domains which are characterised by a different width of tectonic zones (**Fig. 1**): 1) The North-eastern Variscan Domain (NVD) is limited by the Bray Fault in the west and the Sudetic fault system (SFS) in the east and comprises the Bohemian Massif, the Vosges-Schwarzwald massifs and associated small outcrops further north (Odenwald and Spessart), as well as the Rhenish massif. 2) The Central Variscan Domain (CVD) is limited by the Bray Fault in the east and the North Pyrenean Fault in the west, and comprises the Variscan outcrops in SW England and Ireland, the Armorican Massif, French Massif Central and Maures-Tanneron Massif in continental France together with Variscan outcrops in Corsica and Sardinia islands. 3) The South-western Variscan Domain (SVD) is formed by the Variscan outcrops in the Iberian Peninsula, namely the Iberian Massif, Pyrenees, Iberian and Catalonia Coast ranges. The Iberian Massif includes the hinge zone and wide southern flank of the Ibero-Armorican oroclinal arc, which continues to the NE in the Armorican Massif.

2.1. The North-eastern Variscan Domain

The tectonic zoning of the NVD was defined by Kossmat (1927) and it is represented by the Rhenohercynian Zone (RHZ) in the northwest, the Saxothuringian Zone and the upper crustal Teplá-Barrandian in the centre, and the deep crustal Moldanubian Zone in the south. Later, an easternmost Brunovistulian Zone was defined by Dudek (1980).

The Rhenohercynian Zone consists of a deformed Avalonian margin in the NW and accreted and imbricated Devonian syn-rift sediments and syn-orogenic Carboniferous flysch (Franke, 1989; Plesch and Oncken, 1999). The western part of the Rhenish Massif consists of the autochthonous Avalonian Cadomian basement, and its Cambrian to Silurian cover that is unconformably overlain by Laurentia or Baltica-derived Lower Devonian clastics (Franke, 2000; Sintubin et al., 2009). The Lower Devonian continental rifting associated with felsic volcanism, which turned to basaltic during the Middle Devonian to early Carboniferous, is the hallmark of the Emsian opening of the Rhenohercynian Ocean. This oceanic domain was closed in the Upper Devonian (Franke, 2000) or early Carboniferous (Zeh and Gerdes, 2010), when a large subduction wedge started to form being associated with a deposition of syn-

orogenic turbidites in the mainly Carboniferous foreland basin. These sediments were derived mainly from a south-easterly active margin of the Saxothuringian basement characterised by Carboniferous arc-type magmatism called the Mid-German Crystalline Rise (Franke, 2000). This unit crops out in the Odenwald, Spessart and Ruhla regions and consists of a Cambro-Ordovician succession of paragneisses and metabasites, late Ordovician-early Silurian granites and Silurian-early Devonian arc-related granitoids. The whole successions terminated with Middle Devonian to Tournaisian sediments, and middle Carboniferous granitoids interpreted as the Rhenohercynian arc (340-325 Ma; Franke, 2000; Zeh and Will, 2010).

The two hundred kilometres wide Saxothuringian Zone (STZ) is represented by a Proterozoic basement overlain by early Palaeozoic to Devonian passive margin volcano-sedimentary sequences and Carboniferous flysch overthrust by Devonian HP nappes (Franke, 2000). In detail, the Saxothuringian basement includes Neoproterozoic to early Cambrian volcano-sedimentary sequences intruded by numerous granitoids in between 570 – 530 Ma. These Cadomian syn-orogenic complexes and late Proterozoic arcs developed along the margin of Gondwana during the oceanic subduction followed by magmatism and clastic sedimentation related to the Cambro-Ordovician (500 – 480 Ma) rifting (Linnemann et al., 2007; Collett et al., 2018). The Palaeozoic pre-orogenic sequences are formed by Lower Ordovician quartzites and pelites, Silurian graptolite shales, Lower Devonian (cherty) limestones and pelites, Middle Devonian black shales and Upper Devonian limestones. This sequence is unconformably covered by Famennian to Visean syn-orogenic flysch. The eastern Erzgebirge and Sudetic parts of the Saxothuringian Zone are affected by late Carboniferous to early Permian magmatism and volcanism. The boundary between the the Saxothuringian Zone and the hangingwall units are defined by a zone with high deformation and metamorphic contrasts called the Lalaye Lubine Shear Zone (LLSZ) in the French Vosges and the Baden Baden Shear Zone (BBSZ) in the Schwarzwald.

The Teplá-Barrandian Zone (TBZ) is composed of Proterozoic to early Cambrian volcano-sedimentary, weakly metamorphosed, sequences recently interpreted as a Proterozoic accretionary wedge (Ackermann et al., 2020) intruded by late Cambrian mafic bodies and granitoids (Žák et al., 2014). This wedge is unconformably covered by Ordovician to Middle Devonian volcano-sedimentary sequences of the Prague Basin. This sequence consists of Ordovician quartzites, Silurian graptolite shales, Lower Devonian limestones and terminates by Middle Devonian deposition of carbonate and siliciclastic flysch. The whole TBZis further intruded by Upper Devonian to Lower Carboniferous granitoids mainly along its southern and eastern margin.

The core of the belt is formed by the Moldanubian Zone (MZ), which is traditionally divided in two principal ensembles called the Drosendorf and Gföhl units (Fuchs, 1976, Tollmann 1982). The Drosendorf Unit consists of lower Monotonous and upper Varied Groups. The structurally deeper Monotonous Group is composed of a high-grade, most likely Ordovician to Proterozoic metasedimentary sequence (Skrzypek et al., 2012a; Košler et al., 2014, Lindner et al., 2021) and is represented by sometimes migmatized paragneiss, schist, quartzite and amphibolite intercalated with Neoproterozoic gneisses (Finger et al., 2000; Friedl et al., 2000; Lindner et al., 2021). The structurally deepest part of the Monotonous Group is in some places formed by amphibolitized gabbros and leptyno-amphibolite complexes of Cambrian age (Kröner et al., 2000). The Varied Group is represented by paragneiss, schists and marbles associated with amphibolites. The Gföhl Unit is featured by the presence of large HP granulite massifs associated with garnet-spinel peridotites, eclogites and Mg-K syenitic intrusions. The Moldanubian Zone is intruded by tonalites to granodiorites of the late Devonian to early Carboniferous Central Bohemian plutonic complex in the west and by middle Carboniferous granite intrusions of the giant Central Moldanubian pluton in its central part (Žák et al., 2011, 2014).

The easternmost part of the NVD is formed by the Brunia Neoproterozoic basement block consisting of granitoids, migmatites and metasediments unconformably covered by an early Cambrian clastic succession, minor Ordovician and thick Devonian shallow-water sediments and Carboniferous flysch (Dudek, 1980; Hanžl et al., 2019). The boundary between the Moldanubian Zone and the Brunia block is formed by a 30 km wide and up to 300 km long zone of intense deformation and Barrovian metamorphism called the Moravo-Silesian Zone (Suess, 1912). This zone is composed of a stack of Brunia basement-derived nappes imbricated with Devonian sequences and overthrust by the thick Moldanubian nappe along the Moldanubian thrust (Suess, 1912; Schulmann et al., 1991; Štípská et al., 2020).

2.2. The Central Variscan Domain

The CVD includes the Variscan outcrops in SW England and Ireland, the Armorican Massif, French Massif Central and Maures-Tanneron Massif in metropolitan France. The CVD shows similar zoning as the NVD, but the lithological content and tectonic position of key sequences are somewhat different. In SW England, the Rhenohercynian Zone is represented by the deformed Avalonia basement and inverted Devonian basins overthrust by the Devonian Lizard ophiolites (Lo) and imbricated with Carboniferous flysch (Shail and Leveridge, 2009). On the French coast of the English Channel, the Léon Unit consists of paragneisses, orthogneisses and schists and is considered a direct equivalent of the

Saxothuringian Zone (Ballèvre et al., 2009). This unit is intruded by numerous granitoid plutons of Carboniferous age comparable to the intrusive sequence of the Mid-German Crystalline Rise (Faure et al., 2010). Further southeast, the Armorican Massif occurs, composed of three domains named North, Central and South separated by right-lateral shear zones and faults such as Nort-sur-Erdre Fault (NEF). The North Armorican Domain (NAD; **Fig. 1**) is mainly composed of Paleoproterozoic basement gneisses and the Neoproterozoic volcano-sedimentary "Brioverian" succession (Barrois, 199) intruded by Cadomian plutons and affected by early Cambrian migmatization and magmatism (Brun et al., 2001). The Central Armorican Domain (CAD) is formed by Neoproterozoic "Brioverian" detrital/terrigeneous sequences and Cadomian plutons, slightly deformed and uncorformably overlain by pre-orogenic Ordovician, Silurian and Devonian successions (Ballèvre et al., 2014). The Neoproterozoic sedimentation occurred on an active continental margin (Murphy and Nance, 1991) while the Cambrian to Lower Ordovician is considered to represent a passive margin and continental rift associated with bimodal volcanism during the Middle Ordovician. Syn-orogenic Upper-Middle Carboniferous sediments unconformably cover Upper Palaeozoic sequences. The South Armorican Domain (SAD) includes autochthonous Cambrian to Devonian metasediments and volcanics in the SE and schists and gneisses towards the NW (Ballèvre et al., 2014), which were overthrust by an allochthonous nappe stack with several units, of which the Champtoceaux Unit consists of Barrovian metasediments containing eclogitic lenses. In the scheme of Ballèvre et al. (2014), the Champtoceaux Unit is interpreted as a lower allochthonous sheet. In the hangingwall, the Maugues Proterozoic unit occurs, with the Ancenis Palaeozoic basin recently interpreted as equivalent of the TBZ in the NVD on the basis of lithological and paleontological arguments (Paquette et al., 2017; Ballèvre et al., 2019).

The geology of the French Massif Central is characterised, as most of the SAD, by a stack of nappes overlying a schistose para-autochthonous ensemble (Faure et al., 2009). The Parautochthon Unit (PAU) crops out in tectonic windows and consists of low to medium-grade metasediments represented essentially by schist, quartzite and limestone intercalated with mafic metaigneous rocks (Lardeaux et al., 2014). Structurally above the Lower Gneiss Unit (LGU) occurs, consisting of Barrovian paragneisses of possible Proterozoic age and Cambro-Ordovician metaigenous rocks (Ledru et al., 1989; Lardeaux et al., 2014). Higher in the pile, the Upper Gneiss Unit (UGU) includes at its base the Leptyno-Amphibolite Complex (Santallier et al., 1988) which is formed by an assemblage of metagabbros, metabasalts, metatuffs and metasediments associated to ultrabasic rocks (Gardien et al., 1990) with

Cambro-Ordovician magmatic protolith ages (Pin and Lancelot, 1982; Paquette et al., 1995). This unit underwent HP and/or UHP metamorphic conditions (Lardeaux et al., 2001; Berger et al., 2010; Lardeaux et al., 2014) testified by numerous occurrences of Lower-Middle Devonian eclogites (Lotout et al., 2018, 2020; de Hoÿm de Marien et al., 2020) and HP granulites (Pin and Vielzeuf, 1988; Lardeaux et al., 1989). The UGU was interpreted as a relic of subducted oceanic lithosphere or hyper-extended margin forming a subduction mélange (Lardeaux et al., 2014; Lotout et al., 2018). The uppermost part of the pile is represented by a low-grade Cambrian sequence in the SW, represented by the Thiviers-Payzac Unit and the Middle Devonian ophiolite of the Génis-Thiviers-Payzac Unit (Faure et al., 2009). In the NW, a weakly metamorphosed ophiolitic sequence of late Devonian age is above the UGU in the Brévenne area, while in the Morvan area, arc-type volcanic rocks cover the UGU (Pin and Paquette, 1997, 2002). The whole nappe stack is intruded by large volumes of early to middle Carboniferous syn-orogenic granitoids and late Carboniferous post-orogenic granitoids represented mainly by the large Velay intrusion (Ledru et al., 2001). This magmatism was associated with the development of post-orogenic extensional Permian basins (Malavieille et al., 1990; Burg, 1991).

In the south, a sequence of early Palaeozoic sediments occurs, folded together with early Carboniferous flysch interpreted as an external orogenic fold belt (Faure et al., 2009). This sequence surrounds the late Palaeozoic dome of the Montagne Noire, composed mainly of migmatized Cambro-Ordovician orthogneisses (Faure et al., 2014). In the western Maures-Tanneron Massif weakly metamorphosed Silurian sequences are in tectonic contact with Barrovian para- and orthogneisses, while a late Palaeozoic migmatitic dome, including retrogressed eclogites is developed easterly in this massif (Schneider et al., 2014; Gerbault et al., 2018). Edel et al., (2014, 2018) proposed that the Maures-Tanneron Massif formed during Palaeozoic times a joint unit with Corsica and Sardinia, the so-called the Maures-Estérel-Corsica-Sardinia Block. The Autochthon is developed in Sardinia and consists of a Neoproterozoic sequence covered by Cambrian and Ordovician siliciclastic sediments. It is overthrust by a stack of nappes consisting of Lower Palaeozoic sequences with metamorphic grade increasing northwards (Rossi et al., 2009). The internal zone is developed in northern Sardinia and Corsica, and it is represented by early Carboniferous migmatites, HP granulites and Mg-K granitoids (Rossi et al., 2009). In the Maures-Estérel-Corsica-Sardinia micro-plate the Variscan geophysical signatures are severely overprinted by the opening of the Western Mediterranean oceanic domain (Edel et al., 1981, 2014; Chamot-Rooke et al., 1999; Séranne,

1999; Béthoux et al., 2008). Thus these specific data are not included in the various geophysical datasets herafter discussed in this paper.

2.3. The South-western Variscan Domain

The largest outcrop of the Variscan basement in the Iberian Peninsula (SVD) is the Iberian Massif, which occupies its western part. Based mainly on stratigraphic features, the Iberian Massif was divided in tectonic zones by Lotze (1945), which were later revised by Julivert et al. (1972) and Farias et al. (1987).

The South Portuguese Zone (SPZ) represents the Rhenohercynian Zone in Iberia. It is a south-verging thrust belt formed by a terrigenous and volcanic sequence consisting of Upper Devonian shallow-water slates and quartzites, an early Carboniferous volcano-sedimentary complex, mostly felsic, and early to late Carboniferous syn-orogenic flysch (Silva et al., 1990). This sequence is underthrust beneath the Ossa Morena Zone along a suture characterised by the Pulo do Lobo Devonian accretionary prism (Silva et al., 1990; Onézime et al., 2002; Rubio Pascual et al., 2013) and a tectonic mélange with pieces of eclogites and Lower Ordovician oceanic rocks, the latter probably being relics of the Rheic Ocean (Araújo and Ribeiro, 1996; Pedro et al., 2010). Although no units older than Devonian crop out in the SPZ, detrital zircon age populations (Braid et al., 2011; Rodrigues et al., 2015; Pérez-Cáceres et al., 2016) and inherited zircons in granitoids (de la Rosa et al., 2002; Gladney et al., 2014) suggest that their source was the basement of Avalonia.

The Ossa-Morena Zone (OMZ) is a slate belt including Neoproterozoic basement with an important Cadomian imprint (Bandrés et al., 2004), characterised by arc-type magmatism that continued during the Cambrian reflecting arc collapse, and ended by rift-related early Ordovician bimodal and alkaline magmatism in the north (García Casquero et al., 1985; Ochsner, 1993). The Palaeozoic sequence is rather complete and of shallow-water type (Robardet and Gutiérrez Marco, 1990). Early Variscan high-P metamorphism at its southern and northern boundaries suggests that the OMZ is limited by sutures. However, in the north no oceanic assemblages exist, rather suggesting an aborted rift. The boundary between OMZ and the easterly Central Iberian Zone (CIZ) is defined by the Badajoz-Córdoba Shear Zone (BCSZ).

The Central Iberian Zone (CIZ) is formed by a terrigenous Ediacaran succession overlain by shallow-water Palaeozoic slates, quartzites and carbonates. The whole sequence is similar to that of the CAD and the autochthonous part of the SAD, which together with the Pyrenees and Catalonia Coast Ranges represent the northern branch of the Ibero-Armorican Arc (IAA; **Fig. 1**). Structurally, the CIZ is a wide slate belt with abundant upright folds that

occupies the axial part of the Iberian Massif, and its western and central parts are characterised by voluminous Variscan magmatism.

The West Asturian-Leonese Zone (WALZ) is also a slate belt, characterised by recumbent folds and thrust faults. A terrigenous Ediacaran sequence is followed by a complete Palaeozoic succession similar to but thicker than that of the CIZ. The Cantabrian Zone (CZ) is a thin-skinned foreland thrust belt occupying the core of the Ibero-Armorican Arc. The pre-orogenic Palaeozoic is not always complete due to erosion prior to syn-orogenic sedimentation, mostly of molasse type. These two zones have no equivalent in other Variscan massifs of Europe.

The CIZ, WALZ and CZ are not separated by sutures and are considered as a coherent terrane, which during most of the Palaeozoic formed part of the wide northern Gondwana platform (Gutiérrez-Marco et al., 1999; Robardet, 2002, 2003; Martínez Catalán et al., 2004). The OMZ can be also interpreted as part of the same platform, although an early Ordovician rift probably separated it from the mainland.

The Galicia-Trás-os-Montes Zone (GTMZ) is an allochthonous nappe stack emplaced onto the CIZ during the early Carboniferous. It includes a Parautochthon with stratigraphic similarities to the CIZ, although more distal (Dias da Silva et al., 2014, 2015; Martínez Catalán et al., 2020), and three allochthonous groups that were piled up during the Devonian, forming an accretionary wedge. Their characteristics are summarized in several publications (Martínez Catalán et al., 2009; Arenas et al., 2016) and correlated with equivalent groups of the Armorican and Bohemian Massifs (Ballèvre et al., 2014; Martínez Catalán et al., 2020).

The Lower Allochthon is formed by monotonous terrigenous sediments intruded by Cambro-Ordovician granitoids ranging in composition from calcalkaline to peralkaline. Detrital zircon ages suggest proximity to the West African craton. The Lower Allochthon represents the outermost part of the hyper-extended margin of NW Gondwana, which underwent subduction during its incorporation into an accretionary wedge during the late Devonian. The Middle Allochthon includes several slices of Cambro-Ordovician and Lower Devonian oceanic units derived from an intervening ocean between Gondwana and the peri-Gondwana terrane, the later forming the Upper Allochthon. The oceanic units were accreted during the middle Devonian age.

The Upper Allochthon consists of (Neoproterozoic-?) Cambrian terrigenous sequences intruded by granitoids and basic rocks forming two suites, tholeiitic and calcalkaline. The Upper Allochthon is interpreted as a peri-Gondwana terrane rifted away from NW Gondwana during the late Cambrian terrane dispersion and opening of the Rheic Ocean (Martínez

Catalán et al., 2021). While subduction of the outboard oceanic domain was responsible for calcalkaline Cambro-Ordovician magmatism, slab roll back caused back-arc extension, and tholeiitic magmas, which were emplaced in the part of the rifted terrane facing Gondwana. During the late Devonian subduction of this part, the accretion of the early-Variscan orogenic wedge started.

3. Sutures, magmatic arcs and orogen-scale shear zones

Three main oceanic suture zones are recognized in the European Variscan belt. One suture testifies the closure of the Devonian Rhenohercynian Ocean in the NW part of Central Europe and in SW Iberia. Another oceanic suture is identified inside the large central European allochthon here called the Mid-Variscan Allochthon (Fig. 1). Since this suture has been named after the massifs where it occurs (Matte, 2001, 2007), it could be referred to as the Teplá-Massif Central-Galicia-Brittany suture (Matte, 2001). However, as it is preserved inside the Mid-Variscan Allochthon, a short name, Mid-Variscan suture, is proposed. It is thought to represent a branch of the Ordovician Rheic oceanic realm, but also includes pieces of Silurian and Lower Devonian oceanic lithosphere (Martínez Catalán et al., 2020, 2021). A third subduction zone is identified in the Bohemian Massif and northern Vosges and affects the Saxothuringian Zone (Mazur and Aleksandrowski, 2001; Edel and Schulmann, 2009; Guy et al., 2011; Jeřábek et al., 2016; Konopásek et al., 2019).

The Rhenohercynian suture in the NVD is represented by Devonian ophiolitic sequences in the Giessen nappe and by Devonian eclogites at the base of the Saxothuringian domain in Odenwald (Franke, 2000). In the CVD, this suture is represented in Cornwall by the early Devonian Lizard ophiolites and eclogitic bodies in the Léon domain (Shail and Leveridge, 2009; Ballèvre et al., 2014). In the SVD, the Rhenohercynian suture is characterised by HP rocks in the south of the Ossa Morena Zone in southern Iberia (Rubio Pascual et al., 2013).

The Mid-Variscan suture occurs inside the Mid-Variscan Allochthon, where it actually makes up the Middle Allochthon (Ballèvre et al., 2014; Martínez Catalán et al., 2020).

In the NVD, the oceanic Middle Allochthon is represented by the Lower-Middle Devonian ophiolitic complexes in the Münchberg and Mariánské Lázně massifs, the Lower Devonian Central Sudetic ophiolite, the Silurian-Devonian mafic and deep marine successions of the Kaczawa Complex and the Cambro-Ordovician Leszczyniec Complex in Poland. The Upper Allochthon is formed by HP units of the Münchberg, Mariánské Lázně, Góry Sowie and Erbendorf-Vohenstrauβ massifs and, above, the thick TBZ and the

Palaeozoic metasediments and metabasites of the Moldanubian Zone. The subduction that gave rise to the Mid-Variscan suture took place during the middle-late Devonian (Ballèvre et al., 2014; Martínez Catalán et al., 2020 and references therein). The relative autochthon in the NVD is represented by the Saxothuringian Zone.

In the CVD, the Mid-Variscan suture is defined by a belt of HP rocks in the SAD, where the Champtoceaux and Ile-de-Groix eclogites and blueschists represent the Lower Allochthon and Les Essarts eclogitic unit and Mauges metasedimentary sequence characterise the Upper Allochthon (Ballèvre et al., 2014). Equivalent units appear in the Massif Central, represented by the Leptyno-Amphibolitic Complex, which includes the Lower and Upper Gneiss units (Ledru et al., 1989; Faure et al., 2009; Lardeaux et al., 2014) that can be ascribed to the Lower and Upper Allochthons, respectively. The Leptyno-Amphibolitic Complex consists of peridotites, gabbros, granitoids and volcanics of Cambro-Ordovician age alternating with metasediments. Early Variscan (Devonian) metamorphism reached eclogite facies and locally UHP conditions. Although the complex is currently interpreted as the Mid-Variscan suture, most of it derives from two conjugated extended continental margins, while only an ophiolitic unit, probably Devonian, represents the Middle Allochthon (Girardeau et al., 1986; Berger et al., 2005). Conversely, both Cambro-Ordovician and Early Devonian oceanic units occur in the Armorican Massif (Ballèvre et al., 2014).

In the SVD, the Mid-Variscan suture is well exposed in the allochthonous complexes of Galicia (NW Spain) and Trás-os-Montes (N Portugal), represented in the Middle Allochthon by oceanic supracrustal units and ophiolites of Cambro-Ordovician and early Devonian ages (Ballèvre et al., 2014; Arenas et al., 2016; Martínez Catalán et al., 2020). These complexes form remnants of a continuous nappe stack thrust over the Parauthochton and the CIZ and preserved as klippen.

The third suture represented by the Saxothuringian subduction system in the NVD and that interpreted as the Mid-Variscan suture are often considered equivalent. However, they should be considered different since a low-grade Saxothuringian Zone forms the Autochthon under the Münchberg and Mariánské Lázně allochthons, which contain the Mid-Variscan suture (Matínez Catalán et al., 2020). The Saxothuringian Autochthon became underthrust beneath the Mid-Variscan Allochthon in a similar way as it occurred in the CVD and SVD, and then, it was subducted beneath itself. While the Mid-Variscan suture is Devonian, the Saxothuringian suture is marked by the presence of eclogites with a MORB-like chemistry and UHP basement rocks all dated at early Carboniferous (Massone et al., 2007; Schmadike et al., 1995; Závada et al., 2021). The Saxothuringian suture was probably initiated in a narrow

oceanic realm that previously had split apart the Saxothuringian Zone, but it largely evolved as a continental subduction zone during the Carboniferous (Konopásek and Schulmann, 2005; Jeřábek et al., 2016; Konopásek et al., 2019). The subducted part of the Saxothuringian Zone crops out in domes roofed by extensional detachments and pierced through the allochthonous Moldanubian Zone as gneissic diapirs derived from the lower plate (Schulmann et al., 2005, 2009, 2014). This Saxothuringian subduction produced HP eclogites and UHP diamond-bearing granulites (Massone et al., 2007, Kotková et al., 2011) cropping out in the Granulitebirge and Erzgebirge domes of the Saxothuringian Zone (Konopásek and Schulmann, 2005), and in the Moldanubian Zone as granulitic domes, thereby defining the cryptic Carboniferous suture of Schulmann et al. (2014).

Granitoids are abundant and often voluminous along and across the Variscan belt. Many of them result from crustal thickening followed by thermal relaxation, crustal melting, and late Variscan crustal and lithospheric extension. Moreover, three magmatic arcs have been identified in the European Variscan belt, which are correlated to the closure of Rhenohercynian, Mid-Variscan and Saxothuringian Oceans.

In the NVD, the Rhenohercynian arc is described as a series of tonalitic to granodioritic intrusions of late Devonian to early Carboniferous age (360-330 Ma; Oncken, 1997; Altherr et al., 1999; Zeh and Will, 2010; Edel et al., 2013). These intrusions were reported from the French Vosges, Odenwald, Spessart and Ruhla outcrops defining the main part of the Mid-German Crystalline Rise (Edel et al., 2018). In the CVD, magmatic rocks of this arc are known from the Léon Unit (Faure et al., 2010), and their volcanic equivalents may be represented in the Massif Central by the 350-330 Ma old Tuffs Anthracifères (Lardeaux et al., 2014). In the SVD, an early Carboniferous (355-335 Ma) magmatic complex straddles both sides of the Rhenohercynian suture: the Northern Sierra de Sevilla Batholith in the SPZ and the basic and ultrabasic Beja-Acebuches Unit in the OMZ. Plutonic rocks include transitional tholeiitic-calcalkaline and truly calcalkaline suites in the SPZ (de la Rosa and Castro, 2004), and represent an arc probably related to the subduction of the Rhenohercynian Ocean, which included an early Carboniferous ephemeral oceanic-like domain, represented by the Beja-Acebuches Unit (Simancas et al., 2006; Azor et al., 2008).

Arc-type magmatism associated with the Mid-Variscan suture is represented in the CVD by small Late Devonian plutons forming the so-called tonalitic line of Limousin units and intruded into both Upper and Lower Gneiss Units (Lardeaux et al., 2014). In addition, andesitic volcanic rocks unconformably cover the Upper Gneiss Unit in the Morvan area and southern Vosges, where an ophiolitic ensemble known as the Brévenne Unit or “Ligne des

Klippes" occurs (Skrzypek et al., 2014). Both volcanic and ophiolitic rocks are of late Devonian age (370 – 360 Ma; Faure et al., 2009; Lardeaux et al., 2014; Skrzypek et al., 2011) and can be related to the subduction of the Mid-Variscan Ocean under the peri-Gondwana terrane forming the Upper Allochthon. Altogether, these volcano-sedimentary and ophiolitic outcrops in the eastern France (Morvan, Brevenne) and "Ligne des Klippes" in Vosges likely represent one large supra-subduction arc and back-arc system of late Devonian age (Lardeaux et al., submitted) polarity of which is defined by the volcanic arc in the north and back-arc in the south in the current coordinates. This supra-subduction edifice is defined by late Devonian andesitic volcanics in the Morvan area and Bruche valley in Vosges representing a volcanic arc. The back arc system includes pillow lavas and deep marine silicic sediments represented by the Brevenne sequence in the west and southern Devono-Carboniferous Vosges basin in the east (Faure et al., 2009; Lardeaux, 2014) All lithologies are weakly metamorphosed and deposited on the Upper Gneiss Unit in the west and basement of unknown age in the east (Lardeaux et al., 2014; Lardeaux et al., submitted). A similar Middle Devonian volcano-sedimentary rocks association is also recognized in the Black Forest Massif (i.e. Badenweiler- Lenzkirch Zone, Hahn et al., 2003; Lardeaux et al., submitted). The Saxothuringian magmatic arc is represented in the NVD by the early Carboniferous calcalkaline tonalitic and gabbroic rocks of the Central Bohemian Plutonic Complex in the Bohemian Massif (Janoušek et al., 2004) and 370 Ma old granodiorite bodies intruding the TBZ (Venera et al., 2000). These magmatic arc intrusions are interpreted to correspond to the southward subduction of the Saxothuringian Ocean (Schulmann et al., 2009).

The main tectonic zones, sutures, and arcs of the European Variscan belt were displaced by large-scale dextral shear zones of Carboniferous age defining the limits of NVD, CVD and SVD. The Sudetic, Bray and North Pyrenean fault systems were interpreted by Arthaud and Matte (1977) as Riedel shears developed inside a dextral megashear active in late Variscan (early Permian) time between the Urals and the Appalachians (Carreras and Druguet, 2014). It has been proposed that some of these fault zones operated already during Late Devonian and Carboniferous times (Matte et al., 1986; Hofmann et al., 2009; Rolin et al., 2009), and were recently interpreted as reactivated oceanic transforms of the Rhenohercynian basin (Edel et al., 2018). However, they cut across previous ductile, mainly dextral but also sinistral shear zones and related folds dated as late Carboniferous (Dallmeyer et al., 1997; Gumiaux et al., 2004; Gutiérrez-Alonso et al., 2015).

4. Geophysical data

We describe first the source of various datasets followed by various procedures of data processing and presentation of results in the form of geophysical maps and sections.

4.1. Gravity and magnetic data sources and existing refraction and reflection seismic sections

The gravity data for the whole Variscan belt were extracted from the EGM2008 model edited by the BGI (International Gravimetric Bureau). For Spain, the BGI data come from the Instituto Geográfico Nacional (1996) and Mezcua et al. (1996). At a scale of countries, we used the data from the Czech Republic (Czech Geological Survey; Polanský and Škvor, 1975; Ibrmajer, 1981), south-eastern Germany (the Leibniz Institut für Angewandte Geophysik (LIAG); Plaumann, 1983, 1991), south-western Germany (Plaumann, 1995; Rotstein et al., 2006), and France (Bureau de Recherches Géologiques et Minières). We also digitized published Bouguer maps from Austria, Belgium, Germany (Plaumann, 1995) and the Polish Sudetes (Królikowski and Petecki, 1995; Wybraniec, 1999).

The Magnetic Anomaly Map of the World (Meyer et al., 2017) is not detailed enough for the purpose of this work. The maps presented in this work result from a compilation of aeromagnetic data sets of France (Flight Altitude (FA) = 3000, BRGM), northeast France (FA= 1200 m and 1500 m; Edel and Schaumann, 2009), Spain (FA= 3000, Ardizone et al., 1989), Portugal (FA= 3000, Miranda et al., 1989) and of digitized published maps of south Germany (FA= 1000 m and 1500 m, Bundesanstalt für Bodenforschung und Rohstoffe, 1976; FA=3000 m, Wonik and Hahn, 1990; Bosum and Wonik, 1991), north Austria (FA= 1400 m, Blaumoser, 1992), the Czech Republic (FA= 500 m), the Gulf of Gascogne (FA=500 m, BRGM), Great Britain (FA=305 and 152 m, British Geological Survey, 1998). Interpretative aeromagnetic maps for southern England (Busby and Smith, 2001), western and southern Ireland (Kimbell et al., 2010), Belgium, Germany (Gabriel et al., 2011), the Polish platform (Wybraniec, 1999; Mikołajczak et al., 2019) are also taken into account.

In the sixties and seventies of the last century a great number of refraction and wide-angle reflection seismic profiles were shot through the European Variscan Belt. The principal result was the definition of the crust-mantle boundary topography (the Moho discontinuity) and the boundary between upper and lower crust (the Conrad discontinuity) (e.g., Dezes and Ziegler, 2002). Selected published seismic sections (**Fig. 2**) are used here in order to present 1D velocity/depth models along the Variscan chain. The refraction/wide-angle reflection profiles used in this study are summarized in the table 1 along with a selected collection of deep reflection profiles orthogonal to the main tectonic zones.

4.2. Data processing

4.2.1. Potential field

The potential field signals can be considered as a juxtaposition of multiple sinusoids related to the gravity and magnetic sources located at different crustal levels. One of the objectives of the data filtering is to decompose the gravity and magnetic signals in order to investigate the boundaries and continuities of crustal structures.

The deep structures of the belt can be identified by low-pass filtering (**Fig. 3a**) or upward continuation of the Bouguer anomalies (**Fig. 3b**). In order to analyse the variation of the gravity signal in the crust, the low-pass gravity maps have to be compared with the variation of the crustal thickness. Therefore, a map of the Moho depth (**Fig. 4**) was compiled based on the map published by Dezes and Ziegler (2002) and completed by more recent maps on the Bohemian Massif (Wilde-Piórko et al., 2005), the Rhine Graben (Edel et al., 2007) and Iberia (Palomeras et al., 2017). Similarly, the long and short wavelengths, assuming to be related to the lower and upper crustal gravity signal respectively, have been removed to better illustrate the gravity characteristics of the intermediate crust (**Fig. 3c**). Also, the shallow structures of the belt are enhanced by high-pass filtering (**Fig. 3d**) or first vertical derivative of the Bouguer anomaly (**Fig. 3e**). However, these procedures trigger an artefact along the oceanic – continental boundary showing positive and negative belts on the resulting map, respectively (**Fig. 3d**). As these belts have no significance in terms of crustal density, a limit based on the horizontal gradient of the long-wavelength maps has been drawn on the filtered maps to avoid misinterpretation (**Figs. 3c, d**).

The procedure of gravity signal analysis through various filtering techniques is shown in **Fig. 5** using the Bohemian Massif as an example, whose some key geological features are sketched in **Fig. 5a**. The Bouguer map (**Fig. 5b**) and its first derivative (**Fig. 5c**) are shown together with the tilt angle (**Fig. 5d**) and contours of upward continuations (**Fig. 5e**). The tilt angle (**Fig. 5d**) is a transformation of the vertical derivative of the Bouguer anomaly that also locates subvertical boundaries and faults (Miller and Singh, 1994; Verduzco et al., 2004). In addition, it estimates the depths of structures (Salem et al., 2007). The horizontal gradients of the first and second vertical derivatives are maximum along the lateral boundaries of geophysical structures. In particular, the 0 isoline of the second vertical derivative is collinear with these boundaries, provided they are subvertical. Upward continuation of the gravity anomalies attenuates the short-wavelength anomalies and consequently illustrates the effect of the deep structures. Thus, successive upward continuations of the second vertical derivative and the juxtaposition of the resulting maxima show the orientation of the lateral boundaries of

the gravity bodies with depth and indicate the dip of major boundaries (**Fig. 5e**). This technique is equivalent to multiscale edge detection (e.g. Holden et al. 2000; Godin et al., 2014; Vos et al., 2006).

The magnetic anomalies are portrayed in three maps covering the NVD, CVD and SVD domains (**Fig. 6**). The flight levels of different areas of north-eastern France, southern Germany and northern Austria aeromagnetic surveys are 1000, 1200 and 1500 m. Because of this small difference, the effect of the flight level differences for the vertical derivative maps reduced to the pole is negligible and consequently is not taken into account. It is not the case for the Czech survey that was measured at a mean flight level of 500 m. Therefore, for the magnetic map of central-eastern Europe (**Fig. 6a**) a magnetic levelling has been done and the derivatives were continued upwards by 500 m. In contrast, the map of Wonik and Hahn (1990) at a flight level of 3000 m was continued downward by 1500 m. For **Figs. 6b** (France) and **5c** (Iberia), that were measured at a level of 3000 m, no continuation was applied. The reductions to the pole of the magnetic anomalies were applied to solve the problem of the asymmetry of a magnetic anomaly due to a non-vertical inclination of the magnetization. Then, the first vertical derivatives of the magnetic anomalies reduced to the pole were performed (**Fig. 6**). The resulting three maps represent the magnetic structures that are further compared to gravity anomalies for better defining subsurface structures. First and second vertical derivatives of the magnetic maps reduced to the pole were used to delineate the boundaries of subvertical magnetic bodies and faults (**Fig. 5f**). As for a same body, the intensity of magnetic anomaly reduced to the pole is proportional to the intensity of the first vertical derivative of the gravity anomaly, the comparison of both maps facilitates their interpretation.

4.2.2. Seismic experiments

In order to illustrate the thickness and velocities of the different layers of the Variscan belt, published 1D velocity/depth logs and 1D models extracted from 2D velocity models are projected on a series of profiles nearly orthogonal to the axis of the belt (**Fig. 2**). To make easier the comparison between deep reflection seismic sections, a common line drawing has been performed on available sections with a good definition. Collinear reflections have been interpolated in order to extract the structural features, part of which delineates crustal units with a common seismic signal (in colour). To make the seismic profiles more legible and comparable, all other sections are presented with interpolated reflectors. For the Iberian sections, the interpretation was done directly on the published sections (Pérez-Estaún et al.,

1994; Simancas et al., 2003). Four sections (Boh9HR, Dekorp-2S and Dekorp-2N, Dekorp 1C; **Fig. 2**) intersect the Saxothuringian zone and the Rhenohercynian/Saxothuringian sutures zones in the NVD. Three sections, and SWAT 2-3, SWAT 6-7 and SWAT 9-10, cross the Variscan front and four sections and Ecors-Dekorp, ECORS-Nfr, ARMOR-2, ARMOR-1 cross the internal Variscan zone in the CVD (**Fig. 2**). In the SVD the IBERSEIS section crosses the Rhenohercynian suture in the southern flanks of the Ibero-Armorican arc, while the sections ESCIN-1, ESCIN 3.2 and 3.3 (initially called ESCICANTABRICA-1, Pérez-Estaún et al., 1994) and ALCUDIA cross the CIZ, WALZ and CZ (**Fig. 2**).

5. Results viewed to the scale of the Variscan belt

The results of source collection and data processing are presented in a series of gravity and magnetic maps as well as seismic profiles and are described and discussed in the following sections.

5.1. Main features from gravity maps

At a large scale, the wavelengths > 150 km, 450-150 km and 250-25 km, the upward continuation by 2.5 km and the vertical derivative (**Fig. 3**), reflect the thickness of the crust and its mean density (Edel and Weber, 1995; Plaumann, 1988; Baptiste, 2016; Baptiste et al., 2016). The Moho map (**Fig. 4**) is further used here to better constrain the crustal thickness. A clear correlation between crustal thickness and gravity lows exists along the Teisseyre-Tornquist Zone (TTZ) at the SW limit of the East European Platform. As expected, a strong negative anomaly on the Alpine and Carpathian belts is due to the duplication of the crust during the Alpine convergence (**Fig. 3**). For the same reason, the Pyrenees are associated with a negative but less extended anomaly. In the Carpathians, a distinct gravity low coincides with the outer fold-and-thrust belt suggesting that the deep position of the crystalline basement also contributes to a negative gravity anomaly. The increasing gravity high west of Britain and the Paris Basin is explained by thinning of the crust towards the Atlantic Sea.

5.1.1. Long-wavelength anomaly and upward continuation maps

The long-wavelength gravity map (**Fig. 3a**) and the upward continuation map (**Fig. 3b**) show a large negative anomaly in the main part of Iberia, which is not associated with increasing Moho depth. The minimum of this gravity low is located in the central and eastern part of the Central Iberian Zone (CIZ) at its contact with the West Asturian-Leonese Zone (WALZ). Another gravity low in south-eastern Iberia is related to the crustal thickening in the Betics range. A low-density crust also characterises the southern part of the Massif Central and the Moldanubian Zone of the Bohemian Massif. Less pronounced negative anomalies

occur in the Paris Basin, and further east at the contact of the European Variscan belt with the Baltica cratonic crust. In the latter case, gravity lows are a combined effect of a deep basement, low density of the upper crust and lateral changes of the crustal thickness (Mikołajczak et al., 2019). Some negative anomalies also occur in the northern half of Avalonia. In the east of the Variscan belt, the northern part of the Saxothuringian Zone is characterised by a positive ridge.

5.1.2. Intermediate wavelengths gravity map

In the intermediate wavelength gravity map (**Fig. 3c**), that reflects the density of the intermediate crust, the structure of the Variscan belt is still poorly expressed. In general, areas where Carboniferous and early Palaeozoic granites crop out coincide with negative anomalies, indicating that the low density felsic granitoid bodies are deeply rooted. In particular, this is the case of the Moldanubian Zone of the Bohemian Massif, French Massif Central, Vosges and the Saxothuringian late Carboniferous granitoid province. In the Paris Basin, the gravity lows are mainly due to Armorican Cadomian granites (Baptiste et al., 2016). The intermediate wavelengths emphasize the felsic magmatism of the western part of the Massif Central and northern Aquitain Basin. In Iberia, the gravity lows dominate in the CIZ and correlate with zones of late Carboniferous magmatism. A prominent low, which remains after removing the ocean-continental boundary artefact, coincides with the core of the Ibero-Armorican Arc in the Cantabrian zone, where granites are very rare, but the crust is up to 36 km thick. The negative anomalies of south-eastern Iberia observed in the long-wavelength map (**Fig. 3a**), which correlate with the thickened crust of the Betics range (> 35 km; **Fig. 4**), are also well pronounced in the intermediate wavelength map (**Fig. 3c**).

Gravity highs are present in the northern and eastern half of the Saxothuringian Zone, the TBZ and its western extensions, the Kraichgau and the Saverne-Sarrebourg anomalies, north of the Vosges, respectively (Edel and Weber, 1995; Edel and Schulmann, 2009). West of the Bray Fault, the upper crust of the Manche-English Channel shows also high densities, in particular in the northern part of the Armorican Massif, where Cadomian magmatic rocks crop out (Brun et al., 2001). In the Moldanubian Zone, the NE–SW positive gravity belt continues through the Schwarzwald gneiss core and southern Vosges toward the eastern Massif Central. It is not excluded that part of this high gravity belt is related to the elevated Moho that borders the Alpine low in the north and west.

5.1.3. Short wavelengths and derivatives maps

Short wavelength filters, vertical derivatives and tilt angle are used to define boundaries of dense or light upper crustal bodies as well as faults and other discontinuities. In

the short wavelength and vertical derivative maps (**Fig. 3d, e**) the structure of the Variscan belt is well expressed, and the maps can be tentatively converted into geological maps of the pre-Mesozoic basement. This has been done with the high pass filtering of the three Variscan domains (**Figs. 7, 8** and **9**). With the exceptions of Mesozoic and Cenozoic sedimentary basins such as the Aquitain and Paris basins, the northern Upper Rhine Graben and the Polish Basin, the gravity lows mainly represent Carboniferous granites and to a lesser extent Cadomian and Ordovician granites, Carboniferous gneiss domes or felsic granulite domes (**Figs. 7** and **8**).

In Iberia (**Fig. 9**), the effects of the Alpine orogeny obscure the anomalies related to the Variscan basement. Lows in the Betics range (BeR), as well as those of the Pyrenean Chain (PyC) and their continuation to the west at the southern border of the Cantabrian Mountains (CM) result from Alpine crustal thickening, as can be appreciated when comparing with the topography of the Moho (**Fig. 4**). Inside the outcropping Variscan basement, lows correspond to Carboniferous granitoids and late Variscan gneiss domes. Other NW-SE and NE-SW alternations of lows and highs are related to two conjugated families of late Variscan faults (Arthaud and Matte, 1977), but their gravity signature was acquired by their reactivation during Mesozoic extension and Cenozoic compression.

The gravity highs are due to rocks with densities exceeding the mean crustal value of 2670 kg m^{-3} (in green and dark blue), consisting of early Palaeozoic and Proterozoic sedimentary or mafic magmatic units (**Figs. 7, 8** and **9**). In the NVD, the Rhenohercynian and Mid-Variscan sutures are marked by narrow zones of gravity highs coinciding with outcrops of dense rocks such as eclogites and ultramafics and/or Proterozoic basement (**Fig. 7**). The areas coinciding with less important gravity highs are mainly composed of Proterozoic – Lower Palaeozoic sequences of the Teplá-Barrandian crust, dense Proterozoic Brunia and Saxothuringian formations and thick Palaeozoic volcano-sedimentary basins, represented in the Vosges and Schwarzwald. Highest gravity anomalies coincide with ultramafic ophiolitic sequences or Ordovician mafic intrusions amphibolite complexes. The gravity highs in the northern Variscan foreland are related to the presence of shallow structures related to the late Cretaceous-early Paleogene inversion of the Permian-Mesozoic Basin.

The gravity map of the French Massif Central (**Fig. 8**) shows irregularly scattered gravity highs separated by the main outcrops of gneisses of the Parautochthon and Lower Gneiss Unit. The most prominent gravity highs coincide with complexes of mafic and ultramafic rocks of the Upper Gneiss Units in particular at the boundary between the high-grade rocks and migmatites of the French Massif Central and the Armorican Massif. The low

amplitude gravity highs of the Armorican Massif are formed essentially by the Proterozoic metasedimentary and volcaniclastic parautochthonous sequences. A large gravity high in SW France probably corresponds to dense schists of the Autochthon and Parautochthon.

In Iberia, a large gravity high coincides with the Cenozoic Ebro basin (EbB; **Fig. 9**), a triangular region where the crust is relatively thin (**Fig. 4**). Other maxima occur south of a roughly W-E line bounding the region with abundant Variscan granitoids of the Spanish Central System and partly coinciding with the central stretch of the Tagus Basin (TaB). Both highs separate areas thickened during the Alpine cycle from Cenozoic basins, and do not represent the Variscan crustal configuration. Contrarily, short wavelength positive anomalies coincide with outcropping high-density units, as in the case of the allochthonous complexes of NW Iberia, characterised by large bodies of mafic and ultramafic rocks (Martínez Catalán et al., 2012).

5.2. Main features from magnetic maps

Three maps of the vertical derivative of the aeromagnetic data reduced to the pole have been analysed. That of the NVD is an assemblage of processed data from northeastern France (Edel and Schulmann, 2009), southern Germany (BGR, 1976; Wonik and Hahn, 1990), the Czech Republic (Šalanský, 1994), and northern Austria (Blaumoser, 1992) (**Fig. 6a**). Several magnetic belts can be observed in the map. The first is the northern belt, which partly coincides with the Mid German Crystalline Rise and continues through the Rhine Graben toward the northern Vosges. According to the magnetic susceptibility and remanence (Ayarza and Martínez Catalán, 2007; Martínez Catalán et al., 2012, 2018; Edel and Aïfa, 2001; Baptiste, 2016; Baptiste et al., 2016; Edel, 1985; Edel et al., 1986; 2013; Edel and Weber, 1995; Hrouda et al., 2013, 2014; Žak et al., 2011, 2013, 2019), the rocks responsible for the anomalies generally consist of diorites and granodiorites emplaced in the time range of 345-330 Ma. To the south, an up to 200 km long dyke-like structures (M1 and M2 in Fig. 11a) crosscuts the high density Kraichgau domain. The second belt of magnetic rocks is developed along the Saxothuringian and Mid-Variscan Ocean sutures and corresponds to the outcrops of mafic and ultramafic rocks cropping out in the Mariánské Lázně Complex, Krkonoše Massif and Central Sudetic Ophiolite. The third belt is represented by wide anomalies corresponding to the gabbroic and tonalitic intrusions of the Central Bohemian Plutonic Complex and the Nasavrky pluton. A similar magnetic high can be detected beneath sediments of the Schwabian Jura farther southwest. The fourth belt is composed of anomalies rimming the boundary of the Brunia block and represented by Cambro-Ordovician ophiolitic sequences including ultramafic rocks and eclogites of the Rehberg Massif, Letovice Massif

and Staré Město Belt. The magnetic highs in the Brunia block correspond to diorites of Proterozoic arc (Hanžl et al., 2019). The magnetic belts are cut across by dextral fault systems (Pfahl, Danube, Elbe and Sudetic faults) that are highlighted by high-frequency magnetic highs associated with granodiorite magmatism (Finger et al., 1997).

2D and 3D modelling generally reveal thick dykes, dipping toward NW and mostly widening with depth (Edel et al., 1996; Edel and Schulmann, 2009; unpublished student reports). It is also the case for both southerly dykes that are crossed by the DEKORP-2S seismic profile.

The CVD map (**Fig. 6b**) includes the vertical derivatives of the aeromagnetic map of France (BRGM, 1972), the Bay of Biscay (CNRS-IPGP) and southern England (British Geological Survey, 1998). The Magnetic Anomaly of the Paris Basin (MAPB) is the most prominent linear feature of this map connecting anomalies of the Rhenohercynian arc developed in the east and the corresponding anomalies beneath the Manche-English Channel and Léon unit in northern Brittany. These NE-SW striking anomalies of the central Manche-English Channel show the same orientation and a similar distance from the Lizard ophiolite as those shown by the Rhenohercynian magmatic arc relative to the Rhenohercynian suture trace in the east. Thus, the magnetic bodies are interpreted as the western continuation of the Carboniferous arc, shifted dextrally by the Bray Fault. An array of WNW-ESE trending magnetic lineaments in the central Armorican Massif coincides with the folded Neoproterozoic basement and possibly volcanic sequences. However, the most prominent magnetic anomaly coincides with the belt of Ile-de-Groix – Champtoceaux blueschists and eclogites decorating the Mid-Variscan suture zone.

In southwestern France and the Bay of Biscay continental shelf, the NNW-SSE striking anomalies are aligned to late Carboniferous dextral strike slip fault zones parallel to gravity discontinuities (**Figs. 1** and **8**) that result from regional transpressive deformation (Carreras and Druguet, 2014).

For the SVD, the magnetic map (**Fig. 6c**) shows in the southern part of Iberia a dense pattern of magnetic anomalies that cover the whole of the Ossa-Morena Zone. In outcrops, the anomalies are associated with Cadomian, early Paleozoic and Carboniferous basalts, gabbros, diorites and granites. In northwestern Iberia, two magnetic belts border the eastern and western boundaries of the allochthonous terranes. Both are associated with late Variscan migmatites or/and granitoids. The anomaly in the east coincides with the Lugo gneiss dome, where magnetic minerals grew in extensional detachments during decompression (Martínez Catalán et al., 2018; Ayarza et al., 2021b). In the west, the source may be similar, but

outcropping magnetic rocks are rare, and the detachments may remain buried, as in fact occurs in the southern part of the Lugo dome and its continuation to the Sanabria dome. The aeromagnetic map shows a wide high linking the east and west anomalies, fully surrounding the NW Iberian allochthon of the GTMZ. This suggests that the broad anomaly is related to collapse-driven extensional tectonics following crustal thickening and thermal relaxation (Martínez Catalán et al., 2018). That arcuate structure is paralleled by other magnetic anomalies to the east, less clear in the vertical derivative map than in the aeromagnetic map. These anomalies have contributed to define an oroclinal loop of the Central Iberian Arc (CIA; **Fig. 1**), an orocline first envisaged by Staub (1926) and described in several recent papers (Aerden, 2004; Martínez Catalán, 2012; Shaw et al., 2012; Martínez Catalán et al., 2015, 2021).

5.3. Main features from seismic sections

The main reflective horizons in the reflection seismic sections across the European Variscan belt were interpreted using geological, refraction seismic and potential field methods. An example of the data treatment and the definition of main groups of reflectors is presented with the Boh9HR section (Fig. 10b) (Tomek et al., 1997; Tomek, 2007) where geological, structural and geochronological information were compiled by Maierová et al. (2021). Here, the reflection seismic data were combined with the CEL 09 seismic refraction line (Růžek et al., 2007), where some reflective horizons coincide with main velocity gradients (Fig. 10c). The gravity was subsequently modeled along the section taking into account combination of geological and seismic data, which allowed the attribution of the reflecting horizons to the main geological structures (e.g. Guy et al., 2011; Schulmann et al., 2014). Altogether three types of reflective horizons, which are present in all parts of the Variscan belt, are defined according to their dip directions, intensities of main reflectors and relative age based on cross-cutting relations (Fig. 11a, b, c).

The A-type reflections (violet) are oldest and form either thick moderately dipping horizons or parallel moderately dipping distributed reflectors. The younger B-type moderately to gently dipping reflectors (reddish-pink) are mostly present in the upper and middle-crust, while the youngest C-type reflectors (light blue) are mostly developed in the lower crust where they form thick sub-horizontal horizons parallel to the Moho and sometimes also parallel to main mid-crustal velocity gradients in refraction seismic sections.

5.3.1. Reflection seismic sections

A-type reflections (violet) show a southeast dip in the NVD and CVD and an east to northeast dip in the SVD (**Figs. 10 and 11**) and concentrate in thick zones dipping at a

moderate angle down to the Moho. They constitute the most pronounced features in most sections. In the NVD, we recognise two subparallel belts of A-type reflectors (e.g., Boh9HR, DEKORP-2S), whereas three belts exist in the CVD (e.g., ECORS-DEKORP). However, in the SVD and the English Channel area, only one prominent belt occurs (SWAT-6-7, IBERSEIS, ALCUDIA). In a few sections of the CVD and SVD, A-type reflectors are uniformly distributed in the crust (ECORS-NFr; ARMOR-2; ESCIN-1).

B-type reflections (reddish pink) show a northwest dip in the NVD and a southwest dip in the SVD. As these reflectors often interrupt or deviate the previous A-type reflectors, they generally postdate them. They appear as thick belts that in some cases cross the whole crust as for instance in the Dekorp-2S and the ECORS-DEKORP sections (**Fig. 11a**). In several places, B-type reflectors are associated with igneous intrusions emplaced concordantly to them (DEKORP-2S, Edel et al., 1996; ECORS-DEKORP, Edel and Schulmann, 2009). A similar observation can be made on the SWAT-9 and SWAT-10 sections where the B-type reflectors may be linked to the magmatic bodies responsible for the magnetic anomalies of the English Channel (SWAT9-10) (Fig. 11b). In the CVD, the B-type reflections pass through the magnetic body responsible for the Magnetic Anomaly of the Paris Basin and the Courgent granite (**Fig. 11a**, ECORS-NFr). Farther south, the granitoids and migmatites that stretch along the South Armorican Shear Zone overlie a series of B reflectors (Fig. 11b, ARMOR-2). In southern Iberia, SW dipping reflections occur beneath the Pedroches and Mora granitic bodies. B reflections also dominate in the section crossing the Cantabrian Zone and a small part of the West Asturian-Leonese Zone (Fig.11c, ESCIN-1).

In all sections, C-type reflections (light blue) are flat, in general parallel to the Moho and particularly well developed in the lower crust. The most reflective layers occur in the lowermost crust within the range of 10-15 km above the Moho. In the NVD and CVD, the C-type reflectors at the top of the lower crust are particularly well developed in the Rhenohercynian Zone (**Fig. 11**, DEKORP-2N), the Moldanubian zone of the Bohemian Massif (Boh9HR), and the Armorica south of the Bray Fault (Fig. 11a, ECORS-NFr; Fig. 11b, ARMOR-2). In the SVD, the strongest reflectors occur beneath the OMZ and the adjacent CIZ (Fig. 11c, IBERSEIS), where they form a thick zone separating the upper from lower crust.

The interpreted crustal structures show the similarities of the Boh9HR and the DEKORP-2S profiles in the NVD, in particular the gravity highs of the Teplá-Barrandian and the Kraichgau terranes (**Figs. 10 and 11a)**. Both terranes are bordered by low-density granitic rocks of Thuringia and the Erzgebirge. In both sections forward gravity modelling from

previous studies revealed relatively low densities in the lower crust underneath the important zone of A-type reflectors, favouring a felsic composition (Edel et al., 1996; Guy et al., 2011; Schulmann et al., 2014). The only difference between both models is the presence of magnetic dykes intrusive into the Kraichgau dense body (M1, M2; **Fig. 11a**, DEKORP2S). Further west, the ECORS-DEKORP section north of the northern Vosges shows a similar configuration as the previous profiles. Here, the Saverne-Sarrebourg gravity high is bordered in the north by the Adamswiller low that is due to a felsic ridge (Edel and Schulmann, 2009).

West of the Bray Fault, the Armorican Massif is crossed by the prominent magnetic anomaly of the Paris Basin (MAPB; **Fig. 11b,** ECORS-NFr). In its southern part, the magnetic body has the shape of a large dyke widening with depth (Edel, 2008). The ECORS-NFr cuts the magnetic body in its northern part. There is no clear correlation between the gravity and magnetic anomaly.

5.3.2. Crustal velocities of seismic P waves (Vp)

The velocity structure of the Variscan crust (**Fig. 12**) is imaged by seismic refraction profiles whose location is shown in **Fig. 2**. Several velocity models are derived from each profile and represented as logs, which are numbered consistently with the light blue lines in **Fig. 2**. For the NVD, profile (1), trending NE-SW, shows a thick three-layered crust of Baltica characterised by high velocity lower and middle crust (**Fig. 12**). Farther SW on a distance of c. 300 km, the profile samples the attenuated Baltica margin with thin high velocity lower crust and thick low velocity middle and upper crust (Grad et al., 2002, 2003, 2008; Mazur et al., 2015). Still farther SW, the Sudetes and Teplá-Barrandian are characterised by typical Variscan crust with low-velocities down to the Moho. The southernmost section shows a thin high velocity lower crust corresponding to the underthrusting of the Saxothuringian margin that is also imaged by the Boh9HR seismic line. The following 7 sections are oriented perpendicular to the Variscan belt. The Avalonia crust is sampled by profiles (7) and (8) (**Fig. 12**) and is featured by relatively high velocity (c. 7 km/s) and thick lower crust. Farther SE, the Rhenohercynian Zone is crosscut by profiles (4) to (8) and is characterised either by thin high velocity lower crust of underthrust Avalonia or thick low-velocity crust of the Rhenohercynian wedge. The Saxothuringian crust farther SE is represented by standard three-layered crustal velocity profiles. The Teplá-Barrandian and Moldanubian crust mostly show a typical Variscan velocity structure with low velocities down to the Moho, except for a few sections probably representing relics of the underthrust high velocity Saxothuringian lower crust. Finally, the easternmost Brunia reveals a cratonic-type three-layered crustal structure with a thick high velocity lower crust.

Only profile (9) is available for the CVD, running from Wales in the UK to the French Massif Central (**Fig. 12**). The Avalonia crust extends north of the Bray Fault. The Armorica crust farther SE is similar to that of the Saxothuringian (profiles (2) and (3) in **Fig. 12**). The North Armorican section shows a generally low-velocity crustal profile comparable with the Rhenohercynian wedge. The French Massif Central sections image a thin crust comprising thin high velocity lower crust and thicker low-velocity middle and upper crust (Artemieva and Meissner, 2012).

In the SVD, most of the tectonic zones in the south show cratonic-type crust with the deep Moho (profiles 10 to 14), thick high velocity lower crust and thin upper crust. The northern part of the SVD shows the Moho depth that is exceptionally deep (c. 35-40 km) in the WALZ and CZ with thinner high velocity lower crust and thick upper crust. The IBERSEIS and ALCUDIA profiles show that the SPZ and possibly also the OMZ are featured by the Avalonia-type underthrust crust. The eastern part of these profiles shows probably a velocity structure of the Gondwana margin. The crust in the north of the SVD, imaged by the ESCIN-1 profile (**Fig. 11c**) represents the Variscan foreland thrust belt, characterised by thin-skinned tectonics which was not affected by the gravitational collapse typical of the internal zones.

6. Interpretation of gravity and magnetic anomalies

In this section, the regional distribution of gravity and magnetic anomalies is compared with surface geology of the three studied domains of the European Variscan belt (**Figs. 7, 8** and **9**). The gravity and magnetic lineaments are critically assessed and discussed in the light of succession of the principal deformation events affecting the belt. The gravity and magnetic short wavelength anomalies and their derivatives (**Figs. 3, 5** and **6**) allow defining coincidence between them and the respective geological bodies and, also, trace their full extent beneath the younger sediments. However, the interpretation of several gravity anomalies is based more on geological assumptions than on the direct geophysical datasets. Typical example are large magnetic and gravity highs present at the eastern margin of the Bohemian Massif i.e. those characterizing the mafic complexes of the Brunia basement and anomalies featuring Moldanubian nappe dominated by felsic rocks above the eastern Brunia margin. There, some anomalies, such as those that correlate with the surface expression of the Rehberg ophiolite or large northern gravity high beneath the Moldnubian nappe can be interpreted as deep seated mafic complexes belonging to underlying Brunia basement. This is because the Moldanubian nappe consists essentially of low density felsic migmatites,

granulites and paragneisses (Schulmann et al., 2008). Similar problem can be retrieved in the French Massif Central example, where thehuge late Carboniferous - Permian Velay granite massif (Fig. 8) does not coincide with any gravity low compared to the large gravity anomalies associated to early Carboniferous plutons.

6.1. Geophysical anomalies of the NVD

The map of band pass filtered gravity anomalies with cut off wavelengths of 200-7 km and contours of magnetic units of the NVD (**Fig. 7a**) shows that the gravity highs correspond either to ophiolitic bodies in the east, the Devonian suture zone of the Mid-Variscan Ocean in the west and mafic plutonic rocks mostly of Ordovician age scattered across the belt. For instance, the gravity highs along the eastern margin of the Bohemian Massif correspond to large outcrops of gabbros and ultrabasites of the Cambrian Letovice ophiolite (LtO) in Czech Republic or the Devonian Sudetic ophiolite (SO) in Poland. There is also an important linear NE-SW trending gravity high separating the Saxothuringian Zone (STZ) from the Teplá-Barrandian Zone (TBZ). This gravity high coincides with positive magnetic anomalies and together correspond to outcrops of mafic rocks such as eclogites, metagabbros and ultrabasites of the Mariánské Lázně Complex (MLC) or HP mafic complexes rimming the Saxothuringian basement of the Krkonoše pluton (KP) such as Zelezny Brod and Leszczyniec amphibolite complex. These rocks correlate with the base of the Upper Allochthon and the Cambro-Ordovician oceanic units in the sense of Martínez Catalán et al. (2020) and thus correspond to the trace of an exhumed subduction wedge dominated by eclogites, amphibolites and metagabbros. This NE-SW trending semi-continuous trail of positive anomalies, thus, constitutes the outcropping and subsurface trace of the Carboniferous Saxothuringian and Devonian Mid-Variscan Ocean sutures (Mazur and Aleksandrowski, 2001; Konopásek et al., 2019; Martínez Catalán et al., 2020; Martínez Catalán et al., 2021). The gravity highs in Germany correlate well with the outcrop of the Münchberg (Mü) Complex that is a surface expression of the allochthonous mafic complexes, corresponding to the Mid-Variscan Ocean suture zone. There are also several gravity highs that correlate with mafic intrusions such as the Stod Massif (StM) Ordovician gabbros at the southern corner of the Teplá-Barrandian Zone (TBZ) or late Devonian gabbros and diorites of the Central Bohemian Pluton (CBP). The characteristic feature of gravity map is NW-SE trending narrow gravity highs or boundaries between regional gravity lows and highs corresponding to dextral shear zones and faults exemplified by the Bavarian Fault Zone (Bf), Frankenwald Fault (Ff), Elbe Zone or Sudetic Faults. However, there are several large-scale gravity highs for which the correlation with geology remains obscured such as the Lausitz Block (LzB), Kraichgau

(Kr), Black Forest Gneiss mass (BFGm), Rhenish Massif (RhM) and the Saverne-Sarrebourg High (SSH) anomalies. The specific problem represents the large scale gravity highs at the eastern margin of the Bohemian Massif beneath the Moldanubian nappe (Schulmann et al., 2008). The extent of the Brunia basement beneath the felsic rocks of the Moldanubian nappe (BR-MZ) was determined by the gravity modelling (Guy et al., 2011) and therefore we interpret these anomalies as deep seated expressions of Brunia mafic complexes rather than large mafic bodies, such as Rehberg ophiolite, belonging to the Moldanubian nappe (Fig. 7).

The gravity lows are a prominent feature in the gravity map (**Fig. 7a**) and result from the presence of low-density rocks of different age such as Cadomian and Cambro-Ordovician granitoids (550–480 Ma) of the Saxothuringian Zone represented by the core of the Erzgebirge Massif (EzM) or Izera Massif (IzM). The other prominent feature of the NVD is gravity lows coinciding with early Carboniferous (350–340 Ma) felsic migmatite and granulite bodies typically developed in the Moldanubian Zone (MZ), the Podolsko complex (PdC), Kutna Hora Complex (KC) or the Orlica Śnieżnik dome (OSD). Surprisingly, Saxonian (SGr) and Blanský les (BG) granulite bodies form only low amplitude anomalies, which nevertheless can be well traced in more detailed geophysical maps (Franěk et al., 2011). The most important gravity lows correlate with mid-Carboniferous granite plutons, the most important of which is the Central Bohemian Pluton (CBP), and other significant bodies are the North Vosges arc granitoids (NVgr), Odenwald arc granitoids (OdAr), Central Vosges granite complex (CVgr) and the vast granitoid complex of the Mid-German Crystalline Rise (MGCR) spatially matching to the Rhine Graben shear zone (RSZ) in its southern extremity. The last source of gravity lows is late Carboniferous to Permian (310–280 Ma) granite bodies, which crop out in the Sudetes: the East Sudetic pluton (SdP), Krkonoše pluton (KP) and Sobótka pluton (SP) and Erzgebirge such as Karlsbad pluton (KaP). Permian magmatism and volcanism are abundant in the Erzgebirge, but their contribution to a large-scale negative anomaly of the Erzgebirge core cannot be deduced at the scale of the presented map (**Fig. 7a**).

The combined gravity and magnetic data allow to delineate large tectonic domains at the scale of the whole NVD. For instance, the Teplá-Barrandian Zone (TBZ) and the Kraichgau domain (Kr) are characterised by long wavelength low amplitude gravity highs (8 to 20 mGal) compared to the lower density Moldanubian Zone (MZ; 0 to -20 mGal), which is also characterised by the presence of numerous short wavelength gravity lows. The Brunia Domain (BR) is also well defined by an important and long wavelength gravity high (8 to 20 mGal) compared to the Moldanubian Zone (Guy et al., 2011) and their mutual boundary is defined by a magnetic anomaly as well. Important is also a triangular gravity high north of the

Alps that was interpreted as a Precambrian basement block called Vindelicia (VL; Vollbrecht et al., 1989) potentially similar to Brunia. The central part of the Saxothuringian Zone is also characterised by a long wavelength and low amplitude gravity high (2 to 12 mGal) surrounded by NE-SW trending large scale gravity lows. The gravity high corresponds to Proterozoic to early Palaeozoic sequences and the gravity lows to granitoids of the MGCR and North Vosges in the NW, the Erzgebirge orthogneiss dome and Permian granitoids in the SE. Altogether, the main tectonic zones of the European Variscan belt show distinct geophysical signatures and well-defined boundaries that are displaced by dextral and sinistral strike slip faults of late Carboniferous-Permian age (Edel et al., 2018).

This approach allows us to define a new subsurface geological map of the NVD where the extent of tectonic domains together with small-scale geological units is redefined (**Fig. 7b**). For instance, the Saxothuringian and Mid-Variscan sutures are well visible as a zone separating the Saxothuringian Zone from the Teplá-Barrandian Zone, the Kraichgau and northern Vosges domains. Especially, in the Bohemian Massif the gravity signal of the two sutures merge as the distance between them is very small (e.g., Konopásek and Schulmann, 2005). Similarly, the extent of the Moldanubian Zone and its continuity from the Sudetes in Poland to Vosges in France is well established. The shape of Brunia and Vindelicia basement is well defined as well as the boundary between the Rhenohercynian wedge and the Saxothuringian Zone.

6.2. Geophysical anomalies of the CVD

Likewise in the NVD, the map of band pass filtered gravity anomalies with cut off wavelengths of 200-7 km (**Fig. 8a**) was used to identify bodies and complexes of contrasting density. The CVD can be subdivided, based on gravity signature, into three large domains. The northern one is represented by long wavelength and low amplitude gravity highs (ranging from 2 to 12 mGal), which is perturbed by diffuse gravity lows. This area correlates with the Proterozoic gneisses and schists of the NAD. The central domain roughly corresponds to the French Massif Central and Limousin and includes intermediate gravity signal from -2 to 10 mGal correlating with medium-grade schists and gneisses of the Lower Gneiss Unit. Localised short wavelength and high amplitude gravity highs and lows represent relics of the allochthonous Upper Gneiss Unit and Carboniferous granites intruding the whole sequence, respectively. The southern domain correlates with the Aquitain basin in SW France. It is dominated by fairly uniform intermediate density rocks (-2 to 10 mGal) associated with low amplitude anomalies. The area is characterised by the lack of short wavelength highs and

lows and distinct density contrasts. Altogether this region represents the outcrop of the Parautochthon and Autochthon in the sense of Faure et al. (2009).

A salient characteristic of the central domain is the presence of short wavelength and high amplitude positive anomalies that are scattered across the French Massif Central and form a trail rimming the Armorican Domain. The latter anomalies are in particular the Champtoceaux (ChcU) and Essarts eclogitic unit gravity and magnetic highs coinciding with eclogitic outcrops and their subsurface prolongation farther east beneath the Paris basin. In the French Massif Central (FMC), these anomalies correlate with outcrops of the Upper Gneiss Unit mafic rocks (amphibolites, meta-gabbros, eclogites) such as anomalies of Haut Allier (HAU) or Monts du Lyonnais (MLU) and Najac Unit (NAJU) or ophiolitic mainly volcanic units as the Brévenne ophiolite (Bvop) and Morvan Arc (Mvar) or Génis-Thivier-Payzac unit (GTPU). The trail of anomalies at the Armorican basement and Massif Central defines the northern extremity of the Mid-Variscan Ocean suture such as Baie d'Audierne ultramafics (Baum), while the scattered anomalies in the FMC represent klippen of the eroded Allochthon. There is a specific region of north-eastern France defined by scattered gravity highs of intermediate values ranging from 10 to 15 mGal interrupted by gravity lows corresponding to outcrops of Carboniferous granites. These gravity highs encompasse rocks of Upper Devonian – Lower Carboniferous volcanic and sedimentary sequences outcropping in the southern Vosges Arc (SVAr) and in the Badenweiler-Lenzkirch zone of the southern Schwarzwald (BLZ) in the east, and Morvan, and Brevenne Upper Devonian volcanic sequences in the west. Because of the geochemistry and age of these volcanics and associated gabbros (Pin and Paquette, 1997; Pin and Paquette, 2002; Skrzypek et al., 2012b), the whole domain is interpreted as a late Devonian – early Carboniferous suprasubduction basin (**Fig. 8b**).

Short-wavelength and high-amplitude negative Bouguer anomalies are mainly developed in the FMC and coincide with late Carboniferous granitic intrusions such as Millevaches (Migr), Gueret, (Ggr), Margeride (Mggr), Aigurande (Agr), Morvan (Mvgr) and its eastern prolongation called Morvan-Vosges granite (MVgr), and various leucogranites plutons and granites underlining the South Armorican Shear Zone (SASZ), leucogranite intrusions (Lgr) or granitoids of the central Vosges (CVgr). Important gravity lows also correspond to the outcrops of Ordovician granites (Ogr) in the Armorican Domain such as the Lanvaux orthogneiss (LvOg). Mid-late Carboniferous migmatite domes such as the Montagne Noire (Mnmi), Maures internal zone (Malz) and migmatites of the South Armorican domain coincide also with gravity lows. Surprisingly, the largest FMC granite intrusion represented by the Velay dome does not show any gravity low but coincides with a low amplitude gravity

high, which possibly reflects high-density rocks of the UGU preserved in the roof pendants of the pluton. This may indicate that the Velay dome represents a thin granite-migmatite sheet emplaced parallel and contemporaneously with the Pilat detachment corresponding to a magnetic high (**Fig. 6**) (Mallavieille et al., 1990; Gardien et al., 2021).

A new subsurface geological map of the CVD (**Fig. 8b**) shows the contrasting structural style of the three domains discussed above. The main feature is the Mid-Variscan Ocean suture separating the Armorican Proterozoic basement from gneisses, schists and migmatites of the Variscan nappe stack of the FMC intruded by numerous granitoids. This orogenic domain is well separated from the outcrop of the underlying para-autochthonous medium- to low-grade schists in the south defining the southern domain. The other important feature of this new map is the larger extent of the southern part of the Upper Gneiss Unit compared to existing reconstructions as well as the definition of a wide suprasubduction late Devonian-early Carboniferous basin to the east.

6.3. Geophysical anomalies of the SVD

The SVD, represented by the Iberian Peninsula, is embraced by elongated gravity lows corresponding to the Pyrenees (PyC) and Cantabrian Mountains (CM) in the N and the Betics Range (BeR) in the SE (**Fig. 9a**). However, in the interior of the SVD, the Bouguer anomaly is largely conditioned by the Alpine reactivation of late Variscan faults. Thickened crust at pop-ups and horst striking NE-SW and NW-SE (de Vicente et al., 2018), and marginal sedimentary basins, define elongated lows as, for instance, south of the Spanish Central System (SCS) and the Iberian Chain (IbC).

Inside the Iberian Massif, which represents the largest outcrop of the Variscan basement, most of the CZ, WALZ, CIZ, and OMZ (**Figs. 1** and **5c**) are characterised by low amplitude positive anomalies in the range of 2 to 15 mGal. The isolated short wavelength high amplitude gravity highs in the NW correlate with outcrops of mafic rocks (gabbros, amphibolites, eclogites, peridotites) belonging to the termination of the Mid-Variscan Allochthon in Iberia. These gravity highs also coincide with magnetic anomalies. But unlike in the CVD, the Mid-Variscan Ocean suture is not defined by a linear gravity and magnetic anomaly, because it is only preserved in four more or less rounded klippen: the allochthonous complexes of Cabo Ortegal (COC), Órdenes (OC), Bragança (BC) and Morais (MC). Other gravity maxima are elongated and roughly parallel to the Variscan structural grain. They coincide with slate belts, as at the WALZ/CIZ limit, or with a belt of basic and intermediate Cadomian intrusives, as the Mérida Cadomian Batholith (MCB; Bandrés et al., 2004) and its possible continuation to the NW at the CIZ/OMZ boundary.

Gravity lows related to the Variscan basement correspond to a large Carboniferous magmatic province and late Variscan gneiss domes developed in the northern part of the CIZ and WALZ (Ayarza, and Martínez Catalán, 2007; Martínez Catalán et al., 2018; Ayarza et al., 2021b). These include the Lugo and Sanabria domes (LD, SD) and continue south and southwest up to the Porto-Viseu granitic lineament (PVgl) surrounding the NW Iberian Allochthon. The spectacular 400 km long NW-SE negative anomaly parallel to the OMZ – CIZ boundary is also the expression of a granite lineament, the Pedroches batholith (Pgl) and its continuation to the NW by the granitic lineaments of Nisa-Alburquerque (NAgl) and Cáceres (Cgl).

The subsurface map of the SVD is largely dominated by Alpine structures, although some of them are reactivations of late Variscan strike-slip faults (Arthaud and Matte, 1977). In addition, several gravity highs and lows reveal some older features such as tectonic boundaries and granitic lineaments. The Ibero-Armorican Arc is partly delineated by gravity maxima in the WALZ (**Fig. 9b**) but not the Central Iberian Arc, which is better depicted by the aeromagnetic map. Relatively high-frequency, high amplitude magnetic anomalies characterise the OMZ in SW Iberia. The sources are plutonic and volcanic igneous rocks, mostly basic or intermediate, of Neoproterozoic, Cambrian, Ordovician and Carboniferous age.

6.4. Correlation of gravity and magnetic lineaments

All the lineaments emphasise the structural grain of the Variscan belt. As deduced from the band pass analysis (**Fig. 3**), shallow and deep lineaments are mutually consistent. The lineaments are folded in the SW by the Ibero-Armorican oroclinal arc. In the NE, the lineaments are disrupted and shifted by dextral strike-slip faults of the Danubian-Elbe-Sudetic system. Thus, they adjust to the NW-SE trend of the Baltica margin (Mazur et al., 2020). The major deep-seated lineaments express the location of both the Rhenohercynian and Mid-Variscan Ocean sutures in the CVD and NVD.

In contrast, in the SVD only the Rhenohercynian suture is well visible while the Mid-Varican Ocean suture is only represented by isolated maxima due to its rootless character. Here, the deep-seated lineaments, although parallel to the structural grain, only occasionally coincide with the boundaries of the tectonostratigraphic zones, that actually do not represent oceanic sutures except perhaps that between the CIZ and OMZ, which presently is a late Variscan sinistral shear zone. A roughly E-W lineament in the centre of the Iberian Peninsula, partly bounding to the north the Tagus basin (**Fig. 9b**), cuts across the Variscan structures and is probably an important Mesozoic or Alpine fault.

Some potential faults displacing the lineaments are reoriented by the Ibero-Armorican Arc, which shows it is a late feature. The Central Iberian Arc is not delineated by the Bouguer anomaly, probably because of changes in crustal thickness due to the Alpine overprint. This orocline can be followed in the aeromagnetic map (Aerden, 2004; Martínez Catalán, 2012), although the curvature of anomalies in the hinge zone is obscured by the Meso- and Cenozoic cover, and it is poorly visible in the first vertical derivative map in **Fig. 6c**.

In the CVD and NVD, the main lineaments are disrupted and shifted by the dextral Bray Fault and the sinistral Upper Rhine Graben Fault (Edel et al., 2007). This geometry emphasizes the SW corner of the Avalonia promontory. Furthermore, the position of the Upper Rhine Fault and the dextral Pfahl-Danubian fault system underlies the shape of the Vindelicia basement block to the SE (Vollbrecht et al. 1989).

6.5. Interpretation of density structures of the Variscan Belt

The analysis of the nature of gravity anomalies considered jointly with magnetic anomalies gives a lineament map (**Fig. 13**), which allowed for an updated interpretation of the European Variscan belt. The three domains represented in that figure are peri-Gondwanan. The Rhenohercynian system includes the Avalonian Midlands microcraton and Brabant Massif, as well as the Rhenohercynian and South Portuguese Zones, whose basement is considered Avalonian. The Autochton derives from present northern Africa. It probably remained attached or close to mainland Gondwana during the Paleozoic, although some pieces where detached, such as the Ossa-Morena and part of the Saxothuringian Zone. Perhaps the whole Autochthon was pulled apart to open the Paleotethys Ocean during the Devonian (Stampfli et al., 2013; Martínez Catalán et al., 2021). The Allochthon is an accretionary wedge built along the Devonian that involved an individualized peri-Gondwanan terrane (Upper Allochthon), a stack of oceanic units of late Cambrian, Silurian and Lower Devonian ages (Middle Allochthon) and the outermost margin of the northern African terrane (Lower Allochthon). The latter was first subducted beneath the wedge, and then incorporated to it. During the early Carboniferous, the ensemble was emplaced onto the Autochthon incorporating part of its cover during thrusting (Parautochthon). The three allochthons plus the Parautochthon form the Mid-Variscan Allochton (Martínez Catalán et al., 2021).

Based on the gravity highs (**Fig. 14**), the Variscan belt is divided into the composite structure of the Mid-Variscan Allochthon, the Autochthon and the Avalonian domain. It is important to note that especially in the NVD the gravity highs at the western part of the Bohemian Massif coincide with outcrops of both the Saxothuringian and Mid-Variscan sutures. This is due to the fact that the two sutures are often spatially juxtaposed to each other.

The Allochthon itself is represented by high-density mafic and ultramafic rocks, thick Neoproterozoic terrigenous sediments and a Palaeozoic sequence. The Rhenohercynian suture can be traced from eastern Germany in the NVD to southern Portugal in the SVD following outcrops of mafic rocks and corresponding high-density subsurface bodies. The Gondwana-derived succession of the Autochthon and Parautochthon shows a remarkably similar gravity signal of intermediate to high-density Proterozoic rocks along the whole belt.

Low-density rocks (**Fig. 15**) are widespread across the internal zones of the Variscan belt, but they significantly differ in age along the strike. In the NVD, they are mainly Neoproterozoic to early Carboniferous in age corresponding to either gneisses or felsic granulite bodies, while in the CVD and SVD they represent Cadomian, Cambro-Ordovician, Carboniferous, and early Permian granites. The distribution of granites only vaguely follows the structural trends of the Variscan belt, being in some places clearly discordant. The arrangement of magmatic intrusions can be further detailed based on magnetic anomalies. These anomalies (**Fig. 16**) form two belts broadly aligned to the core of the Variscan orogen. The more external belt correlates with the superposition of two magmatic arcs, Cadomian to Cambro-Ordovician (Bandrés et al., 2004; Linnemann et al., 2008; Sánchez-García et al., 2014) and Rhenohercynian (Edel et al., 2013). The latter is represented by the early Carboniferous granodiorites and diorites cropping out in the Odenwald and Vosges Mountains. The belt continues to the west underneath the English Channel and crops out in the Léon Unit in the form of Carboniferous granitoids (Faure et al., 2010). Finally, the belt reappears across the Ossa-Morena Zone/South Portuguese Zone limit including early Carboniferous diorites granodiorites and metabasites (Pin et al., 2008; Azor et al., 2008, 2009; Pin and Rodríguez, 2009). These rocks are related to the closure of the Rhenohercynian Ocean and form the so-called Rhenohercynian arc. The internal belt continues from the Bohemian Massif in the NVD to the Mont du Lyonnais in the CVD (Baptiste et al., 2016). The belt comprises Upper Devonian to early Carboniferous gabbros, tonalites and granodiorites of the Central Bohemian Plutonic Complex in the NVD and andesite to andesitic basalt volcanic sequences in the southern Schwarzwald, Vosges and Brévenne Units. These igneous rocks are interpreted to reflect magmatic arc activity related to the late Devonian-early Carboniferous subduction of the Mid-Variscan or Saxothuringian Ocean (Martínez Catalán et al., 2021), and form the so-called Saxothuringian arc. It includes the Devonian tonalites of Limousin units, the Brévenne ophiolite and the Morvan arc.

A more internal group of magnetic anomalies defining perfectly the Ibero-Armorican Arc include the Variscan granitoids and migmatites in NW and Central Iberia, but also other magnetic sources in the Ediacaran and Palaeozoic metasediments.

7. Interpretation of seismic reflection and refraction data

This section includes a discussion on the meaning of the types of reflectors identified to the scale of the Variscan belt. The NVD, CVD and SVD show the contrasting seismic structure of the Variscan orogen, which is interpreted in terms of three main Variscan suture systems. Moreover, a subsection presents a P-wave velocity model of the transition between the Variscan belt and the East European Craton.

7.1. Seismic structure of the NVD

In the NVD three parallel southeast dipping belts of A-type reflectors spatially coincide with relics of three fossil subduction zones. The northernmost belt corresponds to the Rhenohercynian subduction system that is constituted of highly reflective oceanic crust overlain by an accretionary wedge progressively thickened towards the SE (**Fig. 11a**, DEKORP-2N). This is coherent with the velocity structure derived from seismic refraction data (profiles (7) to (9) in **Fig. 12** (location in **Fig. 2**), which show a progressive thinning of the cratonic Avalonia crust towards the SE. Avalonia thinning is compensated by thickening of the Rhenohercynian accretionary wedge as imaged by profiles (4), (5) and (9).

The A-type reflectors present in the ECORS-DEKORP, DEKORP-2S and Boh9HR profiles can be correlated with Variscan subduction systems. The best line is represented by the seismic reflection profile Boh9HR (Tomek et al., 1997) (**Fig. 2**). This 200 km long and NW–SE striking line starts at the southern part of the Saxothuringian domain, and crosses successively the TBZ, the Central Bohemian Pluton (CBP), high grade gneisses, migmatites and granulites of the Moldanubian Zone and terminates before reaching the Central Moldanubian Pluton (CMP). The line shows two parallel SE dipping reflective horizons. The south-eastern belt coincides with the outcrop of eclogite-bearing wedge of Devonian age in the Mariánské Lázně Complex (**Fig. 10**, profile Boh9HR). This belt represents a testimony of the Mid-Variscan Ocean suture (Martínez Catalán et al., 2021). The other belt of A-type reflectors, located farther NW, is interpreted as reflections of subducted continental lithosphere of the Saxothuringian plate dated at 350-340 Ma (Konopasek et al., 2019; Martínez Catalán et al., 2020). The zone between the two belts in **Fig. 10** (Boh9HR) corresponds to a layer of partially molten granulitic crust extruded back over the continent

(Schulmann et al., 2009, 2014). Structurally above the south-eastern upper reflective layer, the crust of the Teplá-Barrandian Zone is highly reflective. It is characterised by bending of highly reflective horizons with a mean wavelength of 30 km.

The Moldanubian upper crust shows alternations of NW and SE dipping A-type reflective belts (**Fig. 10**) which corresponds to compressive fabrics and upright folding related to extrusion of deep crustal relaminant (Franěk et al., 2011; Maierová et al., 2021). This pattern is best represented by the southernmost part of the profile where moderately southeast-dipping reflective A-type layer mark thrusting of the Gföhl Unit granulite body over mid-crustal rocks. The Moldanubian section shows a highly reflective middle crust represented by the subhorizontal highly reflective bands of B and C types at approximately 18 km depth. This strong mid-crustal reflectivity was interpreted as a result of crustal flow separating deep infrastructure from the supra-structure (Maierová et al., 2016, 2021). The lower crust shows east-dipping reflectors in the northwestern part of the profile interpreted as remnants of A-type reflectors corresponding to the elevated Devonian and possibly also Carboniferous cryptic sutures (Schulmann et al., 2014), while the principal part does not show a clear seismic fabric. The whole crustal section at the southeastern extremity of the profile is relatively transparent.

The whole structure of the three successive subduction systems is also imaged by the ECORS-DEKORP profile where three parallel and SE dipping horizons of A-type reflectors were identified (Edel and Schulmann, 2009). The nature of the Allochthon is revealed by both seismic reflection and refraction profiles, as seen in **Figs. 11a** and **12**, reflection profiles Boh9HR and DEKORP-2S and velocity sections of refraction profiles (3), (4) and (5) respectively. Profiles (1) to (7) in **Fig. 12** show that the TBZ and MZ are both characterised by low-velocity crust down to the Moho or nearly so, which is a unique feature of the Variscan belt. The underthrust Saxothuringian margin can be traced beneath the TBZ crust and possibly also the MZ crust (**Fig. 11a**, DEKORP-2S).

7.2. Seismic structure of the CVD

In the CVD, the sections SWAT-2-3, SWAT-6-7, SWAT-9 and SWAT-10 image the structure of the Variscan front in UK, the Lizard ophiolite (Lo) and the Rhenohercynian wedge beneath the English Channel respectively (**Fig. 11b**). The SWAT-2-3 line reveals a belt of A-type reflectors marking the boundary of the Avalonian basement to the north and the diffuse A-Type reflector to the south marking internal imbrications of the Variscan front. The lower crust beneath the Variscan front is characterised by the presence of both B- and C-type reflectors that can represent late Carboniferous to early Permian extensional fabrics

reactivating the structure of the Rhenohercynian wedge in SW England (Alexander et al., 2019). This pattern is even more pronounced in the southern SWAT-6-7 and SWAT-9 and SWAT-10 lines, which reveal a strong south-dipping band of A-type reflectors coinciding with the Lizard suture (**Fig. 11b**). An important belt of A-type reflectors in the SWAT-10 line can result from accretion of the sedimentary wedge beneath the Armorican upper plate. Here, B-type reflectors were already observed by Alexander et al. (2019) and interpreted as late Carboniferous to early Permian extensional faults. The ARMOR-2 line crosscuting the boundary between the CAD and southerly nappe stack of the SAD, shows a complex seismic pattern (**Fig. 11b**). The southern part of the SAD reveals the presence of two thick horizons of south-dipping A-type reflectors probably marking the boundary between the UGU and LGU, and the LGU and Parautochthon (PAU), respectively (Gapais et al., 2015). Important N- and S-dipping B-type reflectors mark the boundaries of the Champtoceaux and Bois de Céné HP units and can correspond to major detachment zones along which deep crustal units are exhumed to the south and north. Here, the lower crust near the Moho shows extreme reflectivity marked by the dominant presence of C-type reflectors indicating important lower crustal flow. Altogether, the seismic structure of this domain is compatible with late Carboniferous c. 300 Ma extensional deformation affecting the partially molten crust of the PAU (Cagnard et al., 2004; Gapais et al., 2015). Finally, the NE-SW trending line ECORS-NFr is orthogonal to the Bray fault which separates the Armorican crust from the Rhenohercynian type crust (**Fig. 11b**). The profile shows the presence of A-type reflectors and moderate presence of B- and C-type reflectors in the Armorican crust, which is compatible with the early Carboniferous shortening characteristic of the NAD. The Rhenohercynian-type crust shows typical SW-dipping A-type reflectors and dominance of B-type reflectors in the middle crust, as well as important reflective horizons in the lower crust, both compatible with extensional tectonics.

7.3. Seismic structure of the SVD

In the SVD, profile ESCIN-1 across the Cantabrian Zone (CZ) images the foreland thrust belt by a series of reflectors that continue in the adjacent WALZ to the west (**Fig. 11c**). In this case, west-dipping (A-type) and horizontal reflectors correspond to Palaeozoic sedimentary packages bounded by a set of imbricated thrust faults (Pérez-Estaún et al., 1994, 1995). In the E, A-type reflectors occur mainly in the upper crust, imaging the thin-skinned imbrication of the Palaeozoic sequence. In the W, imbrication occurs in the middle crust, where A-type reflectors represent the imbrication of lowermost Paleozoic, Ediacaran a possibly previous crystalline basement. The crust is relatively thick (36 km) compared to

other parts of the Iberian Massif (**Fig. 4**), reflecting moderate thickening by thin-skinned tectonics and the absence of re-equilibration due to gravitational collapse. The lower crust is also thick (10-11 km) and poorly reflective in the CZ, probably little modified since the Cadomian or previous events (Ayarza et al., 2021a). In the W, under the WALZ, E-dipping reflections are common in the lower crust of the Narcea Antiform, probably also reflect an inherited structure.

Profile ESCIN-3 was acquired offshore in the Galician continental platform, and consists of three parts. ESCIN-3.1 provides an image of the accretionary prism of Alpine subduction of the Bay of Biscay oceanic crust (Álvarez-Marrón et al., 1995, 1996), and is not described here. ESCIN-3.2 and ESCIN-3.3 crosses the internal zones of the Iberian Massif, and are described in Álvarez-Marrón et al. (1995, 1996), Martínez Catalán et al. (1995) and Ayarza et al. (1998). Together with ESCIN-1, they provide a nearly complete seismic image of the northern section of the Iberian Massif (**Fig. 2**). Below a Meso- and Cenozoic sedimentary cover characterised by horizontal to low dipping reflections, the upper crust is poorly reflective except in a few parts where A-type events reflect imbricated thrust sheets in the WALZ (**Fig. 11c**). W- and E-dipping reflections in the lowermost upper crust are interpreted as B-type extensional features. The Mid-Variscan Allochthon, which inland would correspond to the uppermost crust of ESCIN-3.2, is not imaged, either due to its structural complexity or because it was eroded. B-type reflectors characterise the lower crust, which is very thin in ESCIN-3.2 and thick in ESCIN-3.3. In the latter, the lower crust includes two reflective packages, the lower of which is interpreted as part of the CZ basement underthrust under the WALZ lower crust (Ayarza et al., 1998; Martínez Catalán et al., 1995, 2018).

While Variscan crustal thickening was moderate in the CZ, increased westward, being large in the western WALZ and CIZ and maximum in the GTMZ, the area is covered by the Mid-Variscan Allochthon (Martínez Catalán et al., 2014). Subsequent thermal relaxation induced late Variscan crustal re-equilibration (Alcock et al., 2015), accompanied by voluminous felsic plutonism, which is probably the cause of the poor reflectivity in the upper crust. In ESCIN-3.2, a couple of dipping reflections in the mantle probably represent a frozen image of delamination during crustal re-equilibration.

The ALCUDIA and IBERSEIS seismic profiles cover the SW half of the Iberian Massif (**Figs. 2** and **11c**). They cut across a little deformed crust in the Central Iberian Zone (CIZ) and one or two sutures bounding the strongly deformed Ossa-Morena (OMZ) and South Portuguese (SPZ) zones, respectively. In ALCUDIA, weak NE and SW-dipping A-type reflections in the upper crust represent the limbs of upright folds affecting Ediacaran and

Palaeozoic low-grade metasediments. In the SW part of the profile, NE-dipping reflectors can be followed from the surface to the Moho, imaging the contact between the CIZ and OMZ, a possible Variscan suture (Martínez Poyatos et al., 2012; Ehsan et al., 2014). C-type horizontal reflections are abundant in the lower crust, which is rather thick, up to 16 km after Ayarza et al. (2021a). These authors interpret the lower crust as essentially pre-Variscan, in accordance with the moderate Variscan crustal shortening and thickening along most of the profile. Thinning of the lower crust at the NE end of the ALCUDIA profile coincides with the outcropping of the Toledo gneiss dome, and is interpreted as evidence of significant crustal re-equilibration in this part of the profile, close to the Spanish Central System, where Variscan thickening was severe and granitoids abundant and voluminous (Andrés et al., 2019).

In the IBERSEIS profile, NE-dipping A-type curved reflections in the upper crust represent listric thrust faults identified at the surface in the OMZ and SPZ. They cut across the metasedimentary and volcanic rocks of Ediacaran to Carboniferous age and the underlying basement, merging downward into a nearly horizontal mid-crustal detachment. This feature, well identified in the SW part, continues to the NE as a lens-shaped area of high reflectivity interpreted as an early Carboniferous intrusion of mafic rocks (Simancas et al., 2003). Below the mid-crustal detachment, a thick and very reflective band represents the lower crust. There, SW-dipping reflections dominate in the SW while in the NE they alternate with NE-dipping events.

A-type reflectors in SW Iberia can be interpreted as reflecting the Rhenohercynian subduction and underthrusting of the Avalonia basement, as in the Rhenish Massif and the southern British Isles (**Fig. 11**, profile IBERSEIS, SWAT 2-3, DEKORP 2N). This image is in agreement with seismic reflection data indicating Avalonia crust beneath the OMZ, as seen in **Fig. 12**, refraction profiles (12) and (13) in the SVD or along refraction profile (9) in the CVD and (7) and (8) in the NVD. The inclined lower crustal reflections overprint previous subhorizontal ones and merge upward with the mid-crustal detachment. In the SVD, Ayarza et al. (2021a) interpreted them as imaging normal faults in an extended continental margin subsequently inverted during Variscan convergence. The margin would be that of Avalonia, according to zircon inheritance in late Palaeozoic sediments (Braid et al., 2011; Pereira et al., 2014; Rodrigues et al., 2015).

7.4. Tectonic significance of A, B and C type reflectors

The A-type reflectors mark events related to the Rhenohercynian subduction in all parts of the Variscan), and the Saxothuringian and Mid-Variscan oceanic subductions. In addition, these reflectors represent the associated distributed deformation of both lower and

upper plates related to Devonian subduction and early Carboniferous collision. Similar reflectors are also present in the Rhenohercynian wedge and farther north at the Variscan front. There, the Devonian normal faults were inverted producing south dipping A-type reflectors parallel to the Rhenohercynian suture (Ayarza et al., 2021a; Alexander et al., 2019).

The B-type reflectors originated during mid-late Carboniferous extension and the melting of the crust manifested by the presence of extensional gneiss domes and syntectonic granitic intrusions across the central part of the Variscan belt (e.g., Faure, 1995; Faure et al., 2009; Martínez Catalán et al., 2014; Žák et al., 2014). This extensional deformation affected the northern and central parts of the CIZ in the SVD, the FMC in the CVD, and the MZ in the NVD and is documented in the Armorican Massif (Gapais et al., 2015), French Vosges (Edel and Schulmann, 2009), Bohemian Massif (Franěk et al., 2011) and Iberia (Simancas et al., 2003). The Rhenohercynian wedge also shows B-type reflectors that are interpreted as a result of the late Carboniferous extensional event (Alexander et al., 2019).

The C-type reflectors that are mostly grouped in the lower crust relfect horizontal flow of the lower crust during late- to post-orogenic equilibration of the crustal thickness following the maximum thickening. It was proposed that this process was related to Permian post-orogenic collapse (Costa and Rey, 1995; Artemieva and Meissner, 2012) that led to the convective removal of thickened root and the replacement by a mafic lower crust. However, the refraction data from both the Rhenohercynian accretionary wedge, the TBZ and the MZ crusts (**Fig. 11a,b** profiles (2) and (3)) reveal the presence of low velocity material across nearly the whole crust. This is in agreement with the fact that, where exhumed, the lower crust is mostly felsic to intermediate (e.g., Franěk et al., 2011; Chopin et al., 2012). The amount of crustal melting dated by granitic plutons suggests mid to late Carboniferous mobilisation of the felsic, buoyant and low-viscosity lower crust rather than Permian extension. However, exceptions occur at least in the CZ, the southern part of the CIZ and the SPZ of Iberia, where the crust was moderately thickened and escaped severe crustal re-equilibration. There, the laminated lower crust is mostly inherited from pre-Variscan events.

7. 5. P-wave velocity model of the East European Craton – Variscan belt transition

The transition between the Variscan orogen and the East European Craton (EEC) is deeply concealed beneath the Permian-Mesozoic Polish Basin. Therefore, the identification of the transition zone between the two domains entirely relies on geophysical and, to a lesser extent, borehole data. Initially, the concept of the Trans-European Suture Zone (TESZ) was introduced postulating a complex zone of terrane accretion to the SW margin of Baltica (e.g.,

Pharaoh, 1999). Eastern Avalonia was a primary candidate to be included in the TESZ (e.g., Winchester et al., 2002). However, the detection of the Baltica lower crust extending as far SW as the Dolsk and Odra Faults (Grad et al., 2002, 2003; Guterch and Grad, 2006; Guterch et al., 2010; **Fig. 17**) made this hypothesis less probable. Therefore, Grad et al. (2002) suggested that the entire section overlying the Baltica lower crust beneath Polish Lowlands is an Avalonian accretionary wedge. This concept, however, was not supported by provenance studies of the lower Palaeozoic sediments from Pomerania (Poprawa, 2006) and rheological considerations (Jarosiński and Dąbrowski, 2006). Therefore, according to the present state of the art the enigmatic domain underneath the Polish Basin represents an attenuated rifted margin of Baltica that is in direct contact with the Variscan domain in SW Poland (Mikołajczak et al., 2019; Mazur et al., 2021). This is consistent with the seismic analysis by Smit et al. (2016), who recognized an Avalonian accretionary complex in a deep substratum of the Palaeozoic Platform much farther to the west.

The transition from the EEC margin to the Variscan orogen is the best demonstrated by the POLONAISE'97 P4 wide-angle reflection and refraction (WARR) profile (**Fig. 17**; Grad et al., 2003). The crust continuing from the Sudetes (Bohemian Massif) across the Odra Fault up to the Dolsk Faut is a two-layer Variscan crust, characteristic of the Bohemian Massif, with low P-wave velocities down to the Moho (6.6 km/s). This is confirmed by the presence of low-grade metamorphic metasediments with a latest Devonian cooling age in the basement of the Wolsztyn Block (**Fig. 17**; Mazur et al., 2006). In contrast, the crust of the EEC is a typical thick cratonic crust with a three-layer velocity structure. The transitional domain between the Dolsk Fault and the Teisseyre-Tornquist Zone (TTZ), corresponding to the area of the Polish Basin, has a strongly attenuated three-layer crust with a lowermost layer representing a continuation of the reflective high-velocity Baltica lower crust (Grad et al., 2002, 2003; Guterch et al., 2010). Furthermore, the transitional domain is underlain by a high-velocity upper mantle (**Fig. 17**). Taking these features jointly with the lack of a tectonic suture along the TTZ (Mazur et al., 2015), the section between the TTZ and Dolsk Fault probably represents an attenuated Ediacaran rifted margin of Baltica (**Fig. 17**). The Dolsk Fault appears on the WARR as a sub-vertical feature (**Fig. 17**) suggesting a strike-slip contact between the EEC margin and the Variscan domain (Mazur et al., 2020). However, the geometry of the fault might be biased by the type of seismic data presented and a thrust of the Variscan crust over the EEC margin cannot be excluded.

8. Discussion

In this section, the relationships between the geophysical data and the main features of the European Variscan belt recently summarized by Martínez Catalán et al. (2021) are discussed. The position of main sutures, magmatic arcs and allochthonous systems are considered in the light of seismic reflection and potential field data presented in this paper. These data allow proposing a new map of the Variscan orogen, which shows the position of the main Devonian and Carboniferous sutures, the magmatic arcs and the extent of the Mid-Variscan Allochthon, while a new supra-subduction Devonian basin is defined (**Fig. 18**). The nature, origin and extent of the "Variscan" orogenic crust is discussed on the basis of existing seismic reflection and refraction data, long-wavelength gravity anomalies and tectonic setting of the Carboniferous magmatic province developed along the axis of the Variscan orogeny (**Fig. 19**). Finally, the Permian modifications of the large-scale Variscan orogenic architecture are discussed based on the shape of geophysical lineaments and their perturbation.

8.1. Geophysical characteristics of suture zones and magmatic arcs

The European Variscan belt is a unique orogen that is covered by comprehensive sets of seismic and potential field data. The combination of both allows for a new interpretation of structure and evolution of the European Variscides. The important outcome of gravity and magnetic study is the identification of a high density and high susceptibility belt that separates the Saxothuringian basement from the RPZ upper plate and the CAD from the French Massif Central (**Fig. 18**). In addition, seismic profiles and published gravity and magnetic models of the sections crossing the NVD (Poh9HR, DEKORP-2S, ECORS-DEKORP, **Fig.11a**) show two parallel and south dipping belts that correspond to zones of primary seismic reflectors (A-type reflectors) associated with dense bodies dipping SE at a moderate angle (cross-sections A and B, **Fig. 18**). This feature is further supported by dip direction of deap seated gravity anomalies indicated by the successive upward continuations of the second vertical derivative (**Figs. 5e and 13**) which generally coincide with locations of main sutures. Here, the southern belt of reflectors confirms the presence of a major suture zone between the Saxothuringian domain and the Mid-Variscan Allochthon predicted by geological surveys (e.g., Schulmann et al., 2009, 2014; Martínez Catalán et al., 2020, 2021). The suture itself is a remnant of the Mid-Variscan Ocean (e.g. Ediacarian to Early Ordovician oceanic lithospheres, Ackerman et al., 2020; Colett et al., 2022) that was closed at Middle Devonian times as testified by ages of ophiolites and eclogites (400 – 390 Ma, Collett at al., 2018; Brueckner and Medaris, 1998; Awdankiewicz et al., 2021). In addition, the profile ARMOR-2 in the CVD also crosses the Mid-Variscan suture between CAD and French Massif Central (Bitri et al., 2003, 2010; Gapais et al., 2015).

In the NVD, the seismic and potential field data also jointly reveal a second suture represented by the second belt of seismic A-type reflectors, located NW and parallel to those reflecting the hangingwall Mid-Variscan suture (**Figs. 10 and 11a**). This reflector is located above the high-velocity and high-density zone representing deeply subducted continental margin of the Saxothruringian block beneath the Mid-Variscan Allochthon in the NVD. This deep continental subduction was dated between 350-340 Ma (e.g., Konopásek and Schulmann, 2005; Konopásek et al., 2019). The low-velocity and low-density zone between both belts of reflectors was formed due to back flow of the previously subducted Saxothuringian crust (e.g. Schulmann et al., 2014; Maierová et al., 2021). The consequence of deep subduction of the Saxothuringian continental crust is its sub-lithospheric relamination beneath the Mid-Variscan Allochthon followed by the formation of HP granulite diapirs that penetrated the whole upper plate lithosphere (Maierová et al., 2021). These low-density diapiric bodies are characterised by gravity lows (**Fig. 7**) and their shape was imaged both by seismic (Franěk et al., 2011) and gravity data (Chopin et al., 2012).

A third major suture, defined mainly by seismic and magnetic data, is located farther NW in the NVD and CVD or in the SW part of the SVD (profiles SWAT-9 and ARMOR-1 for the CVD and IBERSEIS for the SVD) and corresponds to the Rhenohercynian suture (**Fig. 18**). In the SWAT 2-3, DEKORP 2N profiles (**Fig. 11b**) and farther NW occurs another SE dipping more diffuse reflector zone that characterises thrusting of the Rhenohercynian basinal sequences, including the Lizard and Giessen ophiolites, atop the Avalonian basement in SW England (profile SWAT-9) and Germany (profile DEKORP 2N). These features are various manifestations of the oceanic suture developed due to late Devonian to early Carboniferous closure of the Rhenohercynian Ocean (Franke 2000; Shail and Leveridge, 2009; Simancas et al., 2005; Sintubin et al., 2009).

The Mid-Variscan and Rhenohercynian subduction systems have another manifestation through the presence of the Mid-Variscan and Rhenohercynian magmatic arcs (**Fig. 18**), which are expressed by two belts of prominent magnetic anomalies (**Fig. 16**) and represent an excellent proxy for the polarity (E-SE in NVD and CVD, NE in southern SVD in present-day coordinates) and timing of both subduction systems. The ages of arc-type granitoids (gabbros, tonalites, granodiorites) associated to the above-mentioned magnetic highs indicate short-lived subduction of the Rhenohercynian Ocean (340-330 Ma; Zeh and Gerdes, 2010) and long-lasting subduction of the Mid-Variscan Ocean (380-340 Ma, Deiller et al., 2021). This contrast in duration of both arcs activities is also consistent with the

contrasting ages of oceanic lithospheres involved in the Rhenohercynian and Mid-Variscan oceanic subduction systems.

8.2. Geophysical characteristics of the Mid-Variscan Allochthon

Another major outcome of this study are the complex and heterogeneous geophysical characteristics of the Mid-Variscan Allochthon. In the CVD and SVD, the Allochthon is represented by scattered and isolated bodies of high-density rocks (eclogites, ophiolites) while this pattern is missing in the NVD (**Fig. 18**). In the latter, it is represented by a low velocity domain and long wavelength gravity low represented by the Moldanubian Zone and by a gravity high corresponding to the high-density Neoproterozoic TBZ (e.g., Guy et al., 2011; Chopin et al., 2012). Another specific feature of the NVD part of the Moldanubian Zone is the presence of short wavelength gravity lows matching the early Carboniferous high-pressure granulites and gravity highs associated with the high-density ophiolitic bodies. Consequently, the Mid-Variscan Allochthon can be defined as a laterally evolving body that does not have any seismic signature in the SVD and only minor in the CVD (cross-sections C and D, **Fig. 18)**. This first-order geophysical observation corroborates the contrasting CVD and NVD geological characteristics as presented by Lardeaux et al. (2014). The thickness and composition of this body change from the NE, where it is represented by a 30 km thick continental crust, to the SW where the crust of the Allochthon is a few kilometres thick and includes mainly high-density mafic material. In detail, some CVD and SVD allochthonous units show continental character such as the Mauges Unit in France (Ballèvre et al., 2014) or gneisses included in the Upper and Lower Allochthons in Iberia, but the Middle Allochthon in the CVD and SVD is geophysically defined mainly by oceanic rocks.

The central part of the Mid-Variscan Allochthon includes Devonian supra-subduction volcano-sedimentary basinal (both fore-arc and back-arc) sequences (**Fig. 18**) rimmed by the Vosges, the Morvan arc and the Brevenne back-arc ophiolites (Pin and Paquette, 1997; 2002; Skrzypek et al., 2012b). These rocks are characterised by NE-SW trending moderate gravity and magnetic highs, the latter being in direct continuity with magnetic anomalies of the Saxothuringian arc further east (**Fig. 16**). This large late Devonian supra-subduction basin and the Mid-Variscan arc together represent a prominent but overlooked feature of the Mid-Variscan Allochthon, which is very important in the central and north-eastern part of the belt but progressively vanish to the west.

A number of studies demonstrated that geophysical lineaments are the expression of deformation (Molnar, 1984, 1988; Goleby et al., 1989; Burtman and Molnar, 1993; Klemperer, 2006). The gravity and magnetic lineaments presented in our study, both deep and

shallow, are uniformly spaced and oriented parallel to the structural grain of the Variscan belt (**Fig. 13**). It is important to note that the main elongated gravity highs in the autochthonous zones such as CIZ, OMZ and STZ and in the Mid-Variscan Allochthon, are stretched along-strike the whole Variscan belt (**Fig. 14**). This is valid for lineaments deduced from both short and long wavelength anomalies. These features indicate that a large part of the structure of the belt was acquired after the emplacement of the Mid-Variscan Allochthon above the Gondwana crust and is largely related to late-Variscan transpressional tectonics (Martínez Catalán et al., 2021). Therefore, the geophysical lineaments reflect the deformation not only related to the Devonian emplacement of the Allochthon but mainly to the Carboniferous collisional episode and subsequent dextral transpression (Edel et al., 2018).

8.3. Origin, nature and extent of the Variscan orogenic crust

The geophysical data further show that the Variscan belt is shaped by a mosaic of variously reworked cratonic domains usually characterised by high seismic velocities and long wavelength gravity anomalies. These autochthonous domains include lozenge shaped Avalonia, Baltica in the NE, Brunia and Vindelicia in the SE, and Gondwana in the south. We also recognise transitional zones of reworked continental basements corresponding to the entire Saxothuringian Zone and attenuated Baltica margin in the NVD and the northern part of the Gondwana crust in the SVD (**Fig. 19**). Three types of crust can be identified: 1) the cratonic crust rimming the core of the Variscan orogen represented by high-velocity thick lower crust (up to 20 km) and long wavelength gravity highs, 2) the transitional crust developed mainly beneath the STZ, NAD and CIZ, characterised by high-velocity lower crust up to 10 km thick, and middle-upper crust displaying moderately deformed and thickened crust, and 3) the "Variscan" orogenic crust beneath the axial part of the orogen in the NW and central Iberia in the SVD, FMC in the CVD and the TBZ and MZ in the NVD, represented by thin or absent high velocity lower crust and low velocity middle-upper crust (Artemieva and Meissner, 2012) associated with long wavelength gravity lows (Guy et al., 2011; Chopin et al., 2012; Schulmann et al., 2014).

The map of crustal domains (**Fig. 19**) shows that the "Variscan" orogenic crust coincides with a zone of major mid to late Carboniferous magmatic activity that affected both the autochthonous and allochthonous domains of the entire central part of the Variscan belt (**Fig. 15**). This event was related to a major extension and simultaneous mobility of dextral strike-slip faults active at that time as transfer faults (Iglesias Ponce de León and Chokroune, 1980; Martínez Catalán et al., 2014; Edel et al., 2018). Carboniferous extension is also manifested by the seismic B-type reflectors and by short-wavelength negative gravity (-5 to -

20 mGal) and magnetic anomalies, corresponding to intrusive bodies of meta- and per-aluminous granites dated at 335 to 310 Ma (**Fig. 15**). In these areas, extensional reflectors and associated gravity lows are in continuity with surface extensional detachments along which a number of intrusions are syntectonically emplaced (Faure, 1995; Be Mezeme et al., 2007; Faure et al., 2009; Edel et al., 2013; Martínez Catalán et al., 2014, Verner et al., 2014; Žák et al., 2013, 2014). In contrast the late to post-tectonic granites dated at 305 to 290 Ma in the CVD and SVD do not coincide with negative gravity anomalies (**Fig. 15**). In particular, the giant Velay dome (V) in the FMC does not show any gravity signature and is probably formed only by a narrow sheet of anatectic granite parallel to the Pilat detachment (Malavieille et al., 1990; Lardeaux et al., 2014), and thus cannot be interpreted as a deeply rooted "migmatitic core complex" (Vanderharghe et al., 2020). An enigmatic highly reflective lower crust with C-type reflectors is present everywhere in the Variscan belt irrespectively of the composition of the lower crust. This signature can partly correspond to layered intrusions of mafic rocks, referred as seismic lamellae (Behr and Heinrichs, 1987; Mooney and Meissner, 1992), in the SVD and CVD (e.g. Pin and Vielzeuf, 1983) and deformation of deep crustal granulite facies felsic rocks in the NVD (Guy et al., 2011; Schulmann et al., 2014).

The origin of the Variscan crust is a result of two competing processes that evolved along-strike the orogen. The first one corresponds to early Carboniferous thickening of the Mid-Variscan Allochton continental upper crust in the NVD associated with gravity exchanges between the generally felsic lower plate relaminant and the denser upper plate continental rocks with mafic lower crust (Maierová et al., 2016; 2021). The density reversal led to the formation of middle and upper crust that was dominantly felsic, and a relatively thin lower crust that is formed by mafic, probably eclogitic material. By analogy to the Tibet, Maierová et al. (2016) further proposed that the middle – upper crust should be characterised as a low velocity zone and only deep orogenic infrastructure may contain a high-velocity and high-density layer. In the CVD and SVD the Allochthon was relatively thin even if it incorporated parts of the hyper-extended margin of the Gondwana (the Lower Allochthon and Parautochthon, Lardeaux et al., 2014) and its overthrusting induced thickening of the relative autochthon (CIZ and WALZ in Iberia, SAD and Montagne Noire in France) resulting in the generalized Barrovian type Carboniferous metamorphism followed by partial melting of these units (Lardeaux et al., 2014; Alcock et al., 2015). Here, no density reversals developed thanks to a small thickness and low heterogeneity of the locally high-density upper plate precluding the development of Rayleigh-Taylor instability (Gerya et al., 2002; Lexa et al., 2011). However, in both NVD and CVD-SVD parts of the belt, the thickening of the Allochthon and

Autochthon potentially doubled the original crustal thickness in the internal zones of the orogen.

This collisional period was followed by the second process marked by large-scale lithospheric extension associated with widespread magmatism that affected the whole belt between 330 – 310 Ma (**Fig. 15**). The whole Variscan belt was stretched and thinned in the NE-SW direction parallel to the Laurussia margin during giant 2000 km long westward movement of the Gondwana block (Edel et al., 2018). The thickened crust of the internal part of the orogen was thinned to its original thickness or more, while cratonic blocks were merely rearranged in a new plate configuration imposed by a mutual displacement of Laurussia and Gondwana continents. It was the lithospheric thinning associated with an elevated asthenosheric heat flux (e.g. Casini et al., 2015) that was responsible for widespread melting of the crust in the core of the Variscan orogen. The ultimate result of Carboniferous thinning and widespread crustal melting was the development of anomalous structure of the Variscan crust, marked by highly reflective and low-velocity thin lower crust, representing remnants of thinned eclogitic lower crust, and thick low-velocity and low-density middle and upper crust. The synthesis of P-waves velocity logs shows that the lower Variscan crust does not exceed values < 6,7 km/sec (**Fig. 15**). Consequently, this lower crust has to be composed mainly of felsic to intermediate granulites and not of mafic material (Rudnick and Fountain, 1995). High reflectivity of the lower crust of the Moldanubian domain was interpreted by high- and low-velocity lamellae (Mooney and Meissner, 1992) that can be due to lithological (mafic intrusions) and metamorphic-tectonic layering (Artemieva and Meissner, 2012). It is a general consensus that anomalously reflective lower crust results from extensional tectonics either associated with intrusion of thick gabbroic sills (Simancas et al., 2003) or thanks to stretching and lower crustal horizontal flow of Tibetan type eclogite-granulite root. The Variscan middle and upper crust is formed by low velocity gneissic material of standard density intruded by voluminous low-density granitoids. The irregular shape of the Variscan belt, defined by both geophysical data and the extent of the Carboniferous magmatic province, was controlled by the shape of Laurussia (Avalonia and Baltica) and Gondwana (Vindelicia) promontories which activated major wrench shear zones exploited by magmatic intrusions such as the dextral South Armorican Shear Zone (Rolin et al., 2009), the Danubian magmatic belt (Finger et al., 2009) or the sinistral Upper Rhine Graben Fault (Edel et al., 2007).

In contrast to the suggestion of Artemieva and Meissner (2012), we propose that the Permian extensional event was potentially less important in the development of the geophysical character of the Variscan crust. This event was obviously associated with

magmatism and crustal thinning that both were heterogeneously distributed along-strike the belt and particularly in the Western Alps (Lardeaux and Spalla, 1991; Spalla et al., 2014) and Permian basin in NE Europe (Petri et al., 2017). However, in the core of the Variscan belt there is no significant Permian mafic magmatic activity. In the latter, more important is the activity of strike-slip faults that affected the continuity of lineaments and re-activated the network of existing deep-seated Carboniferous discontinuities (Arthaud and Matte, 1977; Edel et al., 2018). Thus the origin and nature of the Variscan lower crust is the result of Carboniferous tectonic processes.

9. Summary

This study presents a continental-scale synthesis of geophysical data (namely gravity, magnetic and seismic data) covering the European Variscan belt. The analyses of these independent and complementary datasets combined with consistent geological interpretations of the different domains of the belt result in a new interpretation of its crustal structures leading to a coherent and innovative large-scale tectonic model of one of the principal collisional systems on the Earth. The extent, nature and origin of the "Variscan" orogenic crust are characterized as follow:

- The location of the Mid-Variscan Allochthon and the Devonian Mid-Variscan and Carboniferous Rhenohercynian sutures are established. The regional extent of the Rhenohercynian arc together with Mid-Variscan and Saxothuringian arc – back arc basin systems are deduced from magnetic and partly gravity data, while a new supra-subduction Devonian basin is defined. The polarities of subduction systems based on geologically-geophysically constrained sutures confirm the non-cylindricity of the Mid-Variscan allochthon.

- The existence of three different types of the continental crust is demonstrated based on a systematic analysis of P wave logs of crustal segments forming the European Variscan belt: (i) cratonic crust marked by a thick, high velocity lower crust, (ii) transitional crust of reworked continental basements characterised by a relatively thin high velocity lower crust and intermediate velocity middle crust, and (iii) a thin Variscan orogenic crust defined by low to intermediate velocity lower and middle crust. These three types of crust are also characterized by large wavelength gravity anomalies ranging from large gravity high for the cratonic crust and gravity low for the Variscan crust.

- The specific "Variscan" orogenic crust originated by Carboniferous extensional thinning and extensive melting of previously thickened "Tibetan" type crust. During the early

Carboniferous, the Mid-Variscan Allochthon continental upper crust emplaced over the autochthonous crust of Gondwana that was previously thickened during Devonian subduction event. This collisional event was mainly in the North-eastern Variscan Domain associated with gravity exchanges between the generally felsic lower plate relaminant and the denser upper plate continental rocks of the Mid-Variscan Allochthon. This collisional period was followed by a large-scale lithospheric extension associated with widespread magmatism that affected the axial part of the Variscan belt between 330 – 310 Ma. On the other hand, the Permian c. 300 – 280 Ma extensional event is restricted to marginal parts of the orogen and was potentially less important in the development of the geophysical character of the Variscan crust.

Acknowledgments. The research for the Iberian Peninsula has been funded by project PID2020-117332GB-C21 of the Spanish Ministry of Science and Innovation, and by research projects SA065P17 and SA084P20 of the regional government Junta de Castilla y León. The Bouguer gravity anomaly data were downloaded from the Bureau Gravimétrique International (BGI), http://bgi.obs-mip.fr. Data of the aeromagnetic map of Spain are property of the Instituto Geográfico Nacional (IGN), www.ign.es/web/ign/portal. This study was supported by the Strategic Research Plan of the Czech Geological Survey-DKRVO/ČGS (2018-2022).

Figures Captions

Fig. 1. Early Permian reconstruction of the Variscan belt. **Variscan domains (VD):** CVD, Central; NVD, North-eastern; SVD, South-western. **Zones (Z):** CZ, Cantabrian; CIZ, Central Iberian; GTMZ, Galicia-Trás-os-Montes; MSZ, Moravo-Silesian Zone; MZ, Moldanubian; OMZ, Ossa-Morena; RHZ, Rhenohercynian; SPZ, South Portuguese; STZ, Saxothuringian; TBZ, Teplá-Barrandian; WALZ, West Asturian-Leonese. **Armorican Domains** (AD): CAD, Central; NAD, North; SAD, South. **Shear zones (SZ)**, **faults (F)** and **fault zones (FZ):** BBSZ, Baden-Baden; BCSZ, Badajoz-Córdoba; BrF: Bray; EFZ, Elbe; JPSZ, Juzbado-Penalva; LLSZ, Lalaye-Lubine; MT, Moldanubian Thrust; NASZ, North Armorican; NEF, Nort-sur-Erdre; NPF, North Pyrenean; PASZ, Posada-Asinara; Pf, Pfahl-Danubian fault system; PTSZ, Porto-Tomar; SASZ, South Armorican (N and S, northern and southern branches); SHF, Sillon Houiller; SISZ, Southern Iberian; SFS, Sudetic fault system; VF, Variscan Front. **Other:** MT, Moldanubian thrust; BM, Basque Massifs; CIA, Central Iberian Arc; Co, Corsica; FMC, French Massif Central; IAA, Ibero-Armorican Arc; Lo,

Lizard ophiolites; MTM, Maures-Tanneron Massif; MGCR, Mid-German Crystalline Rise; MN, Montagne Noire; Sa, Sardinia; SWM, Schwarzwald Massif; VM, Vosges Massif.

Fig.2. Location of seismic reflection profiles roughly orthogonal to the Variscan belt used in Figs. 10 and 11 (in pink). Blue: Transects roughly locating the refraction and wide angle seismic profiles from which a series of Vp/depth logs have been obtained (see Fig. 12).

Fig. 3. Maps of the gravity anomalies derived from the data set of the Bureau Gravimétrique International (http://bgi.obs-mip.fr), and including coast and massif limits (light blue, black), continental platform limits (white, dotted) as well as the main Variscan boundaries and faults (black, dashed). (a) Low pass filtered with wavelengths greater than 150 km. (b) Upward continuation to 2.5 km partially reflecting the main Variscan boundaries and faults. (c) Band pass filtered with wavelengths 450-150 km showing regional anomalies and mainly reflecting density variations of the intermediate crust. The effect of the Moho topography has been significantly reduced by the 450 km filter. The continuous white line indicates the limits on the continental side of the artefact induced by the oceanic/continental boundary. (d) Band pass filtered 250-25 km. The intermediate band pass is representative of the density variations in the upper crust. It shows the structure of the Variscan belt. Excepted young and thick recent basins, gravity lows in red are often associated with granites and meta granites. The gravity highs represent mafic or ultramafic magmatic rocks and in many cases also Neoproterozoic to early Carboniferous metasediments. (e) First vertical derivative imaging some important Variscan structures.

Fig. 4. Topography of the Moho derived from P and S waves seismic data. Compilation by: Dezes and Ziegler (2002, revised according to maps of the British Isles of Kelly et al., 2007), Iberia (Palomeras et al., 2017), Massif Central (Zeyen et al., 1997; Macquet et al., 2014), the Rhinegraben area (Edel et al., 2006), Belgium (Sichien et al., 2012) and the Bohemian Massif (Růžek et al., 2007).

Fig. 5. Example of maps used for the interpretation of geophysical anomalies. (a) Geological map. (b) Bouguer anomaly map. (c) First vertical derivative of the Bouguer map in colour with the isoline 0 of the second vertical derivative represented by a thin, black line. Discontinuities, i.e. boundaries, flexures and faults, are represented by white lines. (d) Tilt angle of the Bouguer anomaly. The negative anomalies (red) are associated with low densities,

while the positive anomalies (green) show bodies with higher densities. The 0 line (thin, black) shows the boundary of bodies with contrasting density, provided it is subvertical. The width of the white belt between red and green represents 2h, h being the average depth of the top of the bodies. Main discontinuities, boundaries and faults are underlined with dashed lines. (e) Zero lines of increasing upward continuations of the second vertical derivative. The upward continuations reflect the density contrasts. The shift of the 0 line indicates the sense of dip of the boundary. (f) Interpretative map showing 1- main boundaries of gravity bodies, 2- faults, 3- secant discontinuities: ductile wrenching zones, transcurrent faults, 4- magnetic discontinuities, 5- gravity and magnetic discontinuities, 6- axes of magnetic bodies. The map shows the main features within the upper crust, not necessarily the basement surface.

Fig. 6. Vertical derivative of aeromagnetic anomalies reduced to the pole of the three Variscan domains. Major Variscan boundaries and some faults are included. (a) North-eastern Variscan Domain. Assemblage of aeromagnetic maps of northeast France (Flight Altitude (FA) = 1200 and 1500 m; Edel and Schulmann, 2009), of digitized published maps of south Germany (FA = 1000 and 1500 m, Bundesanstalt für Bodenforschung und Rohstoffe, 1976; FA = 3000 m, Wonik and Hahn, 1990, Kosum and Wonik, 1991), north Austria (FA = 1400 m, Blaumoser, 1992), and the Czech Republic (FA = 500 m). Interpretative aeromagnetic maps for Germany (Gabriel et al., 2011) and the Polish platform (Wybraniec, 1999, Mikołajczak et al., 2019) are also taken into account. In order to homogenise the maps, those with FA = 3000 and 500 m have been recalculated for the level 1200 m which is the mean FA of the map. (b) Central Variscan Domain. Assemblage of aeromagnetic maps of France (FA = 3000, BRGM) and the Gulf of Gascogne (FA = 500 m, BRGM). Great Britain (FA = 305 and 152 m, British Geological Survey, 1998). (c) South-western Variscan Domain. Assemblage of aeromagnetic maps of Spain (FA = 3000, Ardizone et al., 1989) and Portugal (FA = 3000, Miranda et al., 1989). CZ, Cantabrian Zone; CIZ, Central Iberian Zone; GTMZ, Galicia-Trás-os-Montes Zone; KM, Krkonoše Massif; OMZ, Ossa-Morena Zone; Pi, Pilat detachment SM, Staré Město Belt; SPZ, South Portuguese Zone; WALZ, West Asturian-Leonese Zone; MAPB, magnetic anomaly of the Paris Basin.

Fig. 7. (a) Gravity anomalies in the band pass 200-7 km and contours of magnetic highs of the North-eastern Variscan Domain. (b) Interpretative geophysical map. BBS, Baden-Baden schists; Bf, Bavarian Fault; BFGm, Black Forest Gneiss mass; BG, Blanský les granulites; BLz, Badenweiler-Lenzkirch Zone; BR, Brunia; BR-MZ, Brunia basement

beneath Moldanubian nappe; CBP, Central Bohemian Pluton; CVgr, Central Vosges granite complex; Ef, Elbe Fault; EzM, Erzgebirge Massif; Ff, Frankenwald Fault; GSM, Góry Sowie Massif; Hu: Hunsrück; HuF, Hunsrück Fault; IzM, Izera Massif; KaP, Karlsbad Pluton; KC, Kutna Hora Complex; KP, Krkonoše Pluton; Kr, Kraichgau; LtO, Letovice ophiolite; Ly, Leszczyniec Complex; LzB, Lausitz Block; CMP, Central Moldanubian Pluton; MGCR, Mid-German Crystalline Rise; MgKg, Mg-K granites; MLC, Mariánské Lázně Complex; Mü, Münchberg Complex; MZ, Moldanubian Zone; NVAr, Northern Vosges arc; NVb, Northern Vosges basin; SO, Sudetic ophiolite; OdAr, Odenwald arc; OSD, Orlica-Śnieżnik dome; PdC, Podolsko complex; RbO, Rehberg ophiolite; RSZ, Rhinegraben shear zone; SP, Sobotka Pluton; SdP, Sudetic Pluton; SGr, Saxonian granulites; SSH, Saverne-Sarrebourg High; STZ, Saxothuringian Zone; StM, Stod Massif; SVAr, Southern Vosges Arc; TBZ, Teplá-Barrandian Zone; Vgn, Central Vosges gneisses; VL, Vindelicia; ZB, Zelezny Brod.

Fig. 8. (a) Gravity anomalies in the band pass 200-7 km and contours of magnetic highs of France. (b) Interpretative geophysical map of the Central Variscan Domain. The gravity legend accounts for the interpretation of the anomalies, while the zone legend shows in lighter colours the zonation of the Variscan belt only in the outcropping massifs (white when covered). Ab, Ancenis basin; Baum, Baie d'Audierne ultramafics; BF, Bray fault; BLZ, Badenweiler-Lenzkirch zone; Bvon, Prevenne ophiolite; CAq, Central Aquitanian zone; ChcCU, Champtoceaux Complex Unit; Cmv, Cambrian volcanics; CVgr, Central Vosges granite complex; Ggr, Gueret granite; GTPU, Génis-Thiviers-Payzac Unit; HAU, Haut-Allier units; HuF, Hunsrück fault; Lgn, Léon gneiss nappes;; Lgr, leucogranite; LIMU, Limousin units; LvOg, Lanvaux Orthogneiss; Malz, Maures internal zone; MAPB, Magnetic Anomaly of the Paris Basin;; Mgg, Margeride granite; MLU, Monts du Lyonnais; MNmi, Montagne Noire migmatites; MvAr, Morvan Arc; MVgr, Morvan-Vosges granites; Migr, Millevaches granite; Mvgr, Morvan granites; NAJU, Najac units; NASZ, North Armorican Shear Zone; Agr, Aigurande granites; NVAr, Northern Vosges Arc; NVb, Northern Vosges basin; Ogr, Ordovician granites; PAU, Parautochthon Unit; RSZ, Rhine Graben Shear Zone; SAq, South Aquitanian zone; SASZ-N, South Armorican Shear zone-N; SASZ-S, South Armorican Shear zone-S; SBCmv, Saint-Brieux Cadomian metavolcanics; SMCmi, Saint-Malo Cadomian migmatites; SrM, Serre Massif; SVAr, Southern Vosges Arc; To, tonalite; UGU, Upper Gneiss Unit; Vgn, Central Vosges gneisses; LLSZ, Lalaye-Lubine Shear Zone; FMC, French Massif Central.

Fig. 9. (a) Gravity anomalies in the band pass 200-7 km and contours of magnetic highs of the South-western Variscan Domain, formed by the Iberian Peninsula. (b) Interpretative geophysical map. The gravity legend accounts for the interpretation of the anomalies, while the zone legend shows in lighter colours the zonation of the Variscan belt only in the outcropping massifs (white when covered). BAU, Beja-Acbuches Unit; BC, Bragança Complex; BeR, Betics Range; CCR, Catalonia Coast Ranges; Cgl, Cáceres granitic lineament; CM, Cantabrian Mountains; COC, Cabo Ortegal Complex; DeC, Demanda Chain; DoB, Douro Basin; EbB, Ebro Basin; IbC, Iberian Chain; GuB, Guadalquivir Basin; LD, Lugo Dome; MC, Morais Complex; MCB, Mérida Cadomian Batholith; NAgl, Nisa-Alburquerque granitic lineament; NPF, North Pyrenean Fault; NSb, Northern Sevilla batholith; OC, Órdenes Complex; Pgl, Pedroches granitic lineament; PVgl, Porto-Viseu granitic lineament; PyC, Pyrenean Chain; SCS, Spanish Central System; SD, Sanabria Dome; TaB, Tagus Basin.

Fig. 10. Treatment of reflection and refraction seismic data, modeling of gravity anomalies and extrapolation of geological bodies to depth are used to define three principal types of reflectors and principal tectonic units constituting the Variscan belt as exemplified by Boh9HR seismic line. a) Crustal section across the Bohemian massif based on interpreted structural, geochronological and geophysical data (Maierová et al., 2021). b) Unmigrated seismic section Boh9HR according to Tomek (2007). c) CEL09 refraction seismic line (Hrubcová et al., 2005; Růžek et al., 2007) with superposed line drawing of principal reflectors depicted from Boh9HR line. d) Interpreted and modeled gravity anomalies across the Boh9HR seismic line. The densities (in kg.m-3) of rocks outcropping at the surface are used to characterize gravity anomalies. e) Fully interpreted seismic section with three types of reflectors: A – violet, B – reddish pink, C – light blue. The interpreted tectonic units corresponding to modeled gravity anomalies and velocity P wave gradients are also shown. CBF, Central Bohemian Fault; CBP, Central Bohemian Pluton; v.g. Varied group.

Fig. 11. Interpreted deep seismic sections across different massifs of the Variscan belt including their corresponding gravity and magnetic anomalies. Location is depicted by pink lines in Fig. 2. a) The profiles are DEKORP-2N (migrated) across the northern Variscan front, DEKORP-2S through the Saxothuringian Zone where M1 and M2 locate the magnetic dyke, ECORS-DEKORP (migrated) through the Saxothuringian Zone, and ECORS-NFr (migrated) that crosses the western Paris Basin and the magnetic anomaly of the Paris basin (MAPB). b)

The profiles are represented by ARMOR-2 (migrated), that intersects the South Armorican Domain, SWAT-2-3 (unmigrated), SWAT-9-10 (migrated) crossing British Variscides, and SWAT-6-7 crossing the western part of the English Channel and c) The section ESCIN-1 (ESCICANTABRICA-1; unmigrated) goes through the axial surface of the Cantabrian Arc and ESCIN-3.2 and ESCIN-3.3 sections are located offshore and run parallel to ESCIN-1. The latter sections are the only ones in Iberia that cross the WALZ and CIZ zones together with Mid-Variscan allochthon. ALCUDIA section (migrated) crosses the southern part of the Central Iberian Zone and IBERSEIS (migrated) is crossing the Variscan front in the northern and southern parts of the Ibero-Armorican Arc respectively, and See text for the interpretation of the three types of reflections identified (A, B, C).

Fig. 12. P velocity/depth logs published or extracted from published P velocity sections whose location is depicted by light blue lines in Fig. 2. Many sections are located close to a series of profiles mostly orthogonal to the Variscan belt. The reference for each log is given in the list of authors. Abbreviations not included in the legend: FMC, French Massif Central; MT, Moldanubian thrust; SWM, Schwarzwald Massif; VL, Vindelicia; VM, Vosges Massif. For the location of the logs, see the references in Table 1.

Fig. 13. Gravity and magnetic lineaments derived from the 2nd vertical derivatives and tilt angle. The zone boundaries correspond to the sutures and/or the gravity and magnetic gradients, which can be delineated up to 20 km depth. Most of the gravity and magnetic lineaments display concerned the first 10 km of the crust. Discontinuities and faults are either linear boundaries or secant to the anomalies. Inclined boundaries are deduced from the 2nd vertical derivatives of increasing upward continuation (see Fig. 5e).

Fig. 14. Gravity structures of the Variscan belt reflecting intermediate to high density rocks. Boundaries of the gravity highs are derived from 2nd vertical derivatives of the Bouguer anomaly and/or tilt angle. The concerned rocks mainly consist of Proterozoic and Early Paleozoic compacted metasediments, as well as mafic and ultramafic rocks. The anomalies are colour-coded according to the zone to which they correspond or to a specific interpretation. Zone boundaries and significant gravity or magnetic lineaments are included, as well as some faults transecting the anomalies.

Fig. 15. Gravity structures of the Variscan belt reflecting low density rocks (< 2620 kg m^{-3}). Apart from late Variscan and younger sedimentary basins, the light bodies consist of felsic igneous rocks, dominantly granites and metagranites. a) The granitoid outcrops are shown in the map with colours representing different age intervals. V – Location of Velay dome. Zone boundaries and significant gravity or magnetic lineaments are included, as well as some faults transecting the anomalies. b) Map of gravity lows showing subsurface extension of plutonic bodies across the Variscan belt. Colors indicate age groups. The core of orogen is dominated by Carboniferous granitoids for which arrows show directions of regional extension.

Fig. 16. Magnetic positive anomalies of the Variscan belt representing bodies of relatively high magnetic susceptibility or remanence, mostly igneous rocks including ultrabasic and basic rocks, granitoids and migmatites. Contours derived from vertical derivatives of the map reduced to the pole and tilt angle. The anomalies are colour-coded according to geological interpretation. As in the figures depicting gravity anomalies, zone boundaries, gravity or magnetic lineaments and some faults transecting the anomalies are depicted, but here, additional magnetic lineaments are included.

Fig. 17. Two-dimensional P-wave velocity model for POLONAISE'97 profile P4 derived by ray tracing (modified from Grad et al., 2003). The thick solid lines are layer boundaries, and thin or dashed lines are isovelocity contours in kilometres per second. Model obtained by forward ray-tracing modelling using the SEIS83 package (Červený and Pšenčík, 1983). Colour striping shows the potential extent of the Variscan crust (orange) and Baltica lower crust (blue). The area between the Teisseyre-Tornquist Zone (TTZ) and Dolsk Fault may correspond to the Ediacaran rifted margin (Mikołajczak et al., 2019; Mazur et al., 2021).

Fig. 18. The new tectonic map of the European Variscan belt with updated extent of the mid-Variscan Allochthon based namely on regional distribution of high density bodies and position of Saxothuringian, Mid-Variscan and Rhenohercynian sutures depicted from gravity and magnetic maps. The regional extent of the Rhenohercynian arc together with Mid-Variscan and Saxothuringian arc – back arc basin systems are deduced from magnetic and partly gravity data. Schematic cross-sections across the belt are depicted mainly from seismic data and gravity-magnetic interpreted structures. These sections highlight non-cylindricity of Mid-Variscan allochthon, polarities of subduction systems based on geologically-

geophysically constrained sutures and position of corresponding magmatic arcs and back arc basins. RHZ-w, Rhenohercynian wedge.

Fig. 19. Synthetic map of crustal segments forming the European Variscan belt based on systematic variations of P wave logs. Three types of principal P wave logs are identified corresponding to the cratonic type marked by thick high velocity lower crust, transitional crust marked by three velocity layers and Variscan crust characterized by low to intermediate velocity lower and middle crust. The three types of crust are also characterized by large wavelength gravity anomalies ranging from large gravity high for cratonic crust and gravity low for Variscan crust. The extent of Variscan crust coincides with Carboniferous magmatic province as also shown in the map.

REFERENCES

Ackerman, L., Hajná, J., Žák, J., Erban, V., Sláma, J., Polák, L., Kachlík, V., Strnad, L., Trubač, J., 2020. Architecture and composition of ocean floor subducted beneath northern Gondwana during Neoproterozoic to Cambrian: A palinspastic reconstruction based on Ocean Plate Stratigraphy (OPS). Gondwana Research, 76, 77-97. https://doi.org/10.1016/j.gr.2019.07.001.

Aerden, D.G.A.M., 2004. Correlating deformation in Variscan NW-Iberia using porphyroblasts; implications for the Ibero-Armorican Arc. Journal of Structural Geology, 26, 177-196. https://doi.org/10.1016/S0191-8141(03)00070-1.

Aichroth, B., Prodehl, C., Thybo, H., 1992. Crustal structure along the Central Segment of the EGT from seismic-refraction studies. In: Freeman, R. and Mueller, S. (Eds.). The European Geotraverse, Part 8. Tectonophysics, 207, 43-64. https://doi.org/10.1016/0040-1951(92)90471-H.

Alcock, J.E., Martínez Catalán, J.R., Pascual, F.J.R., Montes, A.L., Fernández, R.D., Barreiro, J.G., Arenas, R., da Silva, I.D., Clavijo, E.G., 2015. 2-D thermal modeling of HT–LP metamorphism in NW and Central Iberia: Implications for Variscan magmatism, rheology of the lithosphere and orogenic evolution. Tectonophysics, 657, 21-37. https://doi.org/10.1016/j.tecto.2015.05.022.

Alexander, A. C., R. K. Shail, and B. E. Leveridge (2019), Late paleozoic extensional reactivation of the rheic–rhenohercynian suture zone in sw england, the english channel and western approaches, in Geological Society Special Publication, edited, pp. 353-373. https://doi.org/10.1144/SP470.19.

Altherr, R., Henes-Klaiber, U., Hegner, E., Satir, M., Langer, C., 1999. Plutonism in the Variscan Odenwald (Germany): from subduction to collision. International Journal of Earth Sciences, 88, 422-443. https://doi.org/10.1007/s005310050276.

Álvarez-Marrón, J., Pérez-Estaún, A., Dañobeitia, J.J., Pulgar, J.A., Martínez Catalán, J.R., Marcos, A., Bastida, F., Aller, J., Ayarza Arribas, P., Gallart, J., González-Lodeiro, F., Banda, E., Comas, M.C., Córdoba, D., 1995. Results from the ESCI-N3.1 and ESCI-N3.2 marine deep seismic profiles in the northwestern Galicia Margin. Revista de la Sociedad Geológica de España, 8, 331-339.

Álvarez-Marrón, J., Pérez-Estaún, A., Dañobeitia, J.J., Pulgar, J.A., Martínez Catalán, J.R., Marcos, A., Bastida, F., Ayarza Arribas, P., Aller, J. Gallart, J., González-Lodeiro, F., Banda, E., Comas, M.C. and Córdoba, D., 1996. Seismic structure of the northern continental margin of Spain from ESCIN deep seismics profiles. Tectonophysics, 264, 153-174. https://doi.org/10.1016/S0040-1951(96)00124-2.

Andrés, J., D. Draganov, M. Schimmel, P. Ayarza, I. Palomeras, M. Ruiz, and R. Carbonell (2019), Lithospheric image of the Central Iberian Zone (Iberian Massif) using global-phase seismic interferometry, Solid Earth, 10(6), 1937-1950. https://doi.org/10.5194/se-10-1937-2019.

Araújo, A.A., Ribeiro, A., 1996. Estrutura dos domínios meridionais da Zona de Ossa-Morena. Estudos sobre a Geologia da Zona de Ossa-Morena (Maciço Ibérico). Livro de homenagem ao Prof. Francisco Gonçalves, Évora, 169-182.

Ardizone, J., Mezcua, J., Socías, I., 1989. Mapa aeromagnético de España Peninsular. Escala 1:1.000.000. Instituto Geográfico Nacional, Madrid.

Arenas, R., Sánchez Martínez, S., Díez Fernández, R., Gerdes, A., Abati, J., Fernández-Suárez, J., Andonaegui, P., González Cuadra, P., López Carmona, A., Albert, R.,

Fuenlabrada, J.M., Rubio Pascual, F.J., 2016. Allochthonous terranes involved in the Variscan suture of NW Iberia: A review of their origin and tectonothermal evolution. Earth-Science Reviews, 161, 140-178. https://doi.org/10.1016/j.earscirev.2016.08.010.

Artemieva, I.M. and Meissner, R., 2012. Crustal thickness controlled by plate tectonics: a review of crust–mantle interaction processes illustrated by European examples. Tectonophysics, 530, 18-49. https://doi.org/10.1016/j.tecto.2011.12.037.

Arthaud, F. and Matte, P., 1977. Late Paleozoic strike-slip faulting in southern Europe and northern Africa: result of a right-lateral shear zone between the Appalachians and the Urals. Geological Society of America Bulletin, 88, 1305-1320. https://doi.org/10.1130/0016-7606(1977)88<1305:LPSFIS>2.0.CO;2.

Awdankiewicz, M., Kryza, R., Turniak, K., Ovtcharova, M., Schaltegger, U., 2021. The Central Sudetic Ophiolite (European Variscan Belt): precise U–Pb zircon dating and geotectonic implications. Geological Magazine, 158, 555-566. https://doi.org/10.1017/S0016756820000722.

Ayarza, P., Martínez Catalán, J.R., Gallart, J., Dañobeitia, J.J., Pulgar, J.A., 1998. Estudio Sísmico de la Corteza Ibérica Norte 3.3: a seismic image of the Variscan crust in the hinterland of the NW Iberian Massif. Tectonics, 17, 171-186. https://doi.org/10.1029/97TC03411.

Ayarza, P., Martínez Catalán, J.R., 2007. Potential field constraints on the deep structure of the Lugo gneiss dome (NW Spain). Tectonophysics, 439, 67-87. https://doi.org/10.1016/j.tecto.2007.03.007.

Ayarza, P., Martínez Catalán, J.R., Martínez García, A., Alcalde, J., Andrés, J., Simancas, J.F., Martí, D., Palomeras, I., de Felipe, I., Juhlin, C., Carbonell, R., 2021a. Evolution of the Iberian Massif as deduced from its crustal thickness and geometry of a mid-crustal (Conrad?) discontinuity. Solid Earth, 12, 1515-1547. https://doi.org/10.5194/se-12-1515-2021.

Ayarza, P, Villalaín, J.J., Martínez Catalán, J.R., Alvarez Lobato, F., Durán Oreja, M., Calvin, P., Recio, C., Suárez Barrios, M., Gómez Martín, E., 2021b. Characterizing the source of the Eastern Galicia Magnetic Anomaly (NW Spain): the role of extension in the origin of magnetization at the Central Iberian Arc. Tectonics, 40, 1-30. https://doi.org/10.1029/2020TC006120.

Azor, A., Rubatto, D., Simancas, J.F., González Lodeiro, F., Martínez Poyatos, D., Martín Parra, L.M., Matas, J., 2008. Rheic Ocean ophiolitic remnants in Southern Iberia questioned by SHRIMP U-Pb zircon ages on the Beja-Acebuches Amphibolites. Tectonics, 27, TC5006, 1-11. https://doi.org/10.1029/2008TC002306.

Azor, A., Rubatto, D., Marchesi, C., Simancas, J.F., González Lodeiro, F., Martínez Poyatos, D., Martín Parra, L.M., Matas, J., 2009. A reply to the comment by C. Pin and J. Rodríguez Aller on "Rheic Ocean ophiolitic remnants in southern Iberia questioned by SHRIMP U-Pb zircon ages on the Beja-Acebuches amphibolites". Tectonics, 28.

Ballèvre, M., Bosse, V., Ducassou, C., Pitra, P., 2009. Palaeozoic history of the Armorican Massif: Models for the tectonic evolution of the suture zones. Comptes Rendus Geoscience, 341, 174-201. https://doi.org/10.1016/j.crte.2008.11.009.

Ballèvre, M., Martínez Catalán, J.R., López-Carmona, A., Pitra, P., Abati, J., Díez Fernández, R., Ducassou, C., Arenas, R., Bosse, V., Castiñeiras, P., Fernández-Suárez, J., Gómez Barreiro, J., Paquette, J.L., Peucat, J.J., Poujol, M., Ruffet, G., Sánchez Martínez, S.,

2014. Correlation of the nappe stack in the Ibero-Armorican arc across the Bay of Biscay: a joint French-Spanish project. In: Schulmann, K., Martínez Catalán, J.R., Lardeaux, J.M., Janousek, V. and Oggiano, G. (Eds.), The Variscan Orogeny: Extent, Timescale and the Formation of the European Crust. Geological Society, London, Special Publications, 405, 77-113. http://dx.doi.org/10.1144/SP405.13.

Ballèvre, M., Brice, D., Lardeux, H., Morzadec, P., Mottequin, B., 2019. Reassignment of Pentamerus davyi Oehlert to Zdimir robustus (Barrande) (Brachiopoda, Devonian): Stratigraphic and palaeogeographic implications. Annales de Paléontologie, 105, 97-108. https://doi.org/10.1016/j.annpal.2019.04.003.

Bandrés, A., Eguíluz, L., Pin, C., Paquette, J.L., Ordóñez, B., Le Fèvre, B., Ortega, L.A., Gil Ibarguchi, J.I., 2004. The northern Ossa-Morena Cadomian batholith (Iberian Massif): magmatic arc origin and early evolution. International Journal of Earth Sciences, 93, 860-885. https://doi.org/10.1007/s00531-004-0423-6.

Baptiste, J., 2016. Cartographie structurale et lithologique du substratum du Bassin parisien et sa place dans la chaîne varisque de l'Europe de l'Ouest. Approches combinées: géophysiques, pétrophysiques, géochronologiques et modélisations 2D. PhD Thesis, Université d'Orléans, 367.

Baptiste, J., Martelet, G., Faure, M., Beccaletto, L., Renard, P.A., Perrin, J., Chen, Y., 2016. Mapping of a buried basement combining aeromagnetic, gravity and petrophysical data: The substratum of southwest Paris Basin, France. Tectonophysics, 683, 333-348. https://doi.org/10.1016/j.tecto.2016.05.049.

Barrois, C., 1899. Brioverian system in a sketch of the geology of Central Brittany. Proc. Geol. Assoc., XVI, 101-132.

Behr, H.J., Engel, W., Franke, W., Giese, P., Weber, K., 1984. The Variscan belt in Central Europe: main structures, geodynamic implications, open questions. Tectonophysics, 109 (1-2), 15-40. https://doi.org/10.1016/0040-1951(84)90168-9.

Behr, H.J., Heinrichs, T., 1987. Geological interpretation of DEKORP 2-S: a deep seismic reflection profile across the Saxothuringian and possible implications for the Late Variscan structural evolution of Central Europe. Tectonophysics 142, 173–202. https://doi.org/10.1016/0040-1951(87)90122-3.

Berger, J., Féménias, O., Mercier, J.C.C., Demaiffe, D., 2005. Ocean-floor hydrothermal metamorphism in the Limousin ophiolites (western French Massif Central): evidence of a rare preserved Variscan oceanic marker. Journal of Metamorphic Geology, 23, 795-812. https://doi.org/10.1111/j.1525-1314.2005.00610.x .

Berger, J., Féménias, O., Ohnenstetter, D., Bruguier, O., Plissart, G., Mercier, J.C., Demaiffe, D., 2010. New occurrence of UHP eclogites in Limousin (French Massif Central): age, tectonic setting and fluid-rock interactions. Lithos, 118, 365-382. https://doi.org/10.1016/j.lithos.2010.05.013.

Béthoux N., Tric E., Chéry J. and Beslier M.-O., 2008. Why is the Ligurian Basin (Mediterranean Sea) seismogenic? Thermomechanical modeling of a reactivated passive margin. Tectonics, 27 (5): 1127-1194. https://doi.org/10.1029/2007TC002232

Be Mezeme, E., Faure, M., Chen, Y., Cocherie, A., Talbot, J.Y., 2007. Structural, AMS and geochronological study of a laccolith emplaced during Late Variscan orogenic extension: the Rocles pluton (SE French Massif Central). International Journal of Earth Sciences, 96, 215-228. https://doi.org/10.1007/s00531-006-0098-2.

Bitri, A., Brun, J.P., Truffert, C., Guennoc, P., 2001. Deep seismic imagin of the Cadomian thrust wedge of Northern Brittany. Tectonophysics, 331, 65-80. https://doi.org/10.1016/S0040-1951(00)00236-5.

Bitri, A., Ballèvre, M., Brun, J.P., Chantraine, J., Gapais, D., Guennoc, P., Gumiaux, C., Truffert, C., 2003. Imagerie sismique de la zone de collision hercynienne dans le Sud-Est du Massif armoricain (projet Armor 2/programme Géofrance 3D). Comptes Rendus Geoscience, 335, 969-979. https://doi.org/10.1016/j.crte.2003.09.002.

Bitri, A., Brun, J.P., Gapais, D., Cagnard, F., Gumiaux, C., Chantraine, J., Martelet, G., Truffert, C., 2010. Deep reflection seismic imaging of the internal zone of the South Armorican Hercynian belt (western France) (ARMOR 2/programme Géofrance 3D). Comptes Rendus Geoscience, 342, 448-452. https://doi.org/10.1016/j.crte.2010.03.006.

Blaumoser, N.H., 1992. Eine erste gesamte aeromagnetische Karte von Österreich und ihre Transformationen. Mitt. Österr. Geol. Ges. 84, 185-203.

Bleibinhaus, F., Bopp, M., Simon, M., Gebrande H., 1999. 3-D Prestack-migration of wide-angle data from a Variscan Transition Zone. Pure and Applied Geophysics, 156, 173-186. https://doi.org/10.1007/s000240050295.

Bosum, W., Wonik, T., 1991. Magnetic anomaly pattern of Central Europe. Tectonophysics, 195, 253-259. https://doi.org/10.1016/0040-1951(91)90213-C.

Braid, J.A., Murphy, J.B., Quesada, C., Mortensen, J., 2011. Tectonic escape of a crustal fragment during the closure of the Rheic Ocean: U-Pb detrital zircon data from the Late Palaeozoic Pulo do Lobo and South Portuguese zones, southern Iberia. Journal of the Geological Society, 168, 383-392. https://doi.org/10.1144/0016-76492010-104.

BRGM, 1972. Carte magnetique de la France. Anomalies détaillées du champ total a l'échelle du 1/1000 000. Ministère du Développement Industriel et Scientifique, Bureau de Recherches Géologiques et Minières, Service, Géologique National. Orléans, col. map 106 x 112 cm, 2 feuilles 64 x 120 cm et 60 x 120 cm. G5831 .C93 1971 .F7 NORTH SHEET; G5831 .C93 1971 .F7 SOUTH SHEET.

Brückl, E., Bleibinhaus, F., Gosar, A., Grad, M., Guterch, A., Hrubcová, P., Keller, G.L., Majdański, M., Šumanovac, F., Tiira, T., Yliniemi,J., Hegedűs, E., Thybo, H., 2007. Crustal structure due to collisional and escape tectonics in the Eastern Alps region based on profiles Alp01 and Alp02 from the ALP 2002 seismic experiment. Journal of Geophysical Research Solid Earth, 112, 1-25. https://doi.org/10.1029/2006JB004687.

Brueckner, H.K., Medaris, L.G., 1998. A tale of two orogens – the contrasting P-T-t history and geochemical evolution of mantle in ultrahigh pressure (UHP) metamorphic terranes of the Norwegian Caledonides and the Czech Variscides. Schweizerische Mineralogische und Petrograph ische Mitteilungen, 78, 293-307.

Brun, J.P., Wenzel, F. and the ECORS-DEKORP team, 1991. Crustal scale structure of the southern Rhinegraben from ECORS-DEKORP seismic reflection data. Geology, 19, 758-762. https://doi.org/10.1130/0091-7613(1991)019<0758:CSSOTS>2.3.CO;2.

Brun, J.P., Guennoc, P., Truffert, C., Vairon, J., 2001. Cadomian tectonics in northern Brittany: a contribution of 3-D crustal-scale modelling. Tectonophysics, 331, 229-246. https://doi.org/10.1016/S0040-1951(00)00244-4.

Burg, J. P. (1991), Syn-migmatization way-up criteria, Journal of Structural Geology, 13(6), 617-623.

Burtman, V.S., Molnar, P., 1993. Geological and geophysical evidence for deep subduction of continental crust beneath the Pamir. Geological Society of America Special Paper 281, 76. https://doi.org/10.1130/SPE281.

Busby, J.P., Smith, N.J.P., 2001. The nature of the Variscan basement in southeast England: evidence from integrated potential field modeling. Geological Magazine, 138, 669-685. 10.1017/S0016756801005751.

Cagnard, F., D. Gapais, J. P. Brun, C. Gumiaux, and J. Van den Driessche (2004), Late pervasive crustal-scale extension in the south Armorican Hercynian belt (Vendeé, France), Journal of Structural Geology, 26(3), 435-449. https://doi.org/10.1016/j.jsg.2003.08.006.

Carreras, J., Druguet, E., 2014. Framing the tectonic regime of the NE Iberian Variscan segment. In: Schulmann, K., Martínez Catalán, J.R., Lardeaux, J.M., Janousek, V. and Oggiano, G. (Eds.), The Variscan Orogeny: Extent, Timescale and the Formation of the European Crust. Geological Society, London, Special Publications, 405, 249-264, http://dx.doi.org/10.1144/SP405.7.

Casini, L., S. Cuccuru, A. Puccini, G. Oggiano, and P. Rossi (2015), Evolution of the Corsica-Sardinia Batholith and late-orogenic shearing of the Variscides, Tectonophysics, 646, 65-78. https://doi.org/10.1016/j.tecto.2015.01.017.

Cazes, M., Torreilles, G., Bois, G., Damotte, B., Galdeano, A., Hirn, A., Mascle, A., Matte, P., Ngoc, P., Raoult, J., 1985. Structure de la croûte hercynienne du Nord de la France: Premiers résultats du profil ECORS. Bulletin de la Société Géologique de France, 1. 925-941. https://doi.org/10.2113/gssgfbull.I 6.925 .

Cerveny, V., and I. Psencik (1983), Gaussian beams and paraxial ray approximation in three-dimensional elastic inhomogeneous media, Journal of Geophysics - Zeitschrift fur Geophysik, 53(1), 1-15.

Chamot-Rooke N., Gaulier J.-M. and Jestin F., 1999. Constraints on Moho depth and crustal thickness in the Liguro-Provençal basin from a 3D gravity inversion: geodynamic implications. Geol. Soc. London Spec. Publ., 156 (1): 37.61. https://doi.org/10.1144/GSL.SP.1999.156.01.04.

Chang, R.H., Neubauer, F., Liu, Y.J., Yuan, S.H., Genser, J., Huang, Q.W., Guan, Q.B., Yi, S.Y., 2021. Hf isotopic constraints for the Austroalpine basement evolution of Eastern Alps: review and new data. Earth-Sci. Rev. 103772 https://doi.org/10.1016/j.earscirev.2021.103772.

Chopin, F., Schulmann, K., Skrzypek, E., Lehmann, J., Dujardin, J.R., Martelat, J.E., Lexa, O., Corsini, M., Edel, J.B., Štípská, P., Pitra, P., 2012. Crustal influx, indentation, ductile thinning and gravity redistribution in a continental wedge: Building a Moldanubian mantled gneiss dome with underthrust Saxothuringian material (European Variscan belt). Tectonics, 31, 1-27. https://doi.org/10.1029/2011TC002951.

Collett, S., Štípská, P., Schulmann, K., Peřestý, V., Soldner, J., Anczkiewicz, R., Lexa, O., Kylander-Clark, A., 2018. Combined Lu-Hf and Sm-Nd geochronology of the Mariánské Lázně Complex: New constraints on the timing of eclogite-and granulite-facies metamorphism. Lithos, 304, 74-94. https://doi.org/10.1016/j.lithos.2018.02.007.

Collett, S., Schulmanna, K., Deiller, P., Štípská, P., Peřestý, V., Ulrich, M., Jiang, Y., de Hoÿm de Marien, L., Míková, J., 2022. Reconstruction of the mid-Devonian HP-HT metamorphic event in the Bohemian Massif (European Variscan belt). Geoscience Frontiers, 13, 101374. https://doi.org/10.1016/j.gsf.2022.101374.

Córdoba, D., Banda, E., Ansorge, J., 1987. The Hercynian crust in northwestern Spain: a seismic survey. Tectonophysics, 132, 321-333. https://doi.org/10.1016/0040-1951(87)90351-9.

Córdoba, D., Banda, E., Ansorge, J., 1988. P-wave velocity-depth distribution in the Hercynian crust of Northwest Spain. Physics of the Earth and Planetary Interiors, 51, 235-248. https://doi.org/10.1016/0031-9201(88)90050-7

Costa, S., Rey, P., 1995. Lower crustal rejuvenation and growth during post-thickening collapse: Insights from a crustal cross section through a Variscan metamorphic core complex. Geology, 23, 905-908. https://doi.org/10.1130/0091-7613(1995)023<0905:LCRAGD>2.3.CO;2.

Dallmeyer, R.D., Martínez Catalán, J.R., Arenas, R., Gil Ibarguchi, J.I., Gutiérrez Alonso, G., Farias, P., Aller, J., Bastida, F., 1997. Diachronous Variscan tectonothermal activity in the NW Iberian Massif: Evidence from $^{40}Ar/^{39}Ar$ dating of regional fabrics. Tectonophysics, 277, 307-337. https://doi.org/10.1016/S0040-1951(97)00035-8.

Damotte, B., Bois, C., 1990. Near-vertical Vibroseis versus large-offset dynamite seismic reflection profiling: example of the ECORS northern France profile. Tectonophysics, 173, 95-106. https://doi.org/10.1016/0040-1951(90)90207-O.

de Hoÿm de Marien, L., Pitra, P., Cagnard, F., Le Bayon, B., 2020. Prograde and retrograde P–T evolution of a Variscan high temperature eclogite, French Massif Central, Haut-Allier. BSGF - Earth Sciences Bulletin, 191, 14. https://doi.org/10.1051/bsgf/2020016 .

Deiller, P., Štípská, P., Ulrich, M., Schulmann, K., Collett, S., Peřestý, V., Hacker, B., Kylander-Clark, A., Whitechurch, H., Lexa, O., Pelt, E., Míková, J., 2021. Eclogite subduction wedge intruded by arc-type magma: The earliest record of Variscan arc in the Bohemian Massif. Gondwana Research, 99, 220-246. . https://doi.org/10.1016/j.gr.2021.07.005.

DEKORP and Orogenic Processes Working Groups, 1999. Structure of the Saxonian granulites: Geological and geophysical constraints on the exhumation of high-pressure/high-temperature rocks in the mid-European Variscan belt. Tectonics, 18, 756-773. https://doi.org/10.1029/1999TC900030

de la Rosa, J., Jenner, J., Castro, A., 2002. A study of inherited zircons in granitoid rocks from the South Portuguese and Ossa-Morena Zones, Iberian Massif: support for the exotic origin of the South Portuguese Zone. Tectonophysics, 352, 245-256. https://doi.org/10.1016/S0040-1951(02)00199-3

de la Rosa, J.D., Castro, A., 2004. Zona Sudportuguesa: Magmatismo de la Zona Sudportuguesa. In: Vera, J.A. (Ed.), Geología de España, SGE-IGME, 2, 215-222.

de Vicente, G., Cunha, P.P., Muñoz-Martín, A., Cloetingh, S.A.P.L., Olaiz, A., Vegas, R., 2018. The Spanish-Portuguese Central System: an example of intense intraplate deformation and strain partitioning. Tectonics, 37, 4444-4469. https://doi.org/10.1029/2018TC005204.

Dezes, P., Ziegler, P.A., 2002. Map of the European Moho. EUCOR URGENT, University Basel.

Dias da Silva, I., Valverde-Vaquero, P., González-Clavijo, E., Díez-Montes, A. and Martínez Catalán, J.R., 2014. Structural and stratigraphical significance of U-Pb ages from the Mora and Saldanha volcanic complexes (NE Portugal, Iberian Variscides). In: Schulmann, K., Martínez Catalán, J.R., Lardeaux, J.M., Janousek, V. and Oggiano, G.

(Eds.), The Variscan Orogeny: Extent, Timescale and the Formation of the European Crust. Geological Society, London, Special Publications, 405, 115-135. http://dx.doi.org/10.1144/SP405.3.

Dias da Silva, Í., Linnemann, U., Hofmann, M., González Clavijo, E., Díez-Montes, A., Martínez Catalán, J.R., 2015. Detrital zircon and tectonostratigraphy of the Parautochthon under the Morais Complex (NE Portugal): implications for the Variscan accretionary history of the Iberian Massif. Journal of the Geological Society, London, 172, 45-61. http://dx.doi.org/10.1144/jgs2014-005.

Dudek, A., 1980. The crystalline basement block of the Outer Carpathians in Moravia: Bruno-Vistulicum. Rozpravy Československá akademie věd - řada matematických a přírodních věd (Rozpr. Čs. Akad.Věd. Ř. mat. přir. Věd), 90, 8, 3-85. Praha.

Edel, J.B., 1985. Magnétisme et paléomagnétisme des roches du socle au sud de l'Anomalie Magnétique du Bassin de Paris. Programme Géologie Profonde de la France. Document B.R.G.M. 95/2 : 17-27.

Edel., J.B., 2008. Structure et nature du socle anté-Permien du Bassin de Paris d'après les données gravimétriques et magnétiques. Le problème de l'Anomalie Magnétique du Bassin de Paris. Geochronique (SGF-BRGM), March 2008, 31-37.

Edel, J.B., Fluck, P., 1989. The upper Rhenish Shield basement (Vosges, Upper Rhinegraben and Schwarzwald): main structural features deduced from magnetic, gravimetric and geological data. Tectonophysics, 169, 303-316. https://doi.org/10.1016/0040-1951(89)90093-0.

Edel, J.B., Weber, K., 1995. Cadomian terranes, wrench faulting and thrusting in the central Europe Variscides: geophysical and geological evidence. Geologische Rundschau, 84, 412-432. https://doi.org/10.1007/BF00260450.

Edel, J.B., Aïfa T., 2001. Paleomagnetic evolution of Armorica in Late Paleozoic times in the light of overprints recorded in Cadomian and Paleozoic units. Tectonophysics, 331, 145-167. https://doi.org/10.1016/S0040-1951(00)00240-7

Edel, J. B., H. Whitechurch, and M. Diraison (2006), Seismicity wedge beneath the Upper Rhine Graben due to backwards Alpine push?, Tectonophysics, 428(1-4), 49-64. https://doi.org/10.1016/j.tecto.2006.08.009.

Edel, J.B., Schulmann, K., 2009. Geophysical constraints and model of the 'Saxothuringian and Rhenohercynian subductions – magmatic arc system' in NE France and SW Germany. Bulletin de la Société Géologique de France, 180, 545-558. https://doi.org/10.2113/gssgfbull.180.6.545.

Edel, J.B., Fuchs, K., Gelbke, C., Prodehl, C., 1975. Deep structure of the Rhinegraben area from seimic refration investigation. Journal of Geophysics, 41, 333-356.

Edel J.B., Montigny R., Royer J.Y., Thuizat R., Trolard, F., 1986. Paleomagnetic investigations and K-Ar dating on the Variscan plutonic massif of the Champ du Feu and its volcanic sedimentary environment, northern Vosges, France. Tectonophysics, 122, 165-185. https://doi.org/10.1016/0040-1951(86)90165-4.

Edel, J.B., Montigny, R., Thuizat, R., 1981. Late Paleozoic rotations of Corsica and Sardinia: new evidence from paleomagnetic and K-Ar studies. Tectonophysics 79 (3–4), 201–223.

Edel, J.B., Arnaud, C., Clauss, M.L., Papillon, E., 1996. The Paleozoic basement of the Süddeutsche Grossscholle" derived from gravimetric and magnetic data, with emphasis on the Kraichgau terrane: Zeitschr. Geol. Wissensch., 24, 41-54.

Edel, J.B., Schulmann, K., Rotstein, Y., 2007. The Variscan tectonic inheritance of the Upper Rhine Graben: evidence of reactivations in the Lias, Late Eocene–Oligocene up to the recent. International Journal of Earth Sciences, 96, 305-325. https://doi.org/10.1007/s00531-006-0092-8.

Edel, J.B., Schulmann, K., Skrzypek, E., Cocherie, A., 2013. Tectonic evolution of the European Variscan belt constrained by palaeomagnetic, structural and anisotropy of magnetic susceptibility data from the Northern Vosges magmatic arc (eastern France). Journal of the Geological Society, London, 170, 785-804. http://dx.doi.org/10.1144/jgs2011-138.

Edel, J.B., Casini, L., Oggiano, G., Rossi P., Schulmann, K., 2014. Early Permian clockwise 90º rotation of the Maures-Estérel-Corsica-Sardinia block confirmed by new palaeomagnetic data and followed by a Triassic 60º clockwise rotation. In: Schulmann, K., Martínez Catalán, J.R., Lardeaux, J.M., Janousek, V. and Oggiano, G. (Eds.), The Variscan Orogeny: Extent, Timescale and the Formation of the European Crust. Geological Society, London, Special Publications, 405, 333-361. http://dx.doi.org/10.1144/SP405.10.

Edel, J.B., Schulmann, K., Lexa, O., Lardeaux, J.-M., 2018. Late Palaeozoic palaeomagnetic and tectonic constraints for amalgamation of Pangea supercontinent in the European Variscan belt. Earth-Science Reviews, 177, 589-612. https://doi.org/10.1016/j.earscirev.2017.12.007.

Ehsan, S.A., Carbonell, R., Ayarza, P., Martí, D., Pérez-Estaún, A., Martínez-Poyatos, D.J., Simancas, J.F., Azor, A., Mansilla, L., 2014. Crustal deformation styles along the reprocessed deep seismic reflection transect of the Central Iberian Zone (Iberian Peninsula). Tectonophysics, 621, 159-174. https://doi.org/10.1016/j.tecto.2014.02.014.

Ehsan, S.A., Carbonell, R., Ayarza, P., Martí, D., Martínez Poyatos, D., Simancas, J.F., Azor, A., Ayala, C., Torné, M., Pérez-Estaún, A., 2015. Lithospheric velocity model across the Southern Central Iberian Zone (Variscan Iberian Massif): The ALCUDIA wide-angle seismic reflection transect. Tectonics, 34, 535-554. https://doi.org/10.1002/2014TC003661.

Enderle, U., Schuster, K., Prodehl, C., Schulze, A., Bribach, J., 1998. The refraction seismic experiment GRANU95 in the Saxothuringian belt, southeastern Germany. Geophysical Journal International, 133, 245-259. https://doi.org/10.1046/j.1365-246X.1998.00462.x.

Farias, P., Gallastegui, G., González Lodeiro, F., Marquínez, J., Martín Parra, L.M., Martínez Catalán, J.R., Pablo Maciá, J.G. de, Rodríguez Fernández, L.R., 1987. Aportaciones al conocimiento de la litoestratigrafía y estructura de Galicia Central. Memórias da Faculdade de Ciências, Universidade do Porto, 1, 411-431.

Faure, M., 1995. Late orogenic Carboniferous extensions in the Variscan French Massif Central. Tectonics, 14, 132-153. https://doi.org/10.1029/94TC02021.

Faure, M., Lardeaux, J.M., Ledru, P., 2009. A review of the pre-Permian geology of the Variscan French Massif Central. Comptes Rendus Geosciences, 341, 202-213. https://doi.org/10.1016/j.crte.2008.12.001.

Faure, M., Sommers, C., Melleton, J., Cocherie, A., Lautout, O., 2010. The Léon Domain (French Massif Armoricain): a westward extension of the Mid-German Crystalline Rise? Structural and geochronological insights. International Journal of Earth Sciences, 99, 65-81. https://doi.org/10.1007/s00531-008-0360-x.

Faure, M., Cocherie, A., Gaché, J., Esnault, C., Guerrot, C., Rossi, P., Wei, L., Qiuli, L., 2014. Middle Carboniferous intracontinental subduction in the outer zone of the Variscan belt (Montagne Noire Axial Zone, French Massif Central): multimethod geochronological approach of polyphase metamorphism. In: Schulmann, K., Martínez Catalán, J.R., Lardeaux, J.M., Janousek, V. and Oggiano, G. (Eds.), The Variscan Orogeny: Extent, Timescale and the Formation of the European Crust. Geological Society, London, Special Publications, 405, 289-311. http://dx.doi.org/10.1144/SP405.2.

Fernández-Viejo, G., Gallart, J., Pulgar, J.A., Córdoba, D., Dañobeitia, J.J., 2000. Seismic signature of Variscan and Alpine tectonics in NW Iberia: Crustal structure of the Cantabrian Mountains and Duero basin. Journal of Geophysical Research, 105, 3001-3018. https://doi.org/10.1029/1999JB900321.

Filippi, M., Spalla, M.I., Pigazzini, N., Diella, V., Lardeaux, J.-M., Zanoni, D., 2021. Cld- St-And-Bearing Assemblages in the Central Southalpine Basement: Markers of an Evolving Thermal Regime during Variscan Convergence. Minerals 11, 1124. https://doi.org/10.3390/min11101124.

Finger, F., Roberts, M.P., Haunschmid, B., Schermaier, A., Steyrer, H.P., 1997. Variscan granitoids of central Europe: their typology, potential sources and tectonothermal relations. Mineralogy and Petrology, 61, 67-96. https://doi.org/10.1007/BF01172478.

Finger, F., Hanžl, P., Pin, C., Von Quadt, A. and Steyrer, H.P., 2000. The Brunovistulian: Avalonian Precambrian sequence at the eastern end of the Central European Variscides?. In: Franke, W., Haak, V., Oncken, O. and Tanner, D. (Eds.), Orogenic Processes: Quantification and Modelling in the Variscan Belt. Geological Society, London, Special Publication, 179, 103-112. http://dx.doi.org/10.1144/GSL.SP.2000.179.01.08.

Finger, F., A. Gerdes, M. René, and G. Riegler (2009), The Saxo-Danubian Granite Belt: Magmatic response to post-collisional delamination of mantle lithosphere below the southwestern sector of the Bohemian Massif (Variscan orogen), Geologica Carpathica, 60(3), 205-212. https://doi.org/10.2478/v10096-009-0014-3.

Fornelli, A., Festa, V., Micheletti, F., Spiess, R., Tursi, F., 2020. Building an Orogen: Review of U-Pb Zircon Ages from the Calabria–Peloritani Terrane to Constrain the Timing of the Southern Variscan Belt. Minerals, 10, 2-31. https://doi:10.3390/min10110944.

Franěk, J., Schulmann, K., Lexa, O., Tomek, Č., Edel, J.B., 2011. Model of syn-convergent extrusion of orogenic lower crust in the core of the Variscan belt: implications for exhumation of high-pressure rocks in large hot orogens. Journal of Metamorphic Geology, 29, 53-78. https://doi.org/10.1111/j.1525-1314.2010.00903.x.

Franke, W., 1989. Tectonostratigraphic units in the Variscan belt of central Europe. Geological Society of America Special Paper, 230, 67-90. https://doi.org/10.1130/SPE230-p67.

Franke, W., 2000. The mid-European segment of the Variscides: tectonostratigraphic units, terrane boundaries and plate tectonic evolution. In: Franke, W., Haak, V., Oncken, O., Tanner, D. (Eds.), Orogenic Processes: Quantification and Modelling in the Variscan Belt. Geological Society, London, Special Publications, 179, 35-61. http://dx.doi.org/10.1144/GSL.SP.2000.179.01.05.

Franke, W., Żelaźniewicz, A., 2000. The eastern termination of the Variscides: terrane correlation and kinematic evolution. In: Franke, W., Haak, V., Oncken, O. and Tanner, D. (Eds.), Orogenic Processes: Quantification and Modelling in the Variscan Belt. Geological Society, London, Special Publications, 179, 63-86. https://doi.org/10.1144/GSL.SP.2000.179.01.06.

Franke, W., Bortfeld, R.K., Brix, M., Drozdzewski, G., Dürbaum, H.J, Giese, P., Janoth, W., Jödicke, H., Reichert, C., Scherp, A., Schmoll, J., Thomas, R., Thünker, M., Weber, K., Wiesner, M.G., Wong, H.K., 1990. Crustal structure of the Rhenish Massif: results of deep seismic reflection lines DEKORP 2-North and 2-North-Q. Geologische Rundschau, 79 (3), 523-566. https://doi.org/10.1007/BF01879201.

Franke, W., Cocks, L.R.M., Torsvik, T.H., 2017. The Palaeozoic Variscan oceans revisited. Gondwana Research, 48, 257-284. https://doi.org/10.1016/j.gr.2017.03.005.

Friedl, G., Finger, F., McNaughton, N.J., Fletcher, I.R., 2000. Deducing the ancestry of terranes: SHRIMP evidence for South America–derived Gondwana fragments in central Europe. Geology, 28 , 1035-1038. https://doi.org/10.1130/0091-7613(2000)28<1035:DTAOTS>2.0.CO;2.

Fuchs, G., 1976. Zur Entwicklung der Böhmischen Masse. Jahrbuch der Geologischen Bundelsansalt, 119, 45-61.

Gabriel, G., Vogel, D., Scheibe, R., Lindner, H., Pucher, R., Wonik, T., Krawczyk, C.M., 2011. Anomalies of the Earth's total magnetic field in Germany – the first complete homogenous data set reveals new opportunities for multiscale geoscientific studies. Geophysical Journal International, 184, 1113-1118. https://doi.org/10.1111/j.1365-246X.2010.04924.x.

Gajewski, D., Prodehl, C., 1987. Seismic refraction investigation of the Black Forest. Tectonophysics, 142, 27-48. https://doi.org/10.1016/0040-1951(87)90293-9.

Gajewski, D., Holbrook, W.S., Prodehl, C., 1987. A three-dimensional crustal model of Southwest Germany derived from seismic refraction data. Tectonophysics, 142, 49-70. https://doi.org/10.1016/0040-1951(87)90294-0.

Gapais, D., J. P. Brun, C. Gumiaux, F. Cagnard, G. Ruffet, and C. Le Carlier De Veslud (2015), Extensional tectonics in the Hercynian Armorican belt (France). An overview, Bulletin de la Societe Geologique de France, 186(2-3), 117-129. https://doi.org/10.2113/gssgfbull.186.2-3.117.

García Casquero, J.L., Boelrijk, N.A.I.M., Chacón, J., Priem, H.N.A., 1985. Rb-Sr evidence for the presence of Ordovician granites in the deformed basement of the Badajoz-Córdoba Belt, SW Spain. Geologische Rundschau, 74, 379-384.

García-Lobón, J.L., Rey-Moral, C., Ayala, C., Martín-Parra, L.M., Matas, J. Reguera, M.I., 2014. Regional structure of the southern segment of Central Iberian Zone (Spanish Variscan Belt) interpreted from potential field images and 2.5 D modelling of Alcudia gravity transect. Tectonophysics, 614, 185-202. https://doi.org/10.1016/j.tecto.2013.12.005.

Gardien V., Tegyey M., Lardeaux J.-M., Misseri M., Dufour E., 1990. Crustal-mantle relationships in the French Variscan chain: the example of the southern Monts du Lyonnais unit (eastern French Massif Central). Journal of Metamorphic Geology, 8, 477-492. https://doi.org/10.1111/j.1525-1314.1990.tb00481.x.

Gardien, V., Martelat, J.-E., Leloup, H.-P., Mahéo G., Bevillard B., Allemand, P., Patrick M., Paquette J.-L., Grosjean A.-S., Faure, M., Chelle-Michou, C., Fellah, C., 2021. Fast exhumation rate during late orogenic extension: the new timing of the Pilat detachment fault (French Massif Central). Gondwana Research, 103, 260-275. https://doi.org/10.1016/j.gr.2021.10.007.

Gerbault, M., Schneider, J., Reverso-Peila, A., Corsini, M., 2018. Crustal exhumation during ongoing compression in the Variscan Maures–Tanneron Massif, France-Geological and

thermo-mechanical aspects. Tectonophysics, 746, 439–458. https://doi.org/10.1016/j.tecto.2016.12.019.

Gerya, T., Perchuk, L., Maresch, W., Willner, A., Van Reenen, D., Smit, C., 2002. Thermal regime and gravitational instability of multi-layered continental crust: implications for the buoyant exhumation of high-grade metamorphic rocks. European Journal of Mineralogy, 14, 687–699. 10.1127/0935-1221/2002/0014-0687.

Girardeau, J., Dubuisson, G., Mercier, J.C.C., 1986. Cinématique de mise en place des ophiolites et nappes cristallophylliennes du Limousin, Ouest du Massif Central français. Bulletin de la Societé Géologique de France, II 5, 849-860. https://doi.org/10.2113/gssgfbull.II.5.849.

Gladney, E.R.,·Braid, J.A., Murphy, J.B., Quesada, C., McFarlane, C.R.M., 2014. U-Pb geochronology and petrology of the late Paleozoic Gil Marquez pluton: magmatism in the Variscan suture zone, southern Iberia, during continental collision and the amalgamation of Pangea. International Journal of Earth Sciences, 103, 1433-1451. https://doi.org/10.1007/s00531-014-1034-5.

Godin, L., and L. B. Harris (2014), Tracking basement cross-strike discontinuities in the Indian crust beneath the Himalayan orogen using gravity data - relationship to upper crustal faults, Geophysical Journal International, 198(1), 198-215. https://doi.org/10.1093/gji/ggu131.

Goleby, B.R., Shaw, R.D., Wright, C., Kennett, B.L.N., Lambeck, K., 1989. Geophysical evidence for 'thick-skinned' crustal deformation in central Australia. Nature, 337, 325-330. https://doi.org/10.1038/337325a0.

Grad, M., Guterch, A., Mazur, S., 2002. Seismic refraction evidence for crustal structure in the central part of the Trans-European Suture Zone in Poland. In: Winchester, J.A., Pharaoh, T.C. and Verniers, J. (Eds.), Palaeozoic Amalgamation of Central Europe. Geological Society, London, Special Publication, 201, 295-309. http://dx.doi.org/10.1144/GSL.SP.2002.201.01.14.

Grad, M., Jensen, S.L., Keller, G.R., Guterch, A., Thybo, H., Janik, T., Tiira, T., Yliniemi, J., Luosto, U., Motuza, G., Nasedkin, V., 2003. Crustal structure of the Trans-European suture zone region along POLONAISE'97 seismic profile P4. Journal of Geophysical Research: Solid Earth, 108. https://doi.org/10.1029/2003JB002426.

Grad, M., Guterch, A., Mazur, S., Keller, G.R., Špičák, A., Hrubcová, P., Geissler, W.H., 2008. Lithospheric structure of the Bohemian Massif and adjacent Variscan belt in central Europe based on profile S01 from the SUDETES 2003 experiment. Journal of Geophysical Research: Solid Earth, 113. https://doi.org/10.1029/2007JB005497.

Grandjean, G., Guennoc, P., Reck, M., Andreo, P., 2001. Refraction/wide-angle reflection investigation of the Cadomian crust between northern Brittany and the Channel Islands. Tectonophysics 331, 45-64. 10.1016/S0040-1951(00)00235-3.

Gumiaux, C., Gapais, D., Brun, J.P., Chantraine, J., Ruffet, G., 2004. Tectonic history of the Hercynian Armorican shear Belt (Brittany, France). Geodinamica Acta, 17, 289-307. https://doi.org/10.3166/ga.17.289-307

Guterch, A., Grad, M., 2006. Lithospheric structure of the TESZ in Poland based on modern seismic experiments. Geological Quarterly, 50, 23-32.

Guterch, A., Wybraniec, S., Grad, M., Chadwick, R.A., Krawczyk, C.M., Ziegler, P.A., Thybo, H., De Vos W., 2010. Crustal structure and structural framework. In:

Doornenbal, J.C. and Stevenson, A.G. (Eds.), Petroleum Geological Atlas of the Southern Permian Basin Area, EAGE Publications, Houten, 11-23.

Gutiérrez-Alonso, G., Collins, A.S., Fernández-Suárez, J., Pastor-Galán, D., González-Clavijo, E., Jourdan, F., Weil, A.B., Johnston, S.T., 2015. Dating of lithospheric buckling: $^{40}Ar/^{39}Ar$ ages of syn-orocline strike-slip shear zones in northwestern Iberia. Tectonophysics, 643, 44-54. https://doi.org/10.1016/j.tecto.2014.12.009.

Gutiérrez-Marco, J.C., Aramburu, C., Arbizu, M., Bernárdez, E., Hacar Rodríguez, M.P., Méndez-Bedia, I., Montesinos López, R., Rábano, I., Truyols, J., Villas, E., 1999. Revisión bioestratigráfica de las pizarras del Ordovícico Medio en el noroeste de España (zonas Cantábrica, Asturoccidental-leonesa y Centroibérica septentrional). Acta Geologica Hispanica, 34, 3-87.

Guy, A., Edel, J.B., Schulmann, K., Tomek, Č., Lexa, O., 2011. A geophysical model of the Variscan orogenic root (Bohemian Massif): Implications for modern collisional orogens. Lithos, 124, 144-157. https://doi.org/10.1016/j.lithos.2010.08.008.

Hann HP, Chen F, Zedler H, Frisch W, Loeschke J., 2003. The Rand Granite in the southern Schwarzwald and its geodynamic significance in the Variscan belt of SW Germany. International Journal of Earth Sciences 92(6), 821–842.

Hanžl, P., Janoušek, V., Soejono, I., Buriánek, D., Svobitka, M., Hrdličková, K., Erban, V., Pin, C., 2019. The rise of the Brunovistulicum: age, geological, petrological and geochemical character of the Neoproterozoic magmatic rocks of the Central Basic Belt of the Brno Massif. International Journal of Earth Sciences, 108, 1165-1199. https://doi.org/10.1007/s00531-019-01700-2.

Hofmann, M., Linnemann, U., Gerdes, A., Ullrich, B., Schauer, M., 2009. Timing of dextral strike-slip processes and basement exhumation in the Elbe Zone (Saxo-Thuringian Zone): the final pulse of theVariscan Orogeny in the Bohemian Massif constrained by LA-SF-ICP-MS U-Pb zircon data. In: Murphy, J.B., Keppie, J.D. and Hynes, A.J. (Eds.), Ancient orogens and modern analogues, Geological Society, London, 327, 197-214. http://dx.doi.org/10.1144/SP327.10.

Holden, D. J., N. J. Archibald, F. Boschetti, and M. W. Jessell (2000), Inferring geological structures using wavelet-based multiscale edge analysis and forward models, Explor. Geophys., 31(4), 617-621. https://doi.org/10.1071/EG00617.

Hrouda, F., Faryad, S.W., Franěk, J., Chlupáčová, M., 2013. Magnetic fabrics in garnet peridotites–pyroxenites and host felsic granulites in the South Bohemian Granulites (Czech Republic): Implications for distinguishing between primary and metamorphism induced fabrics. Gondwana Research, 23, 956-972. https://doi.org/10.1016/j.gr.2012.05.020.

Hrouda, F., Faryad, S.W., Chlupáčová, M., Jeřábek, P., 2014. Magnetic fabric in amphibolized eclogites and serpentinized ultramafites in the Mariánské Lázně Complex (Bohemian Massif, Czech Republic): Product of exhumation-driven retrogression? Tectonophysics, 629, 260-274. https://doi.org/10.1016/j.tecto.2014.01.034.

Hrubcová, P., Środa, P., Spicak, A., Guterch, A., Grad, M., Keller, G.R., Brueckl, E., Thybo H., 2005. Crustal and uppermost mantle structure of the Bohemian massif based on CELEBRATION 2000 data. Journal of Geophysical Research, 110, B11305. https://doi.org/10.1029/2004JB003080.

Hrubcová, P., Środa, P. and CELEBRATION 2000 Working Group., 2008. Crustal structure at the easternmost termination of the Variscan belt based on CELEBRATION 2000 and ALP 2002 data. Tectonophysics, 460, 55-75. https://doi.org/10.1016/j.tecto.2008.07.009.

Hrubcová, P., Geissler, W.H., 2009. The crust-mantle transition and the Moho beneath the Vogtland/West Bohemian Region in the light of different seismic methods. Studia Geophysica et Geodaetica, 53, 275-294. https://doi.org/10.1007/s11200-009-0018-6.

Hrubcová, P., Środa, P., Grad, M., Geissler, W.H., Guterch, A., Vozár, J., Hegedüs, E. and SUDETES 2003 Working Group., 2010. From the Variscan to the Alpine Orogeny: crustal structure of the Bohemian Massif and the Western Carpathians in the light of the SUDETES 2003 seismic data. Geophysical Journal International, 183, 611-633. https://doi.org/10.1111/j.1365-246X.2010.04766.x.

Ibrmajer, J., 1981. Geological interpretation of gravity maps of Czechoslovakia. Geophysical synthesis in Czechoslovakia, Bratislava, 135-148.

Iglesias Ponce de León, M., Choukroune, P., 1980. Shear zones in the Iberian arc. Journal of Structural Geology, 2, 63-68. https://doi.org/10.1016/0191-8141(80)90035-8.

Instituto Geográfico Nacional, 1996. Anomalías gravimétricas Bouguer de la Península Ibérica y Baleares. Escala 1/1.000.000. Madrid.

Janoušek, V., Braithwaite, C.J R., Bowes, D.R., Gerdes, A., 2004. Magma-mixing in the genesis of Hercynian calc-alkaline granitoids: an integrated petrographic and geochemical study of the Sázava intrusion, Central Bohemian Pluton, Czech Republic. Lithos, 78, 67-99. https://doi.org/10.1016/j.lithos.2004.04.046.

Jarosiński, M., Dąbrowski, M., 2006. Modele reologiczne litosfery w poprzek szwu transeuropejskiego w północnej i zachodniej częœci Polski. Pr. Państw. Inst. Geol, 188, 143-166.

Jeřábek, P., Konopásek, J., Záčlová E., 2016. Two-stage exhumation of subducted Saxothuringian continental crust records underplating in the subduction channel and collisional forced folding (Krkonoše-Jizera Mts., Bohemian Massif). Journal of Structural Geology, 89, 214-229, https://doi.org/10.1016/j.jsg.2016.06.008.

Jouffray, F., Spalla, M.I., Lardeaux, J.M., Filippi, M., Rebay, G., Corsini, M., Zanoni, D., Zucali, M., Gosso, G., 2020. Variscan eclogites from the Argentera–Mercantour Massif (External Crystalline Massifs, SW Alps): a dismembered cryptic suture zone. International Journal of Earth Sciences, 109, 1273-1294. https://doi.org/10.1007/s00531-020-01848-2.

Julivert, M., Fontboté, J.M., Ribeiro, A., Conde, L., 1972. Mapa Tectónico de la Península Ibérica y Baleares E. 1: 1 000 000. Instituto Geológico y Minero de España, Madrid.

Kelly, A., R. W. England, and P. K. H. Maguire (2007), A crustal seismic velocity model for the UK, Ireland and surrounding seas, Geophysical Journal International, 171(3), 1172-1184.

Kimbell, G.S., Ritchie, J.D., Henderson, A.F., 2010. Three-dimensional gravity and magnetic modelling of the Irish sector of the NE Atlantic margin. Tectonophysics, 486, 36-54. https://doi.org/10.1016/j.tecto.2010.02.007.

Klemperer, S.L. 2006., Crustal flow in Tibet: geophysical evidence for the physical state of Tibetan lithosphere, and inferred patterns of active flow. In: Law, R.D., Searle, M.P. and Godin, L. (Eds.), Channel flow, ductile extrusion and exhumation in continental collision zones. Geological Society, London, Special Publications, 268, 39-70. http://dx.doi.org/10.1144/GSL.SP.2006.268.01.03.

Konopásek, J., Schulmann, K. 2005., Contrasting Early Carboniferous field geotherms: evidence for accretion of a thickened orogenic root and subducted Saxothuringian crust (Central European Variscides). Journal of the Geological Society, London, 162, 463-470. http://dx.doi.org/10.1144/0016-764904-004.

Konopásek, J., Anczkiewicz, R., Jeřábek, P., Corfu, F., Žáčková, E., 2019. Chronology of the Saxothuringian subduction in the West Sudetes (Bohemian Massif, Czech Republic and Poland). Journal of the Geological Society, London, 176, 492-504. http://dx.doi.org/10.1144/jgs2018-173.

Košler, J., Konopásek, J., Sláma, J. and Vrána, S., 2014. U-Pb zircon provenance of Moldanubian metasediments in the Bohemian Massif. Journal of the Geological Society, London, 171, 83-95. http://dx.doi.org/10.1144/jgs2013-059

Kossmat, F., 1927. Gliederung des varistischen Gebirgsbaues. Abhandlungen des Sächsischen Geologuschen Landesamts, Leipzig, Heft 1, 39 pp., 2 tafel.

Kotková, J., O'Brien, P.J., Ziemann, M.A., 2011. Diamond and coesite discovered in Saxony-type granulite: Solution to the Variscan garnet peridotite enigma. Geology, 39, 667-670. https://doi.org/10.1130/G31971.1.

Królikowski, C. and Petecki, Z., 1995. Gravimetric Atlas of Poland - Polish Geological Institute, Warsaw (Panstw. Inst. Geol. Warszawa.).

Kröner, A., Štipská, P., Schulmann, K., Jaeckel, P., 2000. Chronological constraints on the pre-Variscan evolution of the northeastern margin of the Bohemian Massif, Czech Republic. In: Franke, W., Haak, V., Oncken, O. and Tanner, D. (Eds.), Orogenic processes: Quantification and modelling in the Variscan Belt: Geological Society, London, Special Publications, 179, 175-197. http://dx.doi.org/10.1144/GSL.SP.2000.179.01.12.

Lardeaux, J.M., 2014. Deciphering orogeny: a metamorphic perspective Examples from European Alpine and Variscan belts: Part II: Variscan metamorphism in the French Massif Central–A review. Bulletin de la Société géologique de France, 185, 281-310. https://doi.org/10.2113/gssgfbull.185.5.281

Lardeaux J.-M., Reynard B., Toufour E., 1989. Kornerupine-bearing granulites and post-orogenic decompression of the Monts du Lyonnais, Massif Central, France[Granulites a kornerupine et decompression post-orogenique des Monts du Lyonnais (M.C.F.)].. C. R. Acad. Sci., Paris, II, 308, 1443-1449.

Lardeaux, J.M., Spalla, M.I., 1991. From granulites to eclogites in the Sesia zone (Italian Western Alps): a record of the opening and closure of the Piedmont ocean. Journal of Metamorphic Geology, 9, 35-59. https://doi.org/10.1111/j.1525-1314.1991.tb00503.x.

Lardeaux, J.M., Ledru, P., Daniel, I., Duchene, S., 2001. The Variscan French Massif Central–a new addition to the ultra-high pressure metamorphic 'club': exhumation processes and geodynamic consequences. Tectonophysics, 332, 143-167. https://doi.org/10.1016/S0040-1951(00)00253-5.

Lardeaux, J.M., Schulmann, K., Faure, M., Janoušek, V., Lexa, O., Skrzypek, E., Edel, J.B., Štípská. P., 2014. The Moldanubian Zone in French Massif Central, Vosges/Schwarzwald and Bohemian Massif revisited: Differences and similarities. In: Schulmann, K., Martínez Catalán, J.R., Lardeaux, J.M., Janousek, V. and Oggiano, G. (Eds.), The Variscan Orogeny: Extent, Timescale and the Formation of the European Crust. Geological Society, London, Special Publications, 405, 7-44. https://doi.org/10.1144/SP405.14.

Lardeaux J.M., Schulmann, K., Edel, J.B., (submitted). Vosges and Black Forest. In: Linnemann, U. (Ed.), Geology of the Central European Variscides, Springer.

Ledru, P., Lardeaux, J.M., Santallier, D., Autran, A., Quenardel, J.M., Floc'h J.P., Lerouge, G., Maillet, N., Marchand, J., Ploquin. A., 1989. Où sont les nappes dans le Massif Central Français? Bulletin de la Société Géologique de France, 3, 605-618. https://doi.org/10.2113/gssgfbull.V.3.605 .

Ledru, P., Courrioux, G., Dallain, C., Lardeaux, J.M. Montel, J.M., Vanderhaeghe, O., Vitel, G., 2001. The Velay dome (French Massif Central): melt generation and granite emplacement during orogenic evolution. Tectonophysics, 342, 207-237. https://doi.org/10.1016/S0040-1951(01)00165-2.

Le Gall, B., 1990. Evidence of an imbricate crustal thrust belt in the southern British Variscides - contributions of southwestern approaches traverse (SWAT) deep seismic-reflection profiling recorded through the English-Channel and the Celtic Sea. Tectonics, 9, 283 -302. https://doi.org/10.1029/TC009i002p00283.

Le Gall, B., 1991. Crustal evolutionary model for the Variscides of Ireland and wales from SWAT seismic data. Journal of the Geological Society, London, 148, 759-774. http://dx.doi.org/10.1144/gsjgs.148.4.0759.

Lexa, O., Schulmann, K., Janoušek, V., Štípská, P., Guy, A., Racek, M., 2011. Heat sources and trigger mechanisms of exhumation of HP granulites in Variscan orogenic root. Journal of Metamorphic Geology, 29, 79 - 102. https://doi.org/10.1111/j.1525-1314.2010.00906.x.

Lindner, M., Dörr, W., Reither, D., Finger, F., 2021. The Dobra Gneiss and the Drosendorf Unit in the southeastern Bohemian Massif, Austria: West Amazonian crust in the heart of Europe. Geological Society, London, Special Publications, 503, 185-207. http://dx.doi.org/10.1144/SP502-2019-232.

Linnemann, U., Gerdes, A., Drost, K., Buschmann, B., 2007. The continuum between Cadomian orogenesis and opening of the Rheic Ocean: Constraints from LA-ICP-MS U-Pb zircon dating and analysis of plate-tectonic setting (Saxo-Thuringian zone, northeastern Bohemian Massif, Germany). In: Linnemann, U., Nance, R.D., Kraft, P. and Zulauf, G. (Eds.), The evolution of the Rheic Ocean: From Avalonian-Cadomian active margin to Alleghenian-Variscan collision. Geological Society of America Special Paper, 423, 61-96. https://doi.org/10.1130/2007.2423(03).

Linnemann, U., Pereira, F., Jeffries, T.E., Drost, K., Gerdes, A., 2008. The Cadomian Orogeny and the opening of the Rheic Ocean: The diacrony of geotectonic processes constrained by LA-ICP-MS U–Pb zircon dating (Ossa-Morena and Saxo-Thuringian Zones, Iberian and Bohemian Massifs). Tectonophysics, 461, 21-43. https://doi.org/10.1016/j.tecto.2008.05.002.

Lotout, C., Pitra, P., Poujol, M., Anczkiewicz, R., Van Den Driessche, J., 2018. Timing and duration of Variscan high-pressure metamorphism in the French Massif Central: A multimethod geochronological study from the Najac Massif. Lithos, 308-309, 381-394. https://doi.org/10.1016/j.lithos.2018.03.022.

Lotout, C., Poujol, M., Pitra, P., Anczkiewicz, R., Van Den Driessche, J., 2020. From burial to exhumation: Emplacement and metamorphism of mafic eclogitic terranes constrained through multimethod etrochronology, case study from the Lévézou Massif (French Massif Central, Variscan Belt). Journal of Petrology, 61, 1–27. https://doi.org/10.1093/petrology/egaa046.

Lotze, F., 1945. Zur Gliederung der Varisziden der Iberischen Meseta. Geotektonische Forschungen, 6, 78-92.

Lüschen, E., Wenzel, F., Sandmeyer, K.J., Menges, D., Rühl, Th., Stiller, M., Janoth, W., Keller, F., Söllner, W., Thomas, R., Krohe, A., Stenger, R., Fuchs, K., Willhelm. H., Eisbacher G., 1987. Near-vertical and wide-angle seismic survey in the Black Forest, SW Germany. Journal of Geophysics, 62, 1-30.

Macquet, M., A. Paul, H. A. Pedersen, A. Villaseñor, S. Chevrot, M. Sylvander, and D. Wolyniec (2014), Ambient noise tomography of the Pyrenees and the surrounding regions: Inversion for a 3-D Vs model in the presence of a very heterogeneous crust, Geophysical Journal International, 199(1), 402-415.

Maguire, P., England, R., Hardwick, A., 2011. LISPB DELTA, a lithospheric seismic profile in Britain: analysis and interpretation of the Wales and southern England section. Journal of the Geological Society, 168, 61-82. http://dx.doi.org/10.1144/0016-76492010-030

Maierová, P., K. Schulmann, O. Lexa, S. Guillot, P. Štípska, V. Janoušek, and O. Čadek (2016), European Variscan orogenic evolution as an analogue of Tibetan-Himalayan orogen: Insights from petrology and numerical modeling, Tectonics, 35(7), 1760-1780. https://doi.org/10.1002/2015TC004098.

Maierová, P., Schulmann, K., Štípská, P., Gerya, T., Lexa, O., 2021. Trans-lithospheric diapirism explains the presence of ultra-high pressure rocks in the European Variscides. Communications Earth & Environment, 2, 1-9. https://doi.org/10.1038/s43247-021-00122-w .

Malavieille, J., Guihot, P., Costa, S., Lardeaux, J.M., Gardien, V., 1990. Collapse of the thickened Variscan crust in the French Massif Central: Mont Pilat extensional shear zone and St. Étienne Upper Carboniferous basin. Tectonophysics, 177, 139-149. https://doi.org/10.1016/0040-1951(90)90278-G.

Malinowski, M., Żelaźniewicz, A., Grad, M., Guterch, A., Janik, T., CELEBRATIONWorking Group, 2005. Seismic and geological structure of the crust in the transition from Baltica to Palaeozoic Europe in SE Poland — CELEBRATION 2000 experiment, profile CEL02. Tectonophysics 401, 55–77. https://doi.org/10.1016/j.tecto.2005.03.011.

Marotta, A.M., Spalla, M.I., 2007. Permian-Triassic high thermal regime in the Alps: Result of late Variscan collapse or continental rifting? Validation by numerical modeling. Tectonics 26, TC4016. https://doi.org/10.1029/2006TC002047.

Martínez Catalán, J.R., 2012. The Central Iberian arc, an orocline centered in the Iberian Massif and some implications for the Variscan belt. International Journal of Earth Sciences, 101, 1299-1314. https://doi.org/10.1007/s00531-011-0715-6.

Martínez Catalán, J.R., Ayarza Arribas, P., Pulgar, J.A., Pérez-Estaún, A., Gallart, J., Marcos, A., Bastida, F., Álvarez-Marrón, J., González Lodeiro, F., Aller, J., Dañobeitia, J.J., Banda, E., Cordoba, D., Comas, M.C., 1995. Results from the ESCI-N3.3 marine deep seismic profile along the Cantabrian continental margin. Revista de la Sociedad Geológica de España, 8, 341-354.

Martínez Catalán, J.R., Arenas, R., Díaz García, F. and Abati, J., 1997. Variscan accretionary complex of northwest Iberia: Terrane correlation and succession of tectonothermal events. Geology, 25, 1103-1106. https://doi.org/10.1130/0091-7613(1997)025<1103:VACONI>2.3.CO;2.

Martínez Catalán, J.R., Fernández-Suárez, J., Jenner, G.A., Belousova, E., Díez Montes, A., 2004. Provenance constraints from detrital zircon U-Pb ages in the NW Iberian Massif: implications for Paleozoic plate configuration and Variscan evolution. Journal of the Geological Society, London, 161 , 463-476. http://dx.doi.org/10.1144/0016-764903-054

Martínez Catalán, J.R., Arenas, R., Abati, J., Sánchez Martínez, S., Díaz García, F., Fernández-Suárez, J., González Cuadra, P., Castiñeiras, P., Gómez Barreiro, J., Díez Montes, A., González Clavijo, E., Rubio Pascual, F.J., Andonaegui, P., Jeffries, T.E., Alcock, J.E., Díez Fernández, R., López Carmona, A., 2009. A rootless suture and the loss of the roots of a mountain chain: the Variscan belt of NW Iberia. Comptes Rendus Geoscience, 341, 114-126. https://doi.org/10.1016/j.crte.2008.11.004.

Martínez Catalán, J.R., Álvarez Lobato, F., Pinto, V., Gómez Barreiro, J., Ayarza, P., Villalaín, J.J., Casas, A., 2012. Gravity and magnetic anomalies in the allochthonous Órdenes Complex (Variscan belt, NW Spain): Assessing its internal structure and thickness. Tectonics, 31, 1-18. https://doi.org/10.1029/2011TC003093.

Martínez Catalán, J.R., Rubio Pascual, F.J., Díez Montes, A., Díez Fernández, R., Gómez Barreiro, J., Dias da Silva, Í., González Clavijo, E., Ayarza, P., Alcock, J.E., 2014. The late Variscan HT/LP metamorphic event in NW and Central Iberia: relationships to crustal thickening, extension, orocline development and crustal evolution. In: Schulmann, K., Martínez Catalán, J.R., Lardeaux, J.M., Janousek, V. and Oggiano, G. (Eds.), The Variscan Orogeny: Extent, Timescale and the Formation of the European Crust. Geological Society, London, Special Publications, 405, 225-247. http://dx.doi.org/10.1144/SP405.1.

Martínez Catalán, J.R., Aerden, D.G.A.M., Carreras, J., 2015. The "Castilian bend" of Rudolf Staub (1926): Historical perspective of a forgotten orocline in Central Iberia. Swiss Journal of Geosciences, 108, 283-303. https://doi.org/10.1007/s00015-015-0202-3.

Martínez Catalán, J.R., Ayarza, P., Álvarez Lobato, F., Villalaín, J.J., Durán Oreja, M., Martín Paramio, M., Rodríguez Gómez, S., 2018. Magnetic Anomalies in Extensional Detachments: The Xistral Tectonic Window of the Lugo Dome (NW Spain). Tectonics, 37, 4261-4284. https://doi.org/10.1029/2017TC004887.

Martínez Catalán, J.R., Collett, S., Schulmann, K., Aleksandrowski, P., Mazur, S., 2020. Correlation of allochthonous terranes and major tectonostratigraphic domains between NW Iberia and the Bohemian Massif, European Variscan belt. International Journal of Earth Sciences, 109, 1105-1131. https://doi.org/10.1007/s00531-019-01800-z.

Martínez Catalán, J.R., Schulmann, K., Ghienne, J.F., 2021. The Mid-Variscan Allochthon: Keys from correlation, partial retrodeformation and plate-tectonic reconstruction to unlock the geometry of a non-cylindrical belt. Earth-Science Reviews, 220, 1-65. https://doi.org/10.1016/j.earscirev.2021.103700.

Martínez Poyatos, D., Carbonell, R., Palomeras, I., Simancas, J.F., Ayarza, P., Martí, D., Azor, A., Jabaloy, A., González Cuadra, P., Tejero, R., Martín Parra, L.M., Matas, J., González Lodeiro, F., Pérez-Estaún, A., García Lobón, J.L., Mansilla, L., 2012. Imaging the crustal structure of the Central Iberian Zone (Variscan Belt): The ALCUDIA deep seismic reflection transect. Tectonics, 31, 1-21. https://doi.org/10.1029/2011TC002995.

Massonne, H.J., Kennedy, A., Nasdala, L., Theye, T., 2007. Dating of zircon and monazite from diamondiferous quartzofeldspathic rocks of the Saxonian Erzgebirge – hints at burial and exhumation velocities. Mineralogical Magazine, 71, 407-425. http://dx.doi.org/10.1180/minmag.2007.071.4.407.

Matte, P., Respaut, J.P., Maluski, H., Lancelot, J.R., Brunel, M., 1986. La faille NW-SE du Pays de Bray, un décrochement ductile dextre hercynien: déformation à 330 Ma d'un granite à 570 Ma dans le sondage Pays de Bray 201. Bulletin de la Societé Géologique de France, II, 69-77. https://doi.org/10.2113/gssgfbull.II.1.69.

Matte, P., 1986. Tectonics and plate tectonics model for the Variscan belt of Europe. Tectonophysics, 126, 329-374. https://doi.org/10.1016/0040-1951(86)90237-4.

Matte, P., 1991. Accretionary history and crustal evolution of the Variscan belt in Western Europe. Tectonophysics, 196, 309-337. https://doi.org/10.1016/0040-1951(91)90328-P.

Matte, P., 2001. The Variscan collage and orogeny (480-290 Ma) and the tectonic definition of the Armorica microplate: a review. Terra Nova, 13, 122-128. https://doi.org/10.1046/j.1365-3121.2001.00327.x.

Matte, P., 2007. Variscan thrust nappes, detachments, and strike-slip faults in the French Massif Central: Interpretation of the lineations. In: Hatcher Jr., R.D., Carlson, M.P., McBride, J.H. and Martínez Catalán, J.R. (Eds.), 4-D Framework of Continental Crust. Geological Society of America Memoir, 200, 391-402. https://doi.org/10.1130/2007.1200(20).

Mazur, S., Aleksandrowski, P., 2001. The Tepla(?)/Saxothuringian suture in the Karkonosze-Izera massif, western Sudetes, central European Variscides. International Journal of Earth Sciences, 90, 341-360, https://doi.org/10.1007/s005310000146.

Mazur, S., Aleksandrowski, P., Kryza, R., Oberc-Dziedzic, T., 2006. The Variscan Orogen in Poland. Geological Quarterly, 50, 89-118.

Mazur, S., Mikołajczak, M., Krzywiec, P., Malinowski, M., Buffenmyer, V., Lewandowski, M., 2015. Is the Teisseyre-Tornquist Zone an ancient plate boundary of Baltica? Tectonics, 34, 2465-2477. https://doi.org/10.1002/2015TC003934.

Mazur, S., Aleksandrowski, P., Gągała, Ł., Krzywiec, P., Żaba, J., Gaidzik, K., Sikora, R., 2020. Late Palaeozoic strike-slip tectonics versus oroclinal bending at the SW outskirts of Baltica: case of the Variscan belt's eastern end in Poland. International Journal of Earth Sciences, 109, 1133-1160. https://doi.org/10.1007/s00531-019-01814-7

Mazur, S., Malinowski, M., Maystrenko, Y.P. and Gągała, Ł., 2021. Pre-existing lithospheric weak zone and its impact on continental rifting–the Mid-Polish Trough, Central European Basin System. Global and Planetary Change, 198. https://doi.org/10.1016/j.gloplacha.2021.103417.

Mechie, J., Prodehl, C., Fuchs, K., Kaminski, W., Flick, J., Hirn, A., Ansorge, J., Kind, R., 1982. Progress report on Rhenish Massif seismic experiment. Tectonophysics, 90, 215-230. https://doi.org/10.1016/0040-1951(82)90263-3.

Meissner, R., 1986. Twenty years of deep seismic reflection profiling in Germany – a contribution to our knowledge of the nature of the lower Variscan crust. In: Dawson, J.B., Carswell, D.A., Hall, J. and Wedepohl, K.H. (Eds.), The Nature of the Lower Continental Crust, Geological Society, London, Special Publication, 24, 1-10. http://dx.doi.org/10.1144/GSL.SP.1986.024.01.02.

Meissner, R., 1999. Terrane accumulation and collapse in central Europe: seismic and rheological constraints. Tectonophysics, 305, 93-107. https://doi.org/10.1016/S0040-1951(99)00016-5.

Meyer, B., Saltus, R., Chulliat, A., 2017. EMAG2v3: Earth Magnetic Anomaly Grid (2-arc-minute resolution). Version 3. NOAA National Centers for Environmental Information. https://doi.org/10.7289/V5H70CVX.

Mezcua, J., Gil, A, Benarroch, R., 1996. Estudio gravimétrico de la Península Ibérica y Baleares. Instituto Geográfico Nacional, Madrid, 7.

Mikołajczak, M., Mazur, S., Gągała, Ł., 2019. Depth-to-basement for the East European Craton and Teisseyre-Tornquist Zone in Poland based on potential field data. International Journal of Earth Sciences, 108, 547-567. https://doi.org/10.1007/s00531-018-1668-9.

Miller, H. G., and V. Singh (1994), Potential field tilt—a new concept for location of potential field sources, Journal of Applied Geophysics, 32(2–3), 213-217.

Miranda, J.M., Galdeano, A., Rossignol, J.C., Mendes Victor, L.A., 1989. Aeromagnetic anomalies in mainland Portugal and their tectonic implications. Earth and Planetary Science Letters, 95, 161-172. https://doi.org/10.1016/0012-821X(89)90174-X.

Molnar, P., 1984. Structure and tectonics of the Himalaya: Constraints and implications of geophysical data. Annual Reviews of Earth and Planetary Sciences, 12, 489-518. https://doi.org/10.1146/annurev.ea.12.050184.002421.

Molnar, P., 1988. A review of geophysical constraints on the deep structure of the Tibetan Plateau, the Himalaya, and the Karakorum and their tectonic implications. Philosophical Transactions of the Royal Society, London, Series A, 326, 33-88. https://doi.org/10.1098/rsta.1988.0080.

Mooney, W.D. and Meissner, R., 1992. Multi-genetic origin of crustal reflectivity: a review of seismic reflection profiling of the continental lower crust and Moho. In: D.M. Fountain, R. Arculus and R.W. Kay (Editors), Continental Lower Crust. Developments in Geotectonics, Elsevier, Amsterdam, 23 45- 79.

Mueller, H.J., 1995. Modelling the lower crust by simulation of the in situ conditions: an example from the Saxonian Erzgebirge. Physics of the Earth and Planetary Interiors, 92, 3-15. https://doi.org/10.1016/0031-9201(95)03055-2.

Murphy, J.B., Nance, R.D., 1991. Supercontinent model for the contrasting character of Late Proterozoic orogenic belts. Geology, 19, 469-472. https://doi.org/10.1130/0091-7613(1991)019<0469:SMFTCC>2.3.CO;2.

Neubauer, F., Liu, Y., Dong, Y., Chang, R., Genser, J., Yuan, S., 2022. Pre-Alpine tectonic evolution of the Eastern Alps: From Prototethys to Paleotethys. Earth-Science Reviews, 226, 103923. https://doi.org/10.1016/j.earscirev.2022.103923.

Ochsner, A., 1993. U-Pb geochronology of the Upper Proterozoic-Lower Paleozoic geodynamic evolution in the Ossa-Morena Zone (SW Iberia): constraints on the timing of the Cadomian orogeny. Ph.D. Thesis, University of Zurich, Diss. ETH 10, 392, 249 pp.

Oncken, O., 1997. Transformation of a magmatic arc and an orogenic root during oblique collision and it's consequences for the evolution of the European Variscides (Mid-German Crystalline Rise). Geologische Rundschau, 86, 2-20. https://doi.org/10.1007/s005310050118.

Oncken, O., von Winterfeld, C., Dittmar, U., 1999. Accretion of a rifted passive margin: the late Paleozoic Rhenohercynian fold and thrust belt (Middle European Variscides). Tectonics, 18, 75-91. https://doi.org/10.1029/98TC02763.

Onézime, J., Charvet, J., Faure, M., Chauvet, A., Panis, D., 2002. Structural evolution of the southernmost segment of the West European Variscides: the South Portuguese Zone (SW Iberia). Journal of Structural Geology, 24, 451-468. https://doi.org/10.1016/S0191-8141(01)00079-7.

Palomeras, I., Carbonell, R., Flecha, I., Simancas, F., Ayarza, P., Matas, J., Martínez Poyatos, D., Azor, A., González Lodeiro, F., Pérez-Estaún, A., 2009. Nature of the lithosphere across the Variscan orogen of SW Iberia: Dense wide-angle seismic reflection data. Journal of Geophysical Research, 114, 1-29. https://doi.org/10.1029/2007JB005050.

Palomeras, I., Villaseñor, A., Thurner, S., Levander, A., Gallart, J., Hamafi, M., 2017. Lithospheric structure of Iberia and Morocco using finite-frequency Rayleigh wave tomography from earthquakes and seismic ambient noise. Geochemistry, Geophysics, Geosystems, 18, 1824 - 1840. https://doi.org/10.1002/2016GC006657.

Paquette, J.L., Monchoux, P., Couturier, M., 1995. Geochemical and isotopic study of a norite-eclogite transition in the European Variscan Belt. Implications for U-Pb zircon systematics in metabasic rocks. Geochimica et Cosmochimica Acta, 59, 1611-1622. https://doi.org/10.1016/0016-7037(95)00067-A.

Paquette, J.L., Ballèvre, M., Peucat, J.J., Cornen, G., 2017. From opening to subduction of an oceanic domain constrained by LA-ICP-MS U-Pb zircon dating (Variscan belt, Southern Armorican Massif, France). Lithos, 294-295, 418-437. https://doi.org/10.1016/j.lithos.2017.10.005.

Pedro, J., Araújo, A., Fonseca, P., Tassinari, C., Ribeiro, A., 2010. Geochemistry and U-Pb zircon age of the internal Ossa-Morena zone ophiolite sequences: A remnant of Rheic Ocean in SW Iberia. Ofioliti, 35, 117-130. https://doi.org/10.4454/ofioliti.v35i2.390.

Pereira, M.F., Ribeiro, C., Vilallonga, F., Chichorro, M., Drost, K., Silva, J.B., Albardeiro, L., Hofmann, M., Linnemann, U., 2014. Variability over time in the sources of South Portuguese Zone turbidites: evidence of denudation of different crustal blocks during the assembly of Pangaea. International Journal of Earth Sciences, 103, 1453-1470, https://doi.org/10.1007/s00531-013-0962-8.

Pérez-Cáceres, I., Martínez Poyatos, D., Simancas, J.F., Azor, A., 2016. Testing the Avalonian affinity of the South Portuguese Zone and the Neoproterozoic evolution of SW Iberia through detrital zircon populations. Gondwana Research, 42, 177-192. https://doi.org/10.1016/j.gr.2016.10.010.

Pérez-Estaún, A., Pulgar, J.A., Banda, E., Álvarez-Marrón, J., ESCI-N Research Group., 1994. Crustal structure of the external Variscides in NW Spain from deep seismic reflection profiling. Tectonophysics, 232, 91-118. https://doi.org/10.1016/0040-1951(94)90078-7

Pérez-Estaún, A., Pulgar, J.A., Álvarez-Marrón, J., ESCI-N group. ESCI-N Group: Marcos, A., Bastida, F., Aller, J., Marquínez, J., Farias, P., Alonso, J.L., Gutiérrez, G., Gallastegui, J., Rodríguez, R., Heredia, N., Bulnes, M., Banda, E., Martínez Catalán, J.R., Córdoba, D., Dañobeitia, J.J., Comas, M.C., 1995. Crustal structure of the Cantabrian Zone: seismic image of a Variscan foreland thrust and fold belt (NW Spain). Revista de la Sociedad Geológica de España, 8, 307-319.

Petri, B., Mohn, G., Skrzypek, E., Mateeva, T., Galster, F., Manatschal, G., 2017. U–Pb geochronology of the Sondalo gabbroic complex (Central Alps) and its position within the Permian post-Variscan extension. International Journal of Earth Sciences, 106, 2873-2893. https://doi.org/10.1007/s00531-017-1465-x.

Pharaoh, T.C., 1999. Palaeozoic terranes and their lithospheric boundaries within the Trans-European Suture Zone (TESZ): a review. Tectonophysics, 314, 17-41. https://doi.org/10.1016/S0040-1951(99)00235-8.

Pin, C., Lancelot, J.R., 1982. U-Pb dating of an early Paleozoic bimodal magmatism in the French Massif Central and of its further metamorphic evolution. Contributions to Mineralogy and Petrology, 79, 1-12. https://doi.org/10.1007/BF00376956.

Pin, C., Paquette, J.-L., 1997. A mantle-derived bimodal suite in the Hercynian Belt: Nd isotope and trace element evidence for a subduction-related rift origin of the Late Devonian Brévenne metavolcanics, Massif Central (France). Contributions to Mineralogy and Petrology, 129, 222-238. https://doi.org/10.1007/s004100050334.

Pin, C., Paquette, J.-L., 2002. Le magmatisme basique calcoalcalin d'âge dévono-dinantien du nord du Massif Central, témoin d'une marge active hercynienne: arguments géochimiques et isotopiques Sr/Nd. (Sr-Nd isotope and trace element evidence for a Late Devonian active margin in northern Massif-Central (France)). Geodinamica Acta, 15, 63-77. https://doi.org/10.1080/09853111.2002.10510739.

Pin, C., Rodríguez, J., 2009. Comment on ''Rheic Ocean ophiolitic remnants in southern Iberia questioned by SHRIMP U-Pb zircon ages on the Beja-Acebuches amphibolites'' by A. Azor et al. Tectonics, 28. https://doi.org/10.1029/2009TC002495.

Pin, C., Vielzeuf, D., 1983. Granulites and related rocks in Variscan median Europe: a dualistic interpretation. Tectonophysics, 93, 47-74. https://doi.org/10.1016/0040-1951(83)90233-0.

Pin, C., Vielzeuf, D., 1988. Les granulites de haute-pression de l'Europe moyenne témoins d'une subduction éo-hercynienne. Implications sur l'origine des groupes leptyno-amphiboliques. Bulletin de la Société Géologique de France, 8, 13-20. https://doi.org/10.2113/gssgfbull.IV.1.13.

Pin, C., Fonseca, P.E., Paquette, J.L., Castro, P., Matte, P., 2008. The ca. 350 Ma Beja Igneous Complex: A record of transcurrent slab break-off in the Southern Iberia Variscan Belt? Tectonophysics, 461, 356-377. https://doi.org/10.1016/j.tecto.2008.06.001.

Plaumann, S., 1983. Die Schwerekarte 1:500 000 der Bundesrepublik Deutschland (Bouguer-Anomalien). Blatt Nord. Geologischen Jahrbuch E 27, 3-16. ISBN 978-3-510-96059-0.

Plaumann, S., 1988. Dichtebestimmungen an Kernen der Bohrungen zur Vorerkundung der Tiefbohrlokationen Oberpfalz und Schwarzwald. GeoLate Jb., E41, 71-87.

Plaumann, S., 1991. Die Schwerekarte der Bundesrepublik Deutschland (Bouguer-Anomalien), Blatt Mitte. Geol Jahrb E, 46, 3-16.

Plaumann, S., 1995. Die Schwerekarte der Bundesrepublik Deutschland (Bouguer-Anomalien), Blatt Süd. Geol Jahrb E, 53, 3-13.

Plesch, A., Oncken, O., 1999. Orogenic wedge growth during collision — constraints on mechanics of a fossil wedge from its kinematic record (Rhenohercynian FTB, Central Europe). Tectonophysics, 309, 117-139. https://doi.org/10.1016/S0040-1951(99)00135-3.

Polanský, J., Škvor, V., 1975. Structural–tectonic problems of north-western Bohemia (Summary of Czech. Text). Sborník geologických věd or Journal of Geological Sciences 13, 47-64.

Poprawa, P., Paszkowski, M., Fanning, C.M., Pécskay, Z., Nawrocki, J., Sikorska, M., 2006. Charakterystyka geochronologiczna obszarów źródłowych dla dolnopaleozoicznych utworów z NW kratonu wschodnioeuropejskiego oraz strefy Koszalin-Chojnice; datowania detrytycznych łyszczyków (K/Ar) i cyrkonów (U/Pb SHRIMP). Prace Państwowego Instytutu Geologicznego, 186.

Pulgar, J.A., Gallart, J., Fernández-Viejo, G., Pérez-Estaún, A., Álvarez-Marrón, J., ESCIN Group., 1996. Seismic image of the Cantabrian Mountains in the western extension of the Pyrenees from integrated ESCIN reflection and refraction data. Tectonophysics, 264, 1-19. https://doi.org/10.1016/S0040-1951(96)00114-X.

Regorda, A., Lardeaux, J.-M., Roda, M., Marotta, A.M., Spalla, M.I., 2020. How many subductions in the Variscan orogeny? Insights from numerical models. Geosci. Front. 11, 1025–1052. https://doi.org/10.1016/j.gsf.2019.10.005.

Robardet, M., 2002. Alternative approach to the Variscan Belt of southwestern Europe: Preorogenic paleobiogeographical constraints. In: Martínez Catalán, J.R., Hatcher Jr., R.D., Arenas, R. and Díaz García, F. (Eds.), Variscan-Appalachian Dynamics: The Building of the Late Paleozoic Basement, Geological Society of America, Special Paper, 364, 1-15. https://doi.org/10.1130/0-8137-2364-7.1.

Robardet, M., 2003. The Armorica 'microplate': fact or fiction? Critical review of the concept and contradictory paleobiogeographical data. Palaeogeography, Palaeoclimatology, Palaeoecology, 195, 125-148. https://doi.org/10.1016/S0031-0182(03)00305-5.

Robardet, M., Gutiérrez Marco, J.C., 1990. Sedimentary and faunal domains in the Iberian Peninsula during Lower Paleozoic times. In: Dallmeyer, R.D. and Martínez García, E. (Eds.), Pre-Mesozoic Geology of Iberia. Springer-Verlag, Berlin, 383-395. https://doi.org/10.1007/978-3-642-83980-1_27.

Rodrigues, B., Chew, D.M., Jorge, R.C.G.S., Fernandes, P., Veiga-Pires, C., Oliveira, J.T., 2015. Detrital zircon geochronology of the Carboniferous Baixo Alentejo Flysch Group (South Portugal); constraints on the provenance and geodynamic evolution of the South Portuguese Zone. Journal of the Geological Society, London, 172, 294-308. http://dx.doi.org/10.1144/jgs2013-084

Rolin, P., Marquer, D., Colchen, M., Cartannaz, C., Cocherie, A., Thiery, V., Quenardel, J.M., Rossi, P., 2009. Famenno-Carboniferous (370-320 Ma) strike slip tectonics monitored by syn-kinematic plutons in the French Variscan belt (Massif Armoricain and French Massif Central). Bulletin de la Société Géologique de France, 180, 231-246. https://doi.org/10.2113/gssgfbull.180.3.231.

Rossi, P., Oggiano, G., Cocherie, A., 2009. A restored section of the "southern Variscan realm" accros the Corsica-Sardinia microcontinent. Comptes Rendus Geoscience, 341, 224-238. https://doi.org/10.1016/j.crte.2008.12.005.

Rotstein, Y., Edel, J.B., Gabriel, G., Boulanger, D., Schaming, M., Munschy, M., 2006. Insight into the structure of the Upper Rhinegraben and its basement from a new compilation of Bouguer Gravity. Tectonophysics, 425, 55-70. https://doi.org/10.1016/j.tecto.2006.07.002.

Rubio Pascual, F.J., Matas, J., Martín Parra, L.M., 2013. High-pressure metamorphism in the Early Variscan subduction complex of the SW Iberian Massif. Tectonophysics, 592, 187-199. https://doi.org/10.1016/j.tecto.2013.02.022.

Rudnick, R.L., Fountain, D.M., 1995. Nature and composition of the continental crust: a lower crustal perspective. Reviews of geophysics, 33, 267-309. https://doi.org/10.1029/95RG01302.

Růžek, B., Hrubcova, P., Novotny, M., Spicak, A., Karousova, O., 2007. Inversion of travel times obtained during active seismic refraction experiments Celebration 2000, Alp 2002 and Sudetes 2003. Studia Geophysica et Geodaetica, 51, 141-164. https://doi.org/10.1007/s11200-007-0007-6.

Salem, A., Williams, S., Fairhead, J.D., Ravat, D., Smith, R., 2007. Tilt-depth method: A simple depth estimation method using first-order magnetic derivatives. The Leading Edge, 26, 1502-1505. http://dx.doi.org/10.1190/1.2821934.

Sánchez-García, T., Pereira, M.F., Bellido, F., Chichorro, M., Silva, J.B.,Valverde-Vaquero, P., Pin, C., Solá, A.R., 2014. Early Cambrian granitoids of North Gondwana margin in the transition from a convergent setting to intra-continental rifting (Ossa-Morena Zone, SW Iberia). International Journal of Earth Sciences, 103, 1203-1218. https://doi.org/10.1007/s00531-013-0939-8.

Santallier, D., Briand, B., Ménot, R.P., Piboule, M., 1988. Les complexes leptyno-amphiboliques (C.L.A.): revue critique et suggestions pour un meilleur emploi de ce terme. Bulletin de la Société Géologique de France, 4, 3-12. https://doi.org/10.2113/gssgfbull.IV.1.3

Schmädicke, E., Mezger, K., Cosca, M.A., Okrusch, M., 1995. Variscan Sm-Nd and Ar-Ar ages of eclogite facies rocks from the Erzgebirge, Bohemian Massif. Journal of Metamorphic Geology, 13, 537-552. https://doi.org/10.1111/j.1525-1314.1995.tb00241.x.

Schneider, J., Corsini, M., Reverso-Peila, A., Lardeaux, J.M., 2014. Thermal and mechanical evolution of an orogenic wedge during Variscan collsion: an example in the Maures-Tanneron Massif (SE France). In: Schulmann, K., Martínez Catalán, J.R., Lardeaux, J.M., Janousek, V. and Oggiano, G. (Eds.), The Variscan Orogeny: Extent, Timescale and the Formation of the European Crust. Geological Society, London, Special Publications, 405, 313-331. http://dx.doi.org/10.1144/SP405.4.

Schulmann, K., Ledru, P., Autran, A., Melka, R., Lardeaux, J.M., Urban, M., Lobkowicz, M., 1991. Evolution of nappes in the eastern margin of the Bohemian Massif—a kinematic interpretation. Geologische Rundschau, 80,73-92.

Schulmann, K., Kröner, A., Hegner, E., Wendt, I., Konopásek, J., Lexa, O., Štípská, P., 2005. Chronological constraints on the pre-orogenic history, burial and exhumation of deep-seated rocks along the eastern margin of the Variscan orogen, Bohemian Massif, Czech Republic. American Journal of Science, 305, 407-448. https://doi.org/10.2475/ajs.305.5.407.

Schulmann, K., Konopásek, J., Janousek, V., Lexa, O., Lardeaux, J.-M., Edel, J.-B., Štípská, P., Ulrich, S., 2009. An Andean type Palaeozoic convergence in the Bohemian Massif. Comptes Rendus Geoscience, 341, 266-286. https://doi.org/10.1016/j.crte.2008.12.006.

Schulmann, K., Lexa, O., Janousek, V., Lardeaux, J.-M. and Edel, J.-B., 2014. Anatomy of a diffuse cryptic suture: An example from the Bohemian Massif, European Variscides. Geology, 42 (4), 275-278. https://doi.org/10.1130/G35290.1.

Séranne M., 1999. The Gulf of Lion continental margin (NW Mediterranean) revisited by IBS: an overview. In: B. Durand, L. Jolivet, F. Horvat. and M. Séranne (Eds.), The Mediterranean basins: Tertiary extension within the Alpine Orogen. Geol. Soc. London Spec. Publ., 156: 15-36.

Shail, R.K., Leveridge, B.E., 2009. The Rhenohercynian passive margin of SW England: Development, inversion and extensional reactivation. Comptes Rendus Geoscience, 341, 140-155. https://doi.org/10.1016/j.crte.2008.11.002.

Shaw, J., Johnston, S.T., Gutiérrez-Alonso, G., Weil, A.B., 2012 Oroclines of the Variscan orogen of Iberia: Paleocurrent analysis and paleogeographic implications. Earth and Planetary Science Letters, 329-330, 60-70. https://doi.org/10.1016/j.epsl.2012.02.014.

Sichien, E., J. P. Henriet, T. Camelbeeck, and B. De Baets (2012), Estimating crustal thickness in Belgium and surrounding regions from Moho-reflected waves, Tectonophysics, 560-561, 105-119.

Silva, J.B., Oliveira, J.T., Ribeiro, A., 1990. South Portuguese Zone. Structural outline. In: Dallmeyer, R.D. and Martínez García, E. (Eds.), Pre-Mesozoic Geology of Iberia. Springer-Verlag, Berlin, 348-362.

Simancas, F., Carbonell, R., González Lodeiro, F., Pérez-Estaún, A., Juhlin, C., Ayarza, P., Kashubin, A., Azor, A., Martínez Poyatos, D., Almodóvar, G.R., Pascual, E., Sáez, R., Expósito, I., 2003. Crustal structure of the transpressional Variscan orogen of SW Iberia: SW Iberia deep seismic reflection profile (IBERSEIS). Tectonics, 22, 1-19. https://doi.org/10.1029/2002TC001479.

Simancas, J.F., Tahiri, A., Azor, A., González Lodeiro, F., Martínez Poyatos, D., El Hadi, H., 2005. The tectonic frame of the Variscan-Alleghanian orogen in Southern Europe and Northern Africa. Tectonophysics, 398, 181-198. https://doi.org/10.1016/j.tecto.2005.02.006.

Simancas, J.F., Carbonell, R., González-Lodeiro, F., Pérez-Estaún, A., Juhlin, C., Ayarza, P., Kashubin, A., Azor, A., Martínez Poyatos, D., Sáez, R., Almodóvar, G.R., Pascual, E., Flecha, I., Marti, D., 2006. Transpressional collision tectonics and mantle plume dynamics: the Variscides of Southwestern Iberia. Geological Society, London, Memoirs, 32, 345-354. https://doi.org/10.1144/GSL.MEM.2006.032.01.21.

Sintubin, M., Debacker, T.N., Van Baelen, H., 2009. Early Palaeozoic orogenic events north of the Rheic suture (Brabant, Ardenne): A review. Comptes Rendus Geoscience, 341, 156-173, https://doi.org/10.1016/j.crte.2008.11.012.

Skrzypek, E., Schulmann, K., Štípská, P., Chopin, F., Lehmann, J., Lexa, O., Haloda, J., 2011. Tectonometamorphic history recorded in garnet porphyroblasts: insights from thermodynamic modelling and electron backscatter diffraction analysis of inclusion trails. Journal of Metamorphic Geology, 29, 473-496. https://doi.org/10.1111/j.1525-1314.2010.00925.x.

Skrzypek, E., Štípská, P., Cocherie, A., 2012a. The origin of zircon and the significance of U-Pb ages in high-grade metamorphic rocks: a case study from the Variscan orogenic root (Vosges Mountains, NE France). Contributions to Mineralogy and Petrology, 164, 935-957. https://doi.org/10.1007/s00410-012-0781-1.

Skrzypek, E., Tabaud, A.S., Edel, J.B., Schulmann, K., Cocherie, A., Guerrot, C., Rossi, P., 2012b. The significance of Late Devonian ophiolites in the Variscan orogen: a record from the Vosges Klippen Belt. International Journal of Earth Sciences, 101, 951-972. https://doi.org/10.1007/s00531-011-0709-4

Skrzypek, E., Schulmann, K., Tabaud, A. S. and Edel, J.B., 2014. Palaeozoic evolution of the Variscan Vosges Mountains. In: Schulmann, K., Martínez Catalán, J.R., Lardeaux, J.M., Janoušek, V. and Oggiano, G. (Eds.), The Variscan Orogeny: Extent, Timescale and the Formation of the European Crust. Geological Society, London, Special Publications, 405, 45-75. http://dx.doi.org/10.1144/SP405.8.

Smit, J., Wees, J.D.V. and Cloetingh, S., 2016. The Thor suture zone: From subduction to intraplate basin setting. Geology, 44, 707-710. https://doi.org/10.1130/G37958.1.

Spalla, M.I., Zanoni, D., Marotta, A.M., Rebay, G., Roda, M., Zucali, M., Gosso, G., 2014. The transition from Variscan collision to continental break-up in the Alps: insights from the comparison between natural data and numerical model predictions. Geological

Society, London, Special Publications, 405, 363-400. http://dx.doi.org/10.1144/SP405.11.

Stampfli, G.M., Hochard, C., Vérard, C., Wilhem, C., von Raumer, J., 2013. The formation of Pangea. Tectonophysics, 593, 1-19. https://doi.org/10.1016/j.tecto.2013.02.037.

Staub, R., 1926. Gedanken zum Strukturbild Spaniens. XIV Congrès Géologique International, 3, 949-996.

Šalanský, K., 1995. Magnetic map of the Czech Republic. Český geologický ústav, Praha.

Štípská, P., Schulmann, K., Racek, M., Lardeaux, J.M., Hacker, B.R., Kylander-Clark, A.R.C., Holder, R., Košuličová, M., 2020. Finite pattern of Barrovian metamorphic zones: interplay between thermal reequilibration and post-peak deformation during continental collision—insights from the Svratka dome (Bohemian Massif). International Journal of Earth Sciences, 109, 1161-1187. https://doi.org/10.1007/s00531-019-01788-6.

Suess, F.E., 1912. Die Moravischen Fenster und ihre Beziehungen zum Grundgebirge des hohen Gesenkes. Denkschrift der Kaiserlichen Akademie der Wissenschaften in Wien, Mathematisch-Naturwissenschaftliche Klasse (Math.-nat. Kl.), 88, 541-631.

Tollmann, A., 1982. Großräumiger variszischer Deckenbau im Moldanubikum und neue Gedanken zum Variszikum Europas. Geotektonische Forschungen, v. 64, p. 1–91. ISBN 978-3-510-50030-7

Tomek, Č., 2007. Central parts of the Bohemian Massif revisited: new interpretation of deep reflection seismic line 9HR in West and South Bohemia. In: Special meeting of French and Czech Geological Societies "Mechanics of Variscan Orogeny: a modern view on orogenic research", Orleans September 2007. Géologie de la France, 2, 165.

Tomek, Č., Dvořáková, V., Vrána, S., 1997. Geological interpretation of the 9HR and 503 M seismic profiles in western Bohemia. Geological model of western Bohemia related to the KTB borehole in Germany. Czech Geological Survey, 43-51.

Vanderhaeghe, O., Laurent, O., Gardien, V., Moyen, J.F., Gébelin, A., Chelle-Michou, C., Couzinié, S., Villaros, A., Bellanger, M., 2020. Flow of partially molten crust controlling construction, growth and collapse of the Variscan orogenic belt: the geologic record of the French Massif Central. Bulletin de la Société Géologique de France, 191. https://doi.org/10.1051/bsgf/2020013 .

Veludo, I., Dias, N.A., Fonseca, P.E., Matias, L., Carrilho, F., Haberland, C., Villaseñor, A., 2017. Crustal seismic structure beneath Portugal and southern Galicia (Western Iberia) and the role of Variscan inheritance. Tectonophysics, 717, 645-664. https://doi.org/10.1016/j.tecto.2017.08.018.

Venera, Z., Schulmann, K. and Kröner, A., 2000. Intrusion within a transtensional tectonic domain: the Čistá granodiorite (Bohemian Massif) – structure and rheological modelling. Journal of Structural Geology, 22, 1437-1454. https://doi.org/10.1016/S0191-8141(00)00054-7.

Verduzco, B., J. D. Fairhead, C. M. Green, and C. MacKenzie (2004), New insights into magnetic derivatives for structural mapping, Leading Edge (Tulsa, OK), 23(2), 116-119.

Verner, K., Žák, J., Šrámek, J., Paclíková, J., Zavřelová, A., Machek, M., Finger, F., Johnson, K., 2014. Formation of elongated granite–migmatite domes as isostatic accommodation structures in collisional orogens. Journal of Geodynamics, 73, 100–117. https://doi.org/10.1016/j.jog.2013.10.002.

Vollbrecht, A., Weber, K., Schmoll, J., 1989. Structural model for the Saxothuringian-Moldanubian suture in the Variscan basement of the Oberpfalz (Northeastern Bavaria, F.R.G.) interpreted from geophysical data. Tectonophysics, 157, 123-133. https://doi.org/10.1016/0040-1951(89)90346-6.

Von Raumer JF, Abrecht J, Bussy F, Lombardo B, Ménot RP, Schaltegger, U., 1999. The Palaeozoic metamorphic evolution of the Alpine External Massifs. Schweiz Miner Petrogr Mitt 79, 5–22.

Von Raumer JF, Bussy F, Stampfli, G.M. 2009. The Variscan evolution in the External massifs of the Alps and place in their Variscan framework. C. R. Geosci. 341, 239–252.

Von Raumer, J.F., Bussy, F., Schaltegger, U., Schulz, B., Stampfli, G.M., 2013. Pre-Mesozoic Alpine basements – their place in the European Paleozoic framework. Geol. Soc. Am. Bull. 125, 89–108.

Vos, I. M. A., F. P. Bierlein, M. A. Barlow, and P. G. Betts (2007), Resolving the nature and geometry of major fault systems from geophysical and structural analysis: The Palmerville Fault in NE Queensland, Australia, Journal of Structural Geology, 28(11), 2097-2108.

Wenzel, F., Brun, J.P., Blum, R, ECORS-DEKORP working group, 1991. A deep reflection seismic line across the northern Rhine Graben. Earth And Planetary Science Letters, 104, 140-150. https://doi.org/10.1016/0012-821X(91)90200-2.

Wilde-Piórko, M., Saul, J., Grad, M., 2005. Differences in the crustal and uppermost mantle structure of the Bohemian Massif from teleseismic receiver functions. Studia Geophysica et Geodaetica, 49, 85-107. https://doi.org/10.1007/s11200-005-1627-3.

Winchester, J.A., Pharaoh, T.C., Verniers, J., 2002. Palaeozoic amalgamation of Central Europe: an introduction and synthesis of new results from recent geological and geophysical investigations. In: Winchester, J.A., Pharaoh, T.C. and Verniers, J. (Eds.), Palaeozoic Amalgamation of Central Europe. Geological Society, London, Special Publications, 201, 1-18. http://dx.doi.org/10.1144/GSL.SP.2002.201.01.01.

Wonik, T., Hahn, A., 1990. Compilation of the Central and Northern European aeromagnetic surveys: methods, difficulties, and results. In: Freeman, R. and Mueller, S. (Eds.), Proceedings of the Sixth Workshop European Geotraverse (EGT): Data Compilations and Synoptic Interpretation. European Science Foundation, Strasbourg, 213-224.

Wybraniec, S., 1999. Transformation and visualization of potential field data. Polish Geological Institute Special Paper 1, 1-88.

Žák, J., Verner, K., Finger, F., Faryad, S.W., Chlupáčová, M., Veselovský, F., 2011. The generation of voluminous S-type granites in the Moldanubian unit, Bohemian Massif, by rapid isothermal exhumation of the metapelitic middle crust. Lithos, 121, 25-40. https://doi.org/10.1016/j.lithos.2010.10.002.

Žák, J., Verner, K., Sláma, J., Kachlík, V., Chlupáčová, M., 2013. Multistage magma emplacement and progressive strain accumulation in the shallow-level Krkonoše-Jizera plutonic complex, Bohemian Massif. Tectonics, 32, 1493-1512. https://doi.org/10.1002/tect.20088.

Žák, J., Verner, K., Janoušek, V., Holub, F.V., Kachlík, V., Finger, F., Hajná, J., Tomek, F., Vondrovic, L. and Trubač, J., 2014. A plate-kinematic model for the assembly of the Bohemian Massif constrained by structural relationships around granitoid plutons. In: Schulmann, K., Martínez Catalán, J.R., Lardeaux, J.M., Janousek, V. and Oggiano, G. (Eds.), The Variscan Orogeny: Extent, Timescale and the Formation of the European

Crust. Geological Society, London, Special Publications, 405, 169-196. http://dx.doi.org/10.1144/SP405.9.

Žák, J., Verner, K., Ježek, J., Trubač, J., 2019. Complex mid-crustal flow within a growing granite–migmatite dome: An example from the Variscan belt illustrated by the anisotropy of magnetic susceptibility and fabric modelling. Geological Journal, 54, 3681-3699. https://doi.org/10.1002/gj.3335.

Závada, P., Štípská, P., Hasalová, P., Racek, M., Jeřábek, P., Schulmann, K., Kylander-Clarke, A., Holder, R., 2021. Monazite geochronology in melt-percolated UHP meta-granitoids: An example from the Erzgebirge continental subduction wedge, Bohemian Massif. Chemical Geology, 559, 119919. https://doi.org/10.1016/j.chemgeo.2020.119919.

Zeh, A., Gerdes, A., 2010. Baltica- and Gondwana-derived sediments in the Mid-German Crystalline Rise (Central Europe): Implications for the closure of the Rheic ocean. Gondwana Research, 17, 254-263. https://doi.org/10.1016/j.gr.2009.08.004.

Zeh, A., Will, T., 2010. The Mid-German Crystalline Zone. In: Linnemann, U. and Romer, R.L. (Eds.), Pre-Mesozoic Geology of Saxo-Thuringia - From the Cadomian Active Margin to the Variscan Orogen. Stuttgart, 195-220

Zeis, S., Gajewski, D., Prodehl, C., 1990. Crustal structure of southern Germany from seismic refraction. Tectonophysics 176, 59-86. https://doi.org/10.1016/0040-1951(90)90259-B.

Zeyen, H., Novak, O., Landes, M., Prodehl, C., Driad, L., Hirn, A., 1997. Refraction-seismic investigations of the northern Massif Central (France). Tectonophysics, 275, 99-117. https://doi.org/10.1016/S0040-1951(97)00017-6.

Table 1

Seismic methods	Location	Seismic experiment	Figures	References
REFRACTION	Polish Variscan – East European Craton	POLONAISE '97, P4	Fig.2 (1); Figs.12 and 17	Grad et al. 2003
	Bohemian Massif	S01 S02 S03 S05 S06	Fig.12	Grad et al. 2008
		S04	Fig.2 (2)	Hrubcová et al. 2010
		CEL09 CEL03	Fig.2 (3); Fig.10	Hrubcová et al. 2005 Růžek et al. 2007 Hrubcová and Geissler 2009
		Alp01	Fig.12	Brückl et al. 2007
		GRANU	Fig.12	Enderle et al. 1998
		MVE	Fig.12	Mueller 1995
		Alp04	Fig.12	Hrubcová et al. 2008
		P3	Fig.12	Grad et al. 2003
		P1	Fig.12	Grad et al. 2008
		S10	Fig.12	Hrubcová et al. 2010
		CEL10	Fig.12	Hrubcová et al. 2008
		CEL02	Fig.12	Malinowski et al. 2005
	Southern Germany	EGT	Fig.2 (4),(5); Fig.12	Aichroth et al. 1992 Bleibinhaus et al. 1999 Gajewski et al. 1987 Zeis et al. 1990
	Eastern Germany	Rhenish Massif	Fig.2 (6); Fig.12	Mechie et al. 1982
		Black Forest	Fig.2 (7); Fig.12	Gajewski and Prodehl 1987
	Vosges and upper Rhinegraben	-	Fig.2 (8); Fig.12	Edel et al. 1975
	Southern England	DELTA	Fig.2 (9); Fig.12	Maguire et al. 2011
	Western France	ARMOR-1	Fig.2 (9); Fig.12	Grandjean et al. 2001
	Massif Central	-	Fig.2 (9); Fig.12	Zeyen et al. 1997
	Northwestern Iberia	ESCIN	Fig.2 (10); Fig.12	Ayarza et al. 1998 Córdoba et al. 1987 Fernández-Viejo et al. 2000 Veludo et al. 2017
	Northern and central western Iberia	ESCIN	Fig.2 (11); Fig.12	Pulgar et al. 1996 Fernández-Viejo et al. 2000

				Veludo et al. 2017
	Southern Iberia	IBERSEIS	Fig.2 (12)(13); Fig.12	Palomeras et al. 2009
	Southern-Central Iberia	ALCUDIA	Fig.2 (14); Fig.12	Ehsan et al. 2015
REFLECTION	Bohemian Massif	Boh9HR	Fig.2; Fig. 10	Tomek et al. 1997 Tomek 2007
	Southern Germany	DEKORP-2N	Fig.2; Fig. 11a	Franke et al. 1990
		DEKORP-2S	Fig.2; Fig. 11a	Franke et al. 1990
	Saar-Nahe trough, Northern Vosges, Southern Vosges	DEKORP-1C	Fig.2; Fig. 11a	Lüschen et al. 1987 DEKORP and Orogenic Processes Working Group 1999
		ECORS-DEKORP	Fig.2; Fig. 11a	Brun and Wenzel 1991 Wenzel et al. 1991
	Northern France	ECORS NF	Fig.2; Fig. 11a	Cazes et al. 1985 Damotte and Bois 1990
	English Channel, Northern Armorican Massif	SWAT 2-3, 6-7, 9, 10	Fig.2; Fig. 11b	Le Gall 1990, 1991
		ARMOR-1	Fig.2; Fig. 11b	Bitri 2001
	Southern Armorican Massif	ARMOR-2	Fig.2; Fig. 11b	Bitri et al. 2003, 2010
	Cantabrian Zone	ESCIN-1	Fig.2; Fig. 11c	Pérez-Estaún et al. 1994, 1995
	Northernwestern Iberia	ESCIN-3	Fig.2; Fig. 11c	Álvarez-Marrón et al. 1995, 1996 Martínez Catalán et al. 1995 Ayarza et al. 1998
	Southern and Central Iberia	IBERSEIS	Fig.2; Fig. 11c	Simancas et al. 2003
		ALCUDIA	Fig.2; Fig. 11c	Ehsan et al. 2014

Declaration of interests

☒The authors declare that they have no known competing financial interests or personal relationships that could have appeared to influence the work reported in this paper.

☐The authors declare the following financial interests/personal relationships which may be considered as potential competing interests:

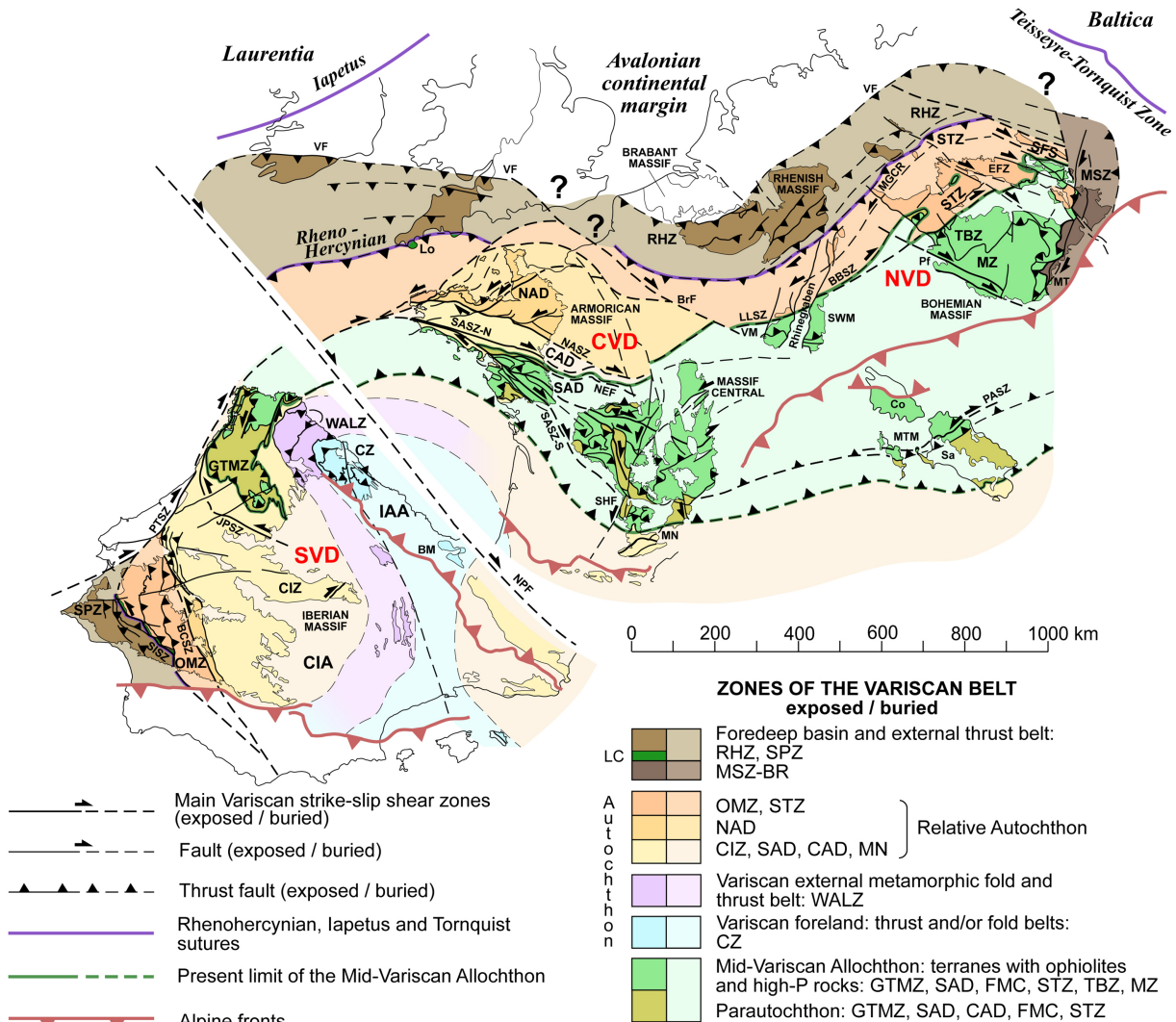
Laurentia
Iapetus
Avalonian continental margin
Baltica
Teisseyre-Tornquist Zone
Rheno-Hercynian
VF
Lo
BRABANT MASSIF
RHENISH MASSIF
RHZ
STZ
MGCR
SFS
EFZ
MSZ
TBZ
MZ
Pf
MT
NVD
BOHEMIAN MASSIF
NAD
ARMORICAN MASSIF
BrF
LLSZ
VM
Rhinegraben
BBSZ
SWM
SASZ-N
NASZ
CAD
CVD
SAD
NEF
MASSIF CENTRAL
Co
PASZ
MTM
Sa
SASZ-S
SHF
MN
WALZ
CZ
GTMZ
PTSZ
JPSZ
IAA
BM
SVD
CIZ
IBERIAN MASSIF
SPZ
BCSZ
OMZ
CIA
NPF
0
200
400
600
800
1000 km
ZONES OF THE VARISCAN BELT
exposed / buried
LC
Foredeep basin and external thrust belt:
RHZ, SPZ
MSZ-BR
Autochthon
OMZ, STZ
NAD
CIZ, SAD, CAD, MN
Relative Autochthon
Variscan external metamorphic fold and thrust belt: WALZ
Variscan foreland: thrust and/or fold belts: CZ
Mid-Variscan Allochthon: terranes with ophiolites and high-P rocks: GTMZ, SAD, FMC, STZ, TBZ, MZ
Parautochthon: GTMZ, SAD, CAD, FMC, STZ
Main Variscan strike-slip shear zones (exposed / buried)
Fault (exposed / buried)
Thrust fault (exposed / buried)
Rhenohercynian, Iapetus and Tornquist sutures
Present limit of the Mid-Variscan Allochthon
Alpine fronts

Figure 1

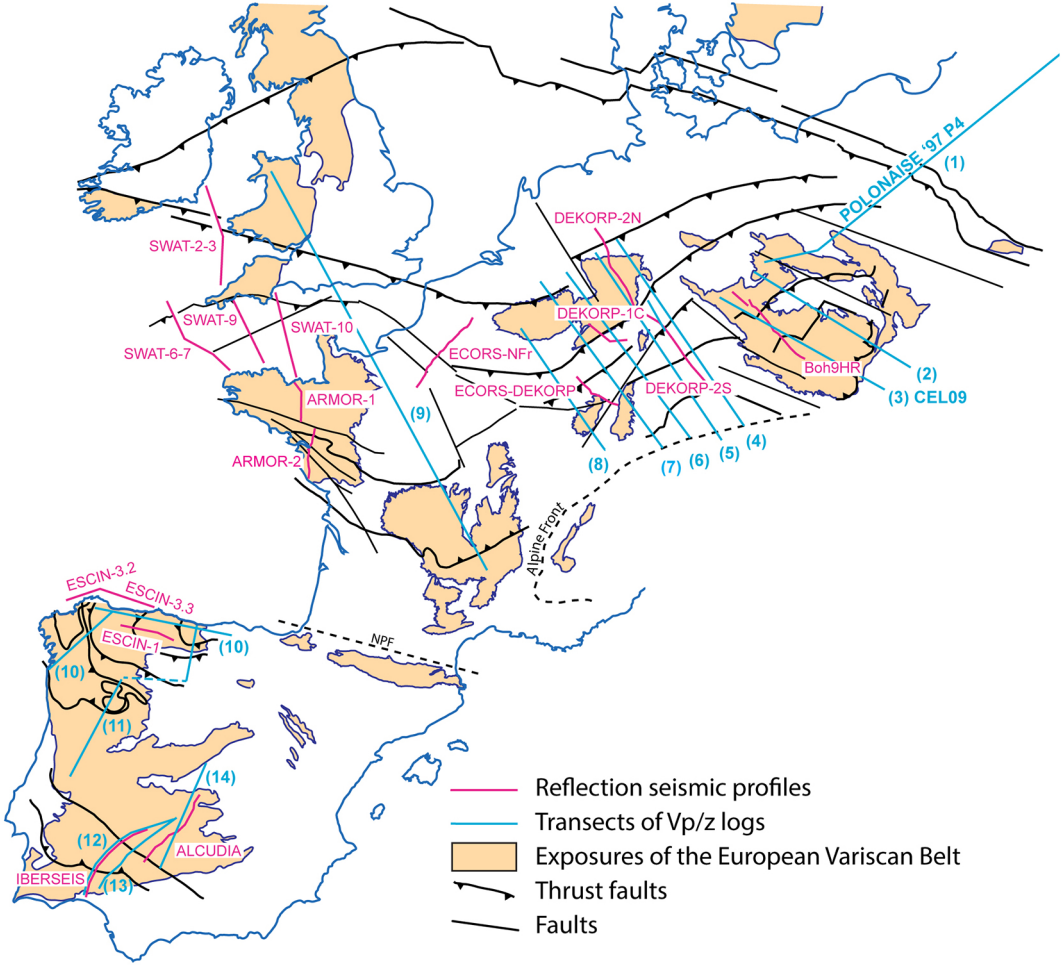
SWAT-2-3
SWAT-9
SWAT-10
SWAT-6-7
ECORS-NFr
ARMOR-1
ARMOR-2
(9)
DEKORP-2N
DEKORP-1C
ECORS-DEKORP
DEKORP-2S
POLONAISE '97 P4
(1)
Boh9HR
(2)
(3) CEL09
(4)
(5)
(6)
(7)
(8)
Alpine Front
NPF
ESCIN-3.2
ESCIN-3.3
ESCIN-1
(10)
(11)
(12)
(13)
(14)
ALCUDIA
IBERSEIS
Reflection seismic profiles
Transects of Vp/z logs
Exposures of the European Variscan Belt
Thrust faults
Faults

Figure 2

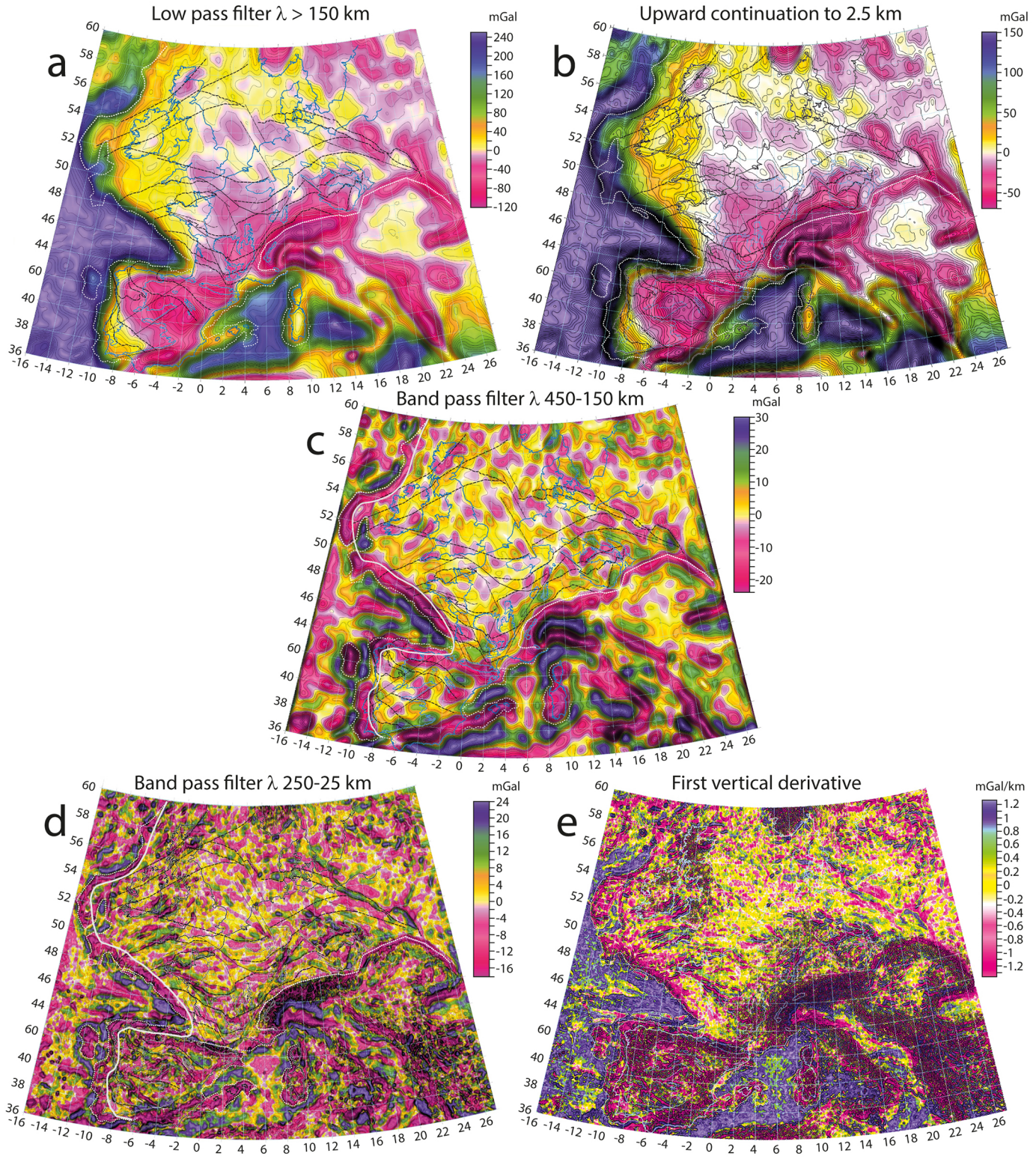
a
Low pass filter λ > 150 km
mGal
240
200
160
120
80
40
0
-40
-80
-120
b
Upward continuation to 2.5 km
mGal
150
100
50
0
-50
c
Band pass filter λ 450-150 km
mGal
30
20
10
0
-10
-20
d
Band pass filter λ 250-25 km
mGal
24
20
16
12
8
4
0
-4
-8
-12
-16
e
First vertical derivative
mGal/km
1.2
1
0.8
0.6
0.4
0.2
0
-0.2
-0.4
-0.6
-0.8
-1
-1.2

Figure 3

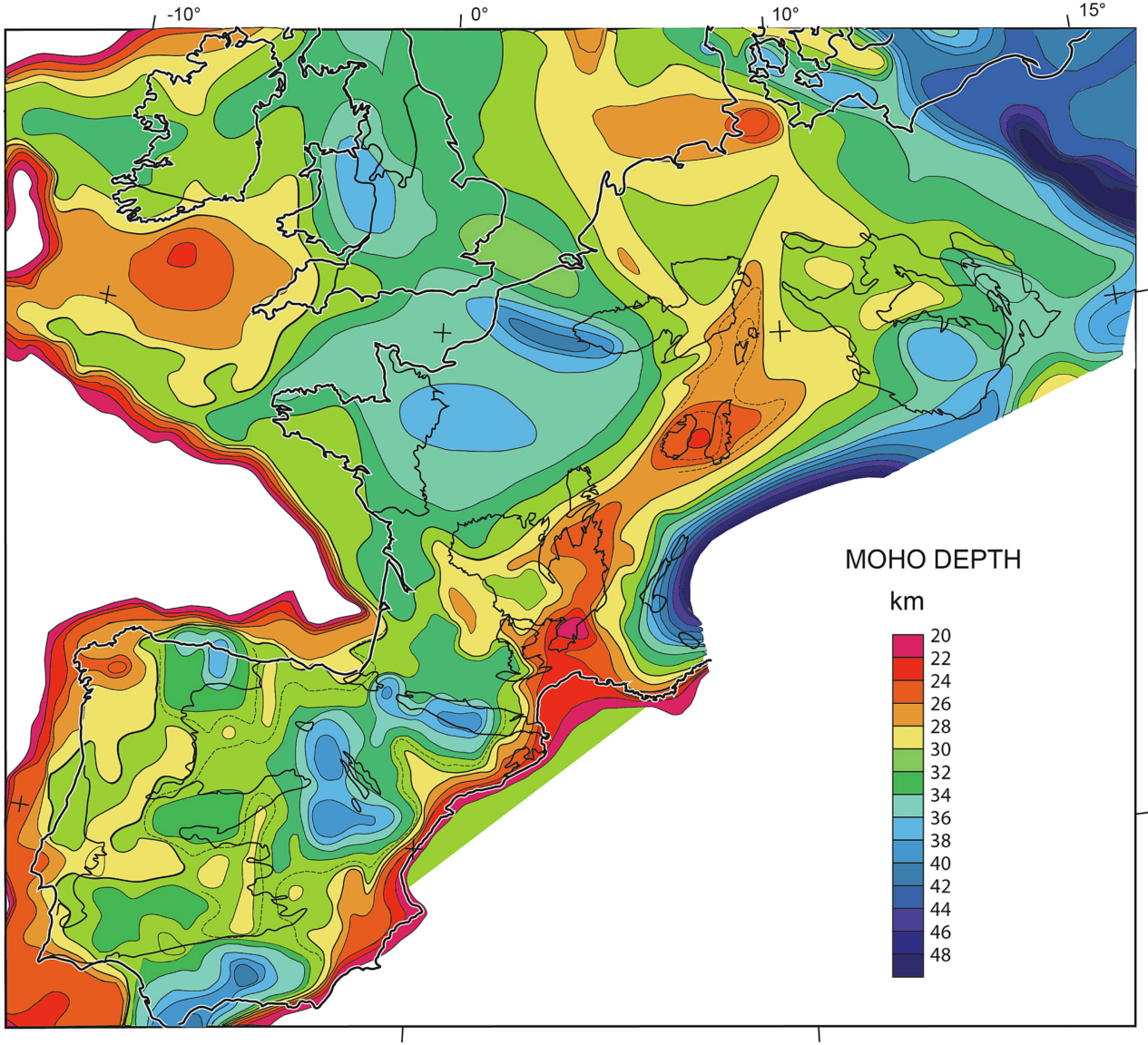
-10°
0°
10°
15°
50°
40°
MOHO DEPTH
km
20
22
24
26
28
30
32
34
36
38
40
42
44
46
48

Figure 4

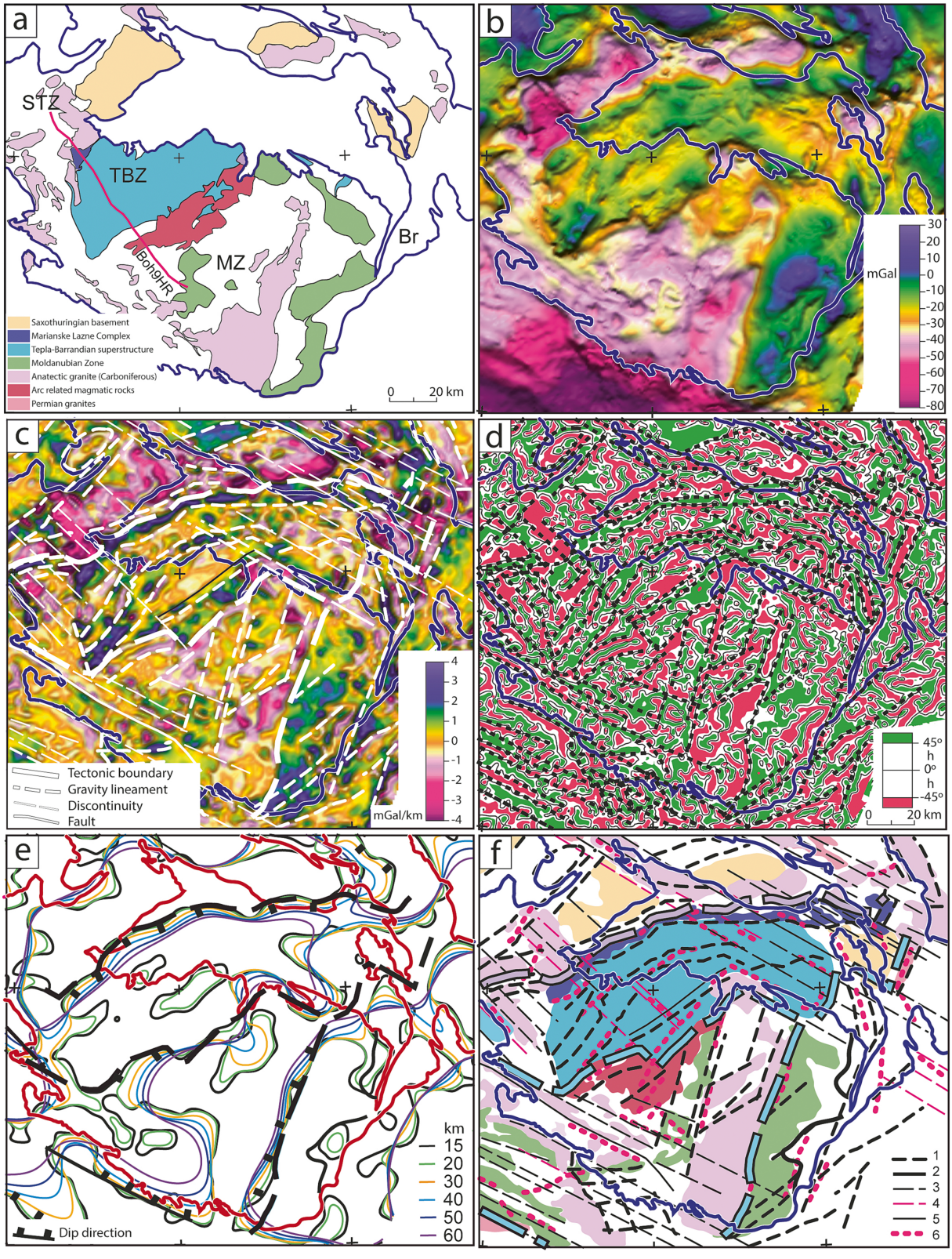
a
STZ
TBZ
MZ
Br
Boh9HR
Saxothuringian basement
Marianske Lazne Complex
Tepla-Barrandian superstructure
Moldanubian Zone
Anatectic granite (Carboniferous)
Arc related magmatic rocks
Permian granites
0
20 km
b
mGal
30
20
10
0
-10
-20
-30
-40
-50
-60
-70
-80
c
Tectonic boundary
Gravity lineament
Discontinuity
Fault
mGal/km
4
3
2
1
0
-1
-2
-3
-4
d
45°
h
0°
h
-45°
0
20 km
e
km
15
20
30
40
50
60
Dip direction
f
1
2
3
4
5
6

Figure 5

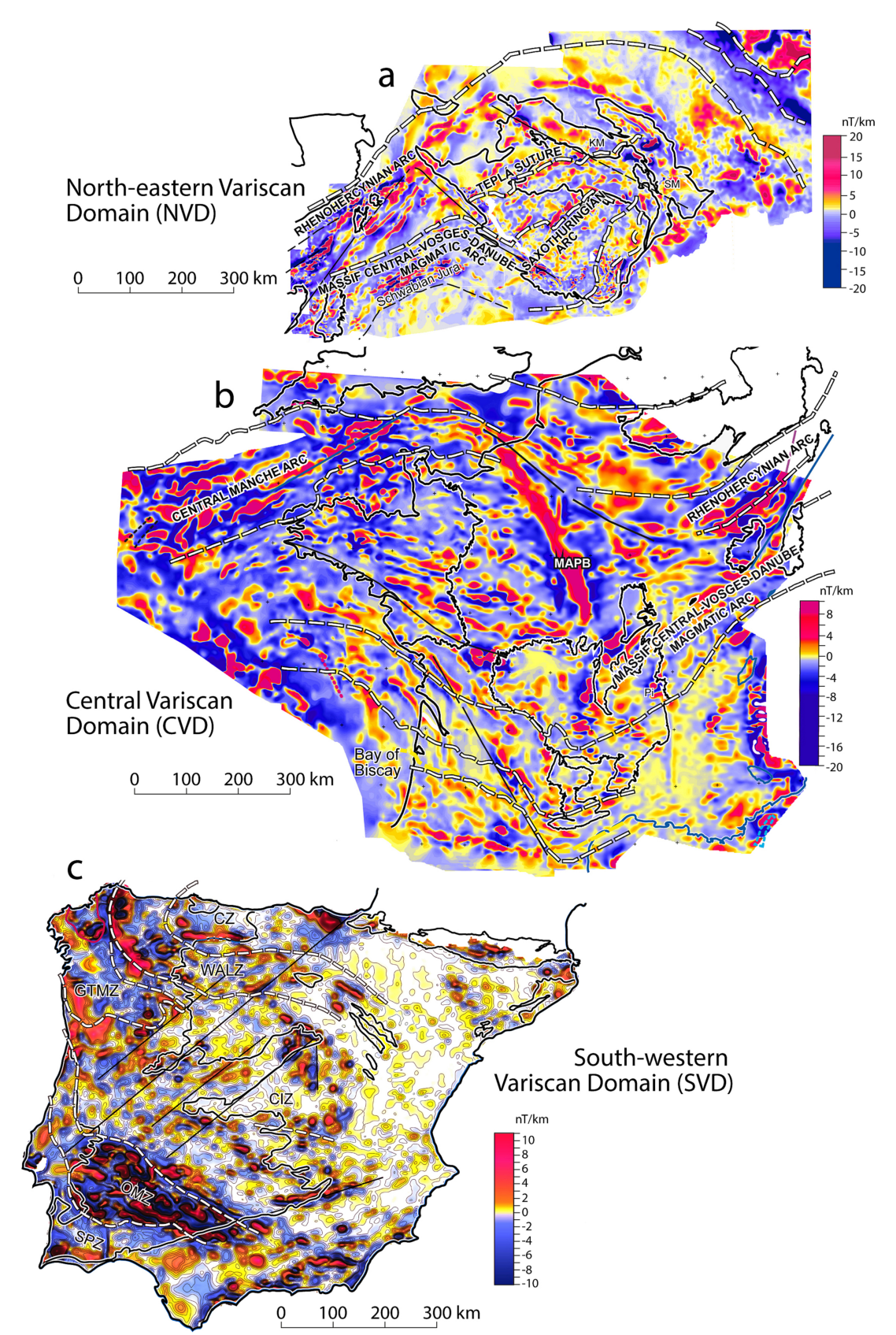
a
North-eastern Variscan Domain (NVD)
0 100 200 300 km
nT/km
20
15
10
5
0
-5
-10
-15
-20
RHENOHERCYNIAN ARC
TEPLÁ SUTURE
KM
SM
MASSIF CENTRAL-VOSGES-DANUBE MAGMATIC ARC
SAXOTHURINGIAN ARC
Schwabian Jura
b
CENTRAL MANCHE ARC
RHENOHERCYNIAN ARC
MAPB
MASSIF CENTRAL-VOSGES-DANUBE MAGMATIC ARC
PL
Central Variscan Domain (CVD)
0 100 200 300 km
Bay of Biscay
nT/km
8
4
0
-4
-8
-12
-16
-20
c
CZ
WALZ
GTMZ
CIZ
OMZ
SPZ
South-western Variscan Domain (SVD)
0 100 200 300 km
nT/km
10
8
6
4
2
0
-2
-4
-6
-8
-10

Figure 6

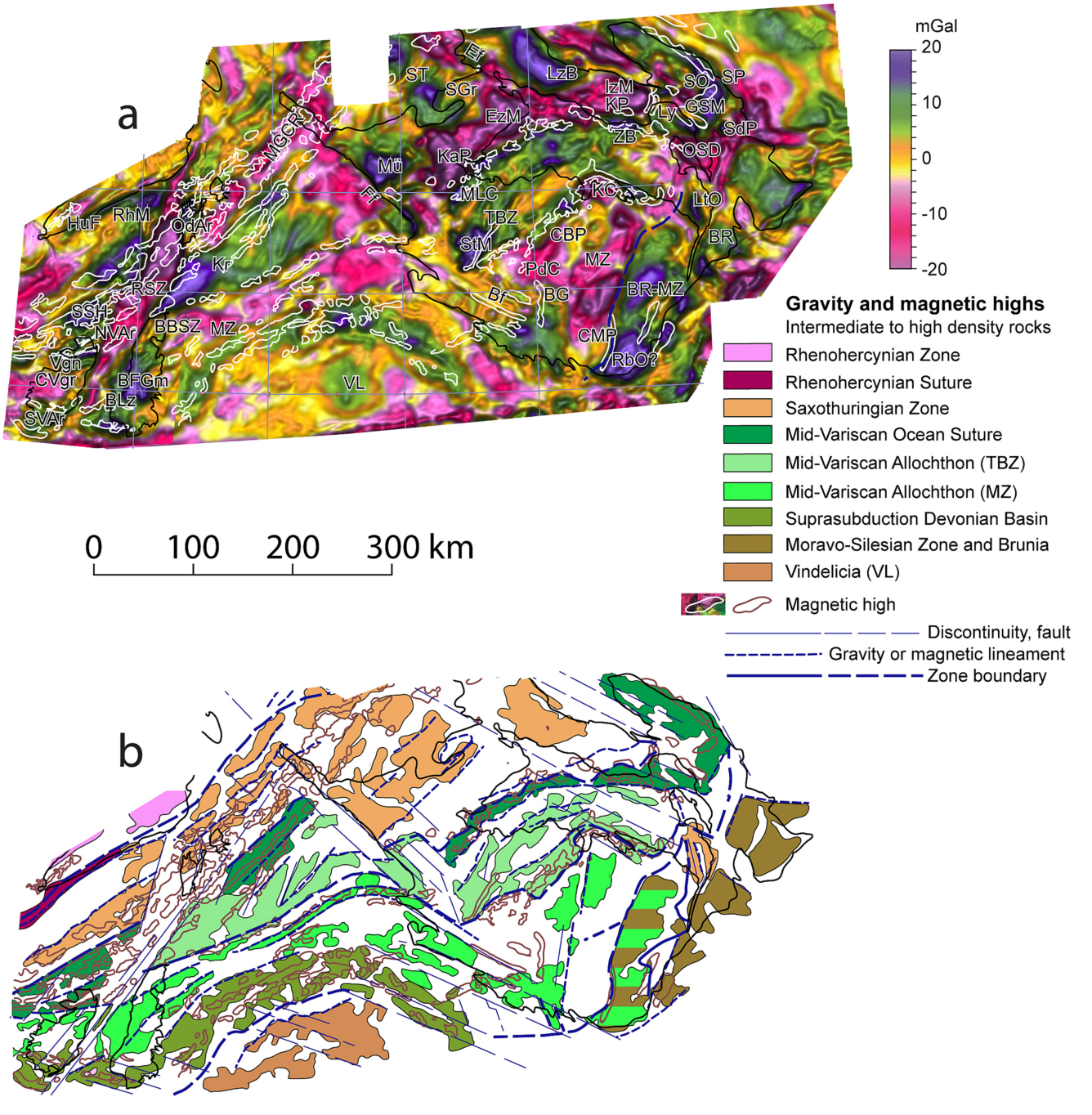
a
b
mGal
20
10
0
-10
-20
ST
SGr
Ef
LzB
IzM
KP
SO
SP
GSM
Ly
SdP
ZB
OSD
EzM
MGCR
KaP
Mü
Fr
MLC
KC
LtO
HuF
RhM
OdAr
TBZ
CBP
BR
StM
MZ
Kr
PdC
RSZ
Bf
BG
BR-MZ
SSHr
NVAr
BBSZ
MZ
CMP
RbO?
Vgn
CVgr
BFGm
VL
BLz
SVAr
0
100
200
300 km
Gravity and magnetic highs
Intermediate to high density rocks
Rhenohercynian Zone
Rhenohercynian Suture
Saxothuringian Zone
Mid-Variscan Ocean Suture
Mid-Variscan Allochthon (TBZ)
Mid-Variscan Allochthon (MZ)
Suprasubduction Devonian Basin
Moravo-Silesian Zone and Brunia
Vindelicia (VL)
Magnetic high
Discontinuity, fault
Gravity or magnetic lineament
Zone boundary

Figure 7

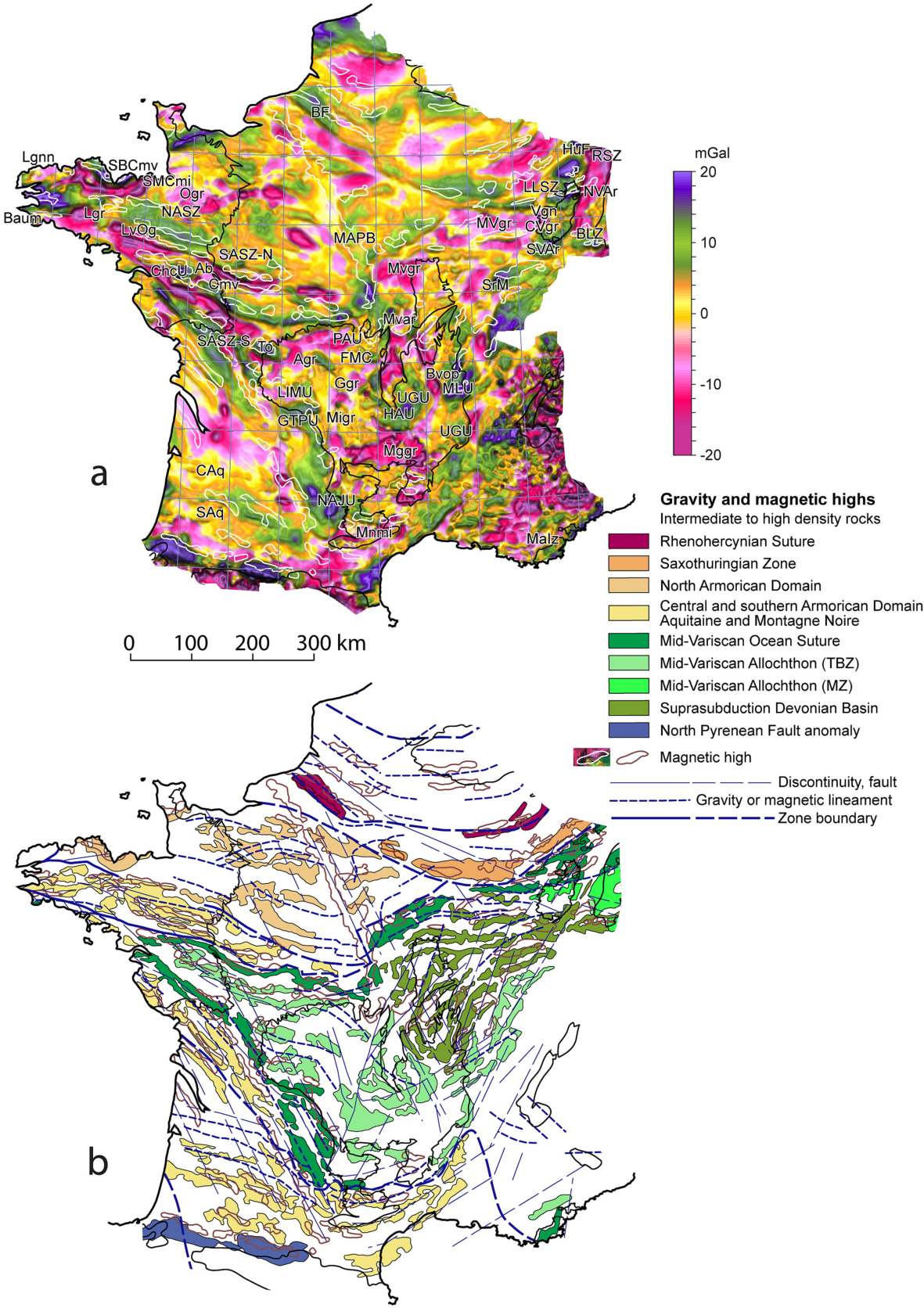
a
b
mGal
20
10
0
-10
-20
0 100 200 300 km
Lgnn
SBCmv
SMCmi
Ogr
NASZ
Lgr
Baum
LvOg
SASZ-N
ChcU
Ab
Cmv
SASZ-S
To
CAq
SAq
BF
MAPB
PAU
Agr
FMC
LIMU
Ggr
GTPU
Migr
NAJU
Mnmi
Mvgr
Mvar
SrM
UGU
HAU
Bvob
MLU
Mggr
HUF
RSZ
LLSZ
NVAr
Vgn
MVgr
CVgr
BtZ
SVAr
Malz
Gravity and magnetic highs
Intermediate to high density rocks
Rhenohercynian Suture
Saxothuringian Zone
North Armorican Domain
Central and southern Armorican Domain, Aquitaine and Montagne Noire
Mid-Variscan Ocean Suture
Mid-Variscan Allochthon (TBZ)
Mid-Variscan Allochthon (MZ)
Suprasubduction Devonian Basin
North Pyrenean Fault anomaly
Magnetic high
Discontinuity, fault
Gravity or magnetic lineament
Zone boundary

Figure 8

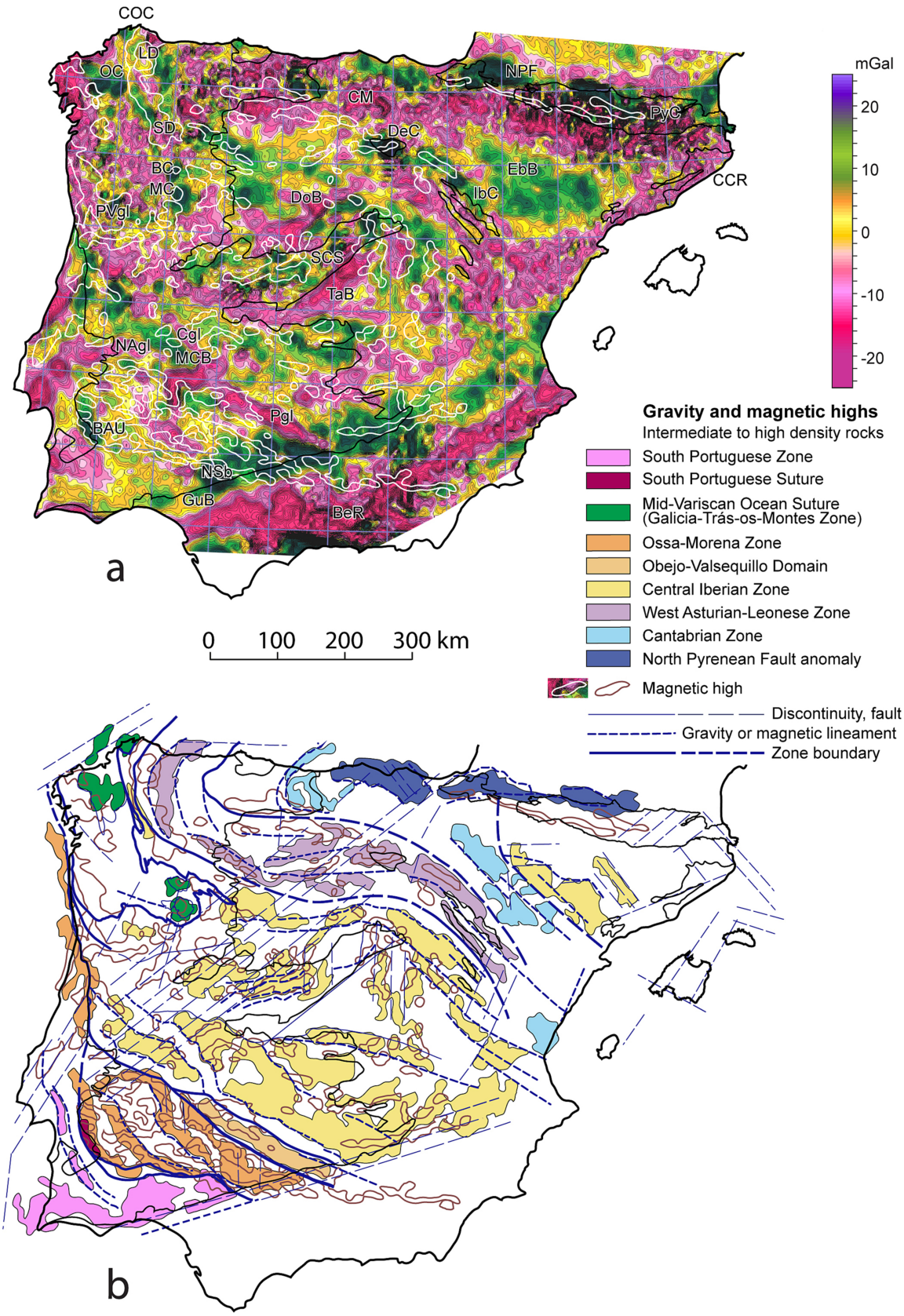
COC
LD
OC
NPF
CM
PyC
SD
DeC
EbB
CCR
BC
MC
IbC
DoB
PVgl
SCS
TaB
NAgl
Cgl
MCB
Pgl
BAU
NSb
GuB
BeR
a
mGal
20
10
0
-10
-20
0 100 200 300 km
Gravity and magnetic highs
Intermediate to high density rocks
South Portuguese Zone
South Portuguese Suture
Mid-Variscan Ocean Suture
(Galicia-Trás-os-Montes Zone)
Ossa-Morena Zone
Obejo-Valsequillo Domain
Central Iberian Zone
West Asturian-Leonese Zone
Cantabrian Zone
North Pyrenean Fault anomaly
Magnetic high
Discontinuity, fault
Gravity or magnetic lineament
Zone boundary
b

Figure 9

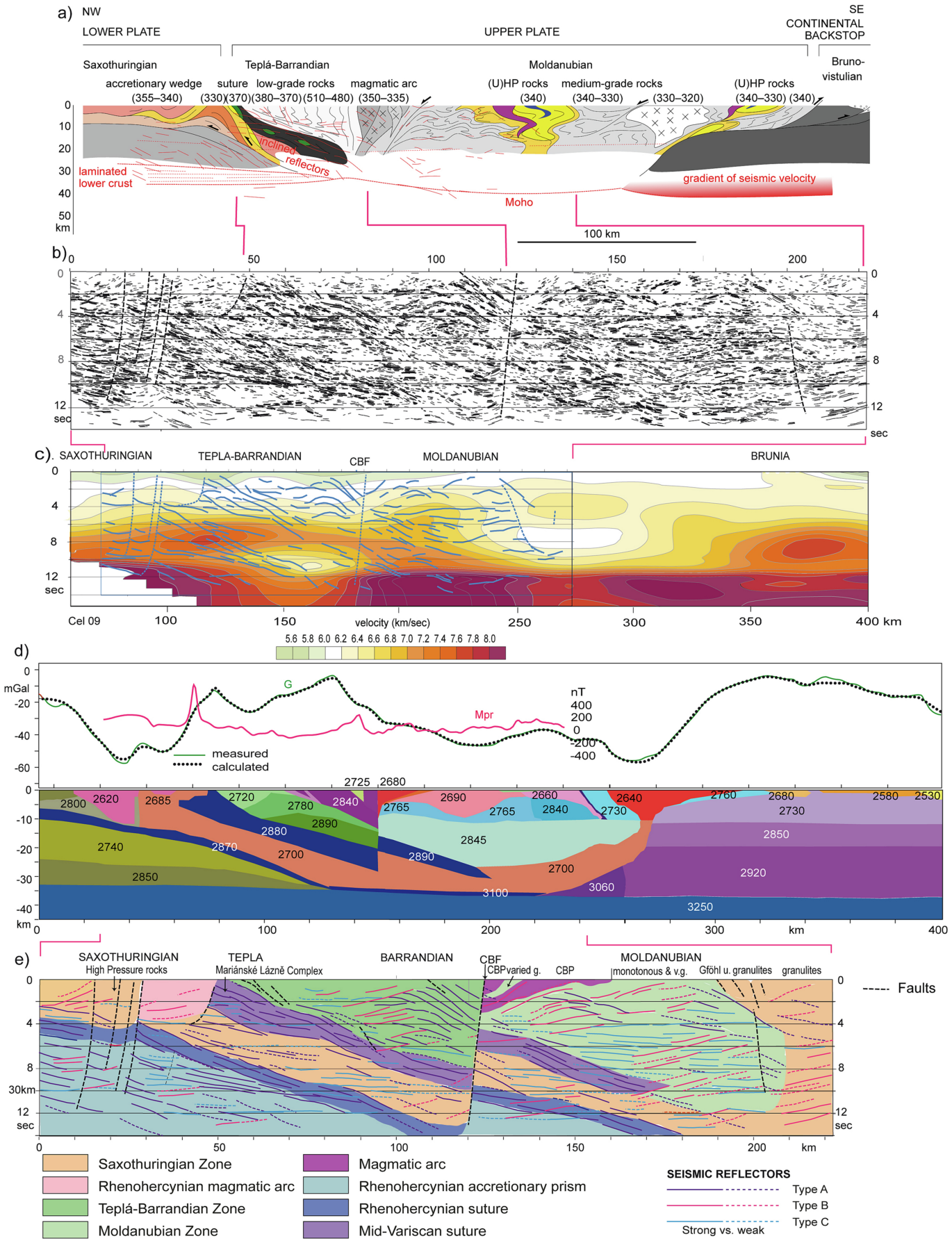
a)
NW
SE
LOWER PLATE
UPPER PLATE
CONTINENTAL BACKSTOP
Saxothuringian
Teplá-Barrandian
Moldanubian
Bruno-vistulian
accretionary wedge (355–340)
suture (330)
low-grade rocks (370)(380–370)
magmatic arc (510–480) (350–335)
(U)HP rocks (340)
medium-grade rocks (340–330)
(330–320)
(U)HP rocks (340–330) (340)
inclined reflectors
laminated lower crust
gradient of seismic velocity
Moho
km
100 km
b)
sec
c)
SAXOTHURINGIAN
TEPLA-BARRANDIAN
CBF
MOLDANUBIAN
BRUNIA
Cel 09
velocity (km/sec)
5.6 5.8 6.0 6.2 6.4 6.6 6.8 7.0 7.2 7.4 7.6 7.8 8.0
d)
mGal
G
Mpr
nT
measured
calculated
2725
2680
2800
2620
2685
2720
2780
2840
2890
2880
2740
2870
2700
2850
2690
2660
2765
2765
2840
2730
2640
2845
2890
2700
3100
3060
2760
2680
2730
2580
2530
2850
2920
3250
km
e)
SAXOTHURINGIAN
High Pressure rocks
TEPLA
Mariánské Lázně Complex
BARRANDIAN
CBF
CBP
varied g.
CBP
MOLDANUBIAN
monotonous & v.g.
Gföhl u. granulites
granulites
Faults
30km
Saxothuringian Zone
Rhenohercynian magmatic arc
Teplá-Barrandian Zone
Moldanubian Zone
Magmatic arc
Rhenohercynian accretionary prism
Rhenohercynian suture
Mid-Variscan suture
SEISMIC REFLECTORS
Type A
Type B
Type C
Strong vs. weak

Figure 10

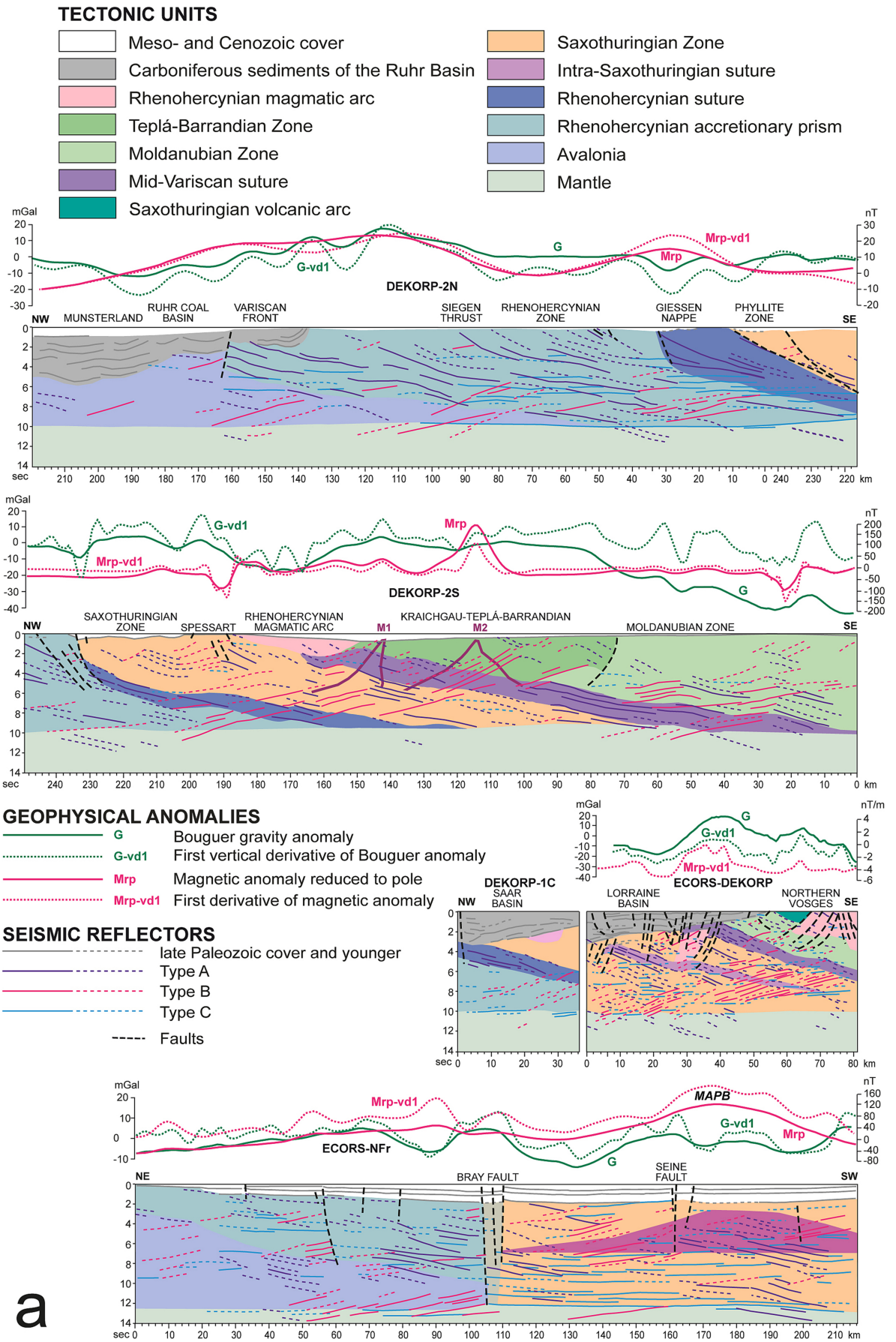
TECTONIC UNITS
Meso- and Cenozoic cover
Carboniferous sediments of the Ruhr Basin
Rhenohercynian magmatic arc
Teplá-Barrandian Zone
Moldanubian Zone
Mid-Variscan suture
Saxothuringian volcanic arc
Saxothuringian Zone
Intra-Saxothuringian suture
Rhenohercynian suture
Rhenohercynian accretionary prism
Avalonia
Mantle
mGal
nT
G
G-vd1
Mrp
Mrp-vd1
DEKORP-2N
NW
MUNSTERLAND
RUHR COAL BASIN
VARISCAN FRONT
SIEGEN THRUST
RHENOHERCYNIAN ZONE
GIESSEN NAPPE
PHYLLITE ZONE
SE
sec
km
DEKORP-2S
SAXOTHURINGIAN ZONE
SPESSART
RHENOHERCYNIAN MAGMATIC ARC
M1
M2
KRAICHGAU-TEPLÁ-BARRANDIAN
MOLDANUBIAN ZONE
GEOPHYSICAL ANOMALIES
Bouguer gravity anomaly
First vertical derivative of Bouguer anomaly
Magnetic anomaly reduced to pole
First derivative of magnetic anomaly
nT/m
ECORS-DEKORP
DEKORP-1C
SAAR BASIN
LORRAINE BASIN
NORTHERN VOSGES
SEISMIC REFLECTORS
late Paleozoic cover and younger
Type A
Type B
Type C
Faults
MAPB
ECORS-NFr
NE
SW
BRAY FAULT
SEINE FAULT
a

Figure 11A

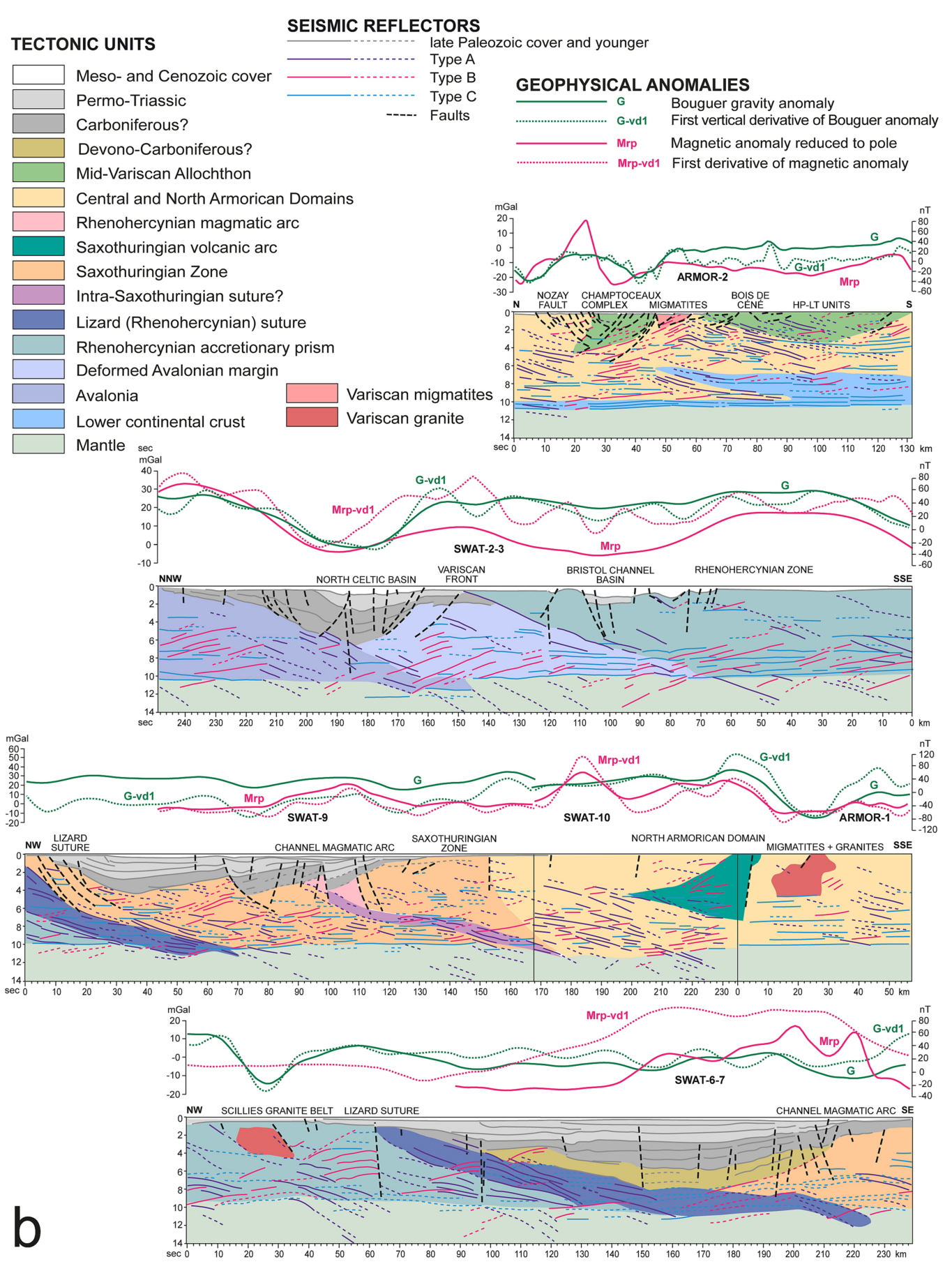
TECTONIC UNITS
Meso- and Cenozoic cover
Permo-Triassic
Carboniferous?
Devono-Carboniferous?
Mid-Variscan Allochthon
Central and North Armorican Domains
Rhenohercynian magmatic arc
Saxothuringian volcanic arc
Saxothuringian Zone
Intra-Saxothuringian suture?
Lizard (Rhenohercynian) suture
Rhenohercynian accretionary prism
Deformed Avalonian margin
Avalonia
Lower continental crust
Mantle
Variscan migmatites
Variscan granite
SEISMIC REFLECTORS
late Paleozoic cover and younger
Type A
Type B
Type C
Faults
GEOPHYSICAL ANOMALIES
G Bouguer gravity anomaly
G-vd1 First vertical derivative of Bouguer anomaly
Mrp Magnetic anomaly reduced to pole
Mrp-vd1 First derivative of magnetic anomaly
mGal
nT
ARMOR-2
N
S
NOZAY FAULT
CHAMPTOCEAUX COMPLEX
MIGMATITES
BOIS DE CÈNE
HP-LT UNITS
SWAT-2-3
NNW
SSE
NORTH CELTIC BASIN
VARISCAN FRONT
BRISTOL CHANNEL BASIN
RHENOHERCYNIAN ZONE
SWAT-9
SWAT-10
ARMOR-1
NW
SE
LIZARD SUTURE
CHANNEL MAGMATIC ARC
SAXOTHURINGIAN ZONE
NORTH ARMORICAN DOMAIN
MIGMATITES + GRANITES
SWAT-6-7
SCILLIES GRANITE BELT
sec
km
b

Figure 11B

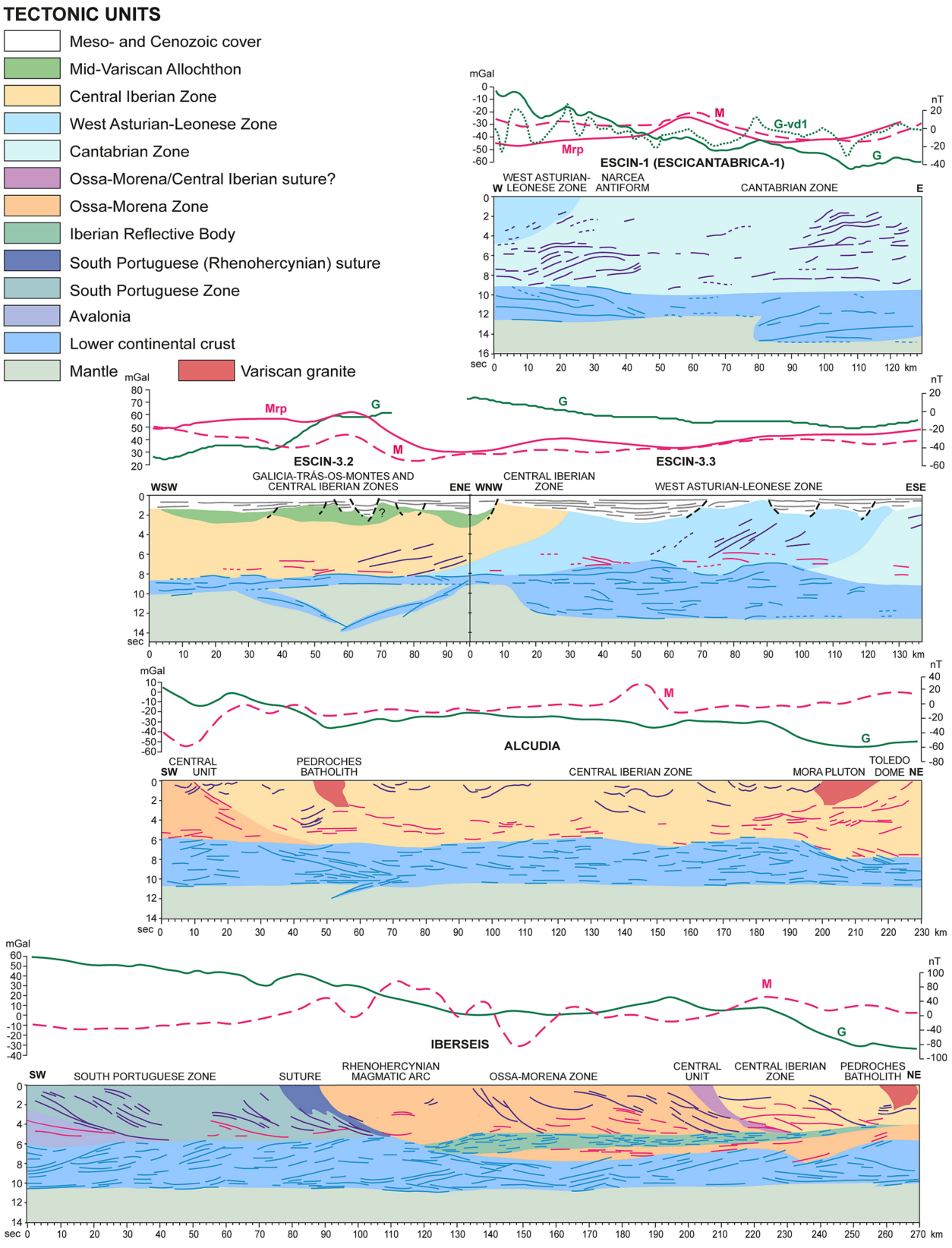
TECTONIC UNITS
Meso- and Cenozoic cover
Mid-Variscan Allochthon
Central Iberian Zone
West Asturian-Leonese Zone
Cantabrian Zone
Ossa-Morena/Central Iberian suture?
Ossa-Morena Zone
Iberian Reflective Body
South Portuguese (Rhenohercynian) suture
South Portuguese Zone
Avalonia
Lower continental crust
Mantle
Variscan granite
mGal
nT
M
G-vd1
Mrp
G
ESCIN-1 (ESCICANTABRICA-1)
W
WEST ASTURIAN-LEONESE ZONE
NARCEA ANTIFORM
CANTABRIAN ZONE
E
sec
km
ESCIN-3.2
ESCIN-3.3
WSW
GALICIA-TRÁS-OS-MONTES AND CENTRAL IBERIAN ZONES
ENE
WNW
CENTRAL IBERIAN ZONE
WEST ASTURIAN-LEONESE ZONE
ESE
ALCUDIA
SW
CENTRAL UNIT
PEDROCHES BATHOLITH
CENTRAL IBERIAN ZONE
MORA PLUTON
TOLEDO DOME
NE
IBERSEIS
SOUTH PORTUGUESE ZONE
SUTURE
RHENOHERCYNIAN MAGMATIC ARC
OSSA-MORENA ZONE
GEOPHYSICAL ANOMALIES
G Bouguer gravity anomaly
G-vd1 First vertical derivative of Bouguer anomaly
M Magnetic anomaly
Mrp Magnetic anomaly reduced to pole
SEISMIC REFLECTORS
Meso- and Cenozoic cover
Type A
Type B
Type C
Faults
C

Figure 11C

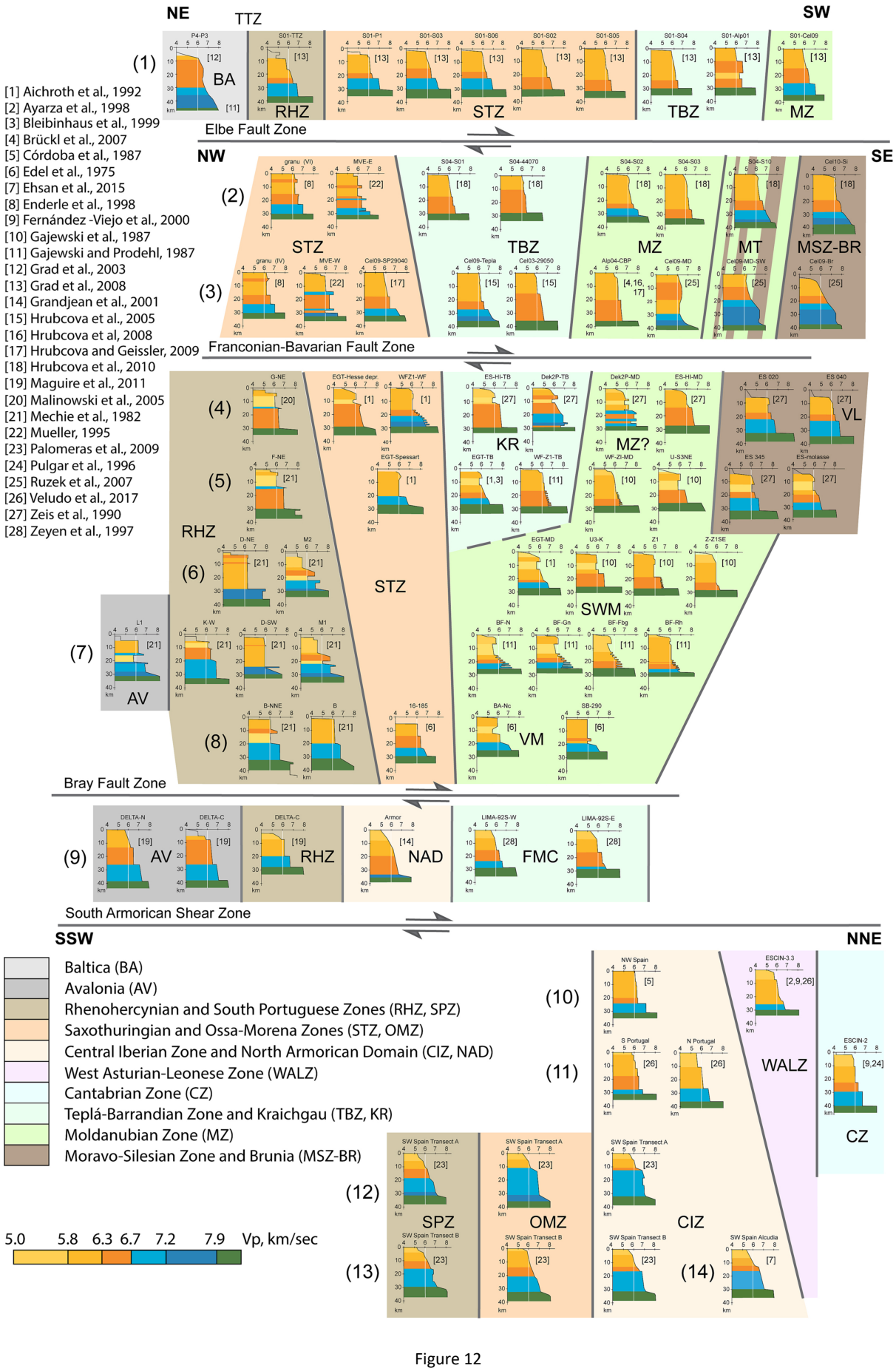

[1] Aichroth et al., 1992
[2] Ayarza et al., 1998
[3] Bleibinhaus et al., 1999
[4] Brückl et al., 2007
[5] Córdoba et al., 1987
[6] Edel et al., 1975
[7] Ehsan et al., 2015
[8] Enderle et al., 1998
[9] Fernández -Viejo et al., 2000
[10] Gajewski et al., 1987
[11] Gajewski and Prodehl, 1987
[12] Grad et al., 2003
[13] Grad et al., 2008
[14] Grandjean et al., 2001
[15] Hrubcova et al., 2005
[16] Hrubcova et al, 2008
[17] Hrubcova and Geissler, 2009
[18] Hrubcova et al., 2010
[19] Maguire et al., 2011
[20] Malinowski et al., 2005
[21] Mechie et al., 1982
[22] Mueller, 1995
[23] Palomeras et al., 2009
[24] Pulgar et al., 1996
[25] Ruzek et al., 2007
[26] Veludo et al., 2017
[27] Zeis et al., 1990
[28] Zeyen et al., 1997

Baltica (BA)
Avalonia (AV)
Rhenohercynian and South Portuguese Zones (RHZ, SPZ)
Saxothuringian and Ossa-Morena Zones (STZ, OMZ)
Central Iberian Zone and North Armorican Domain (CIZ, NAD)
West Asturian-Leonese Zone (WALZ)
Cantabrian Zone (CZ)
Teplá-Barrandian Zone and Kraichgau (TBZ, KR)
Moldanubian Zone (MZ)
Moravo-Silesian Zone and Brunia (MSZ-BR)

Figure 12

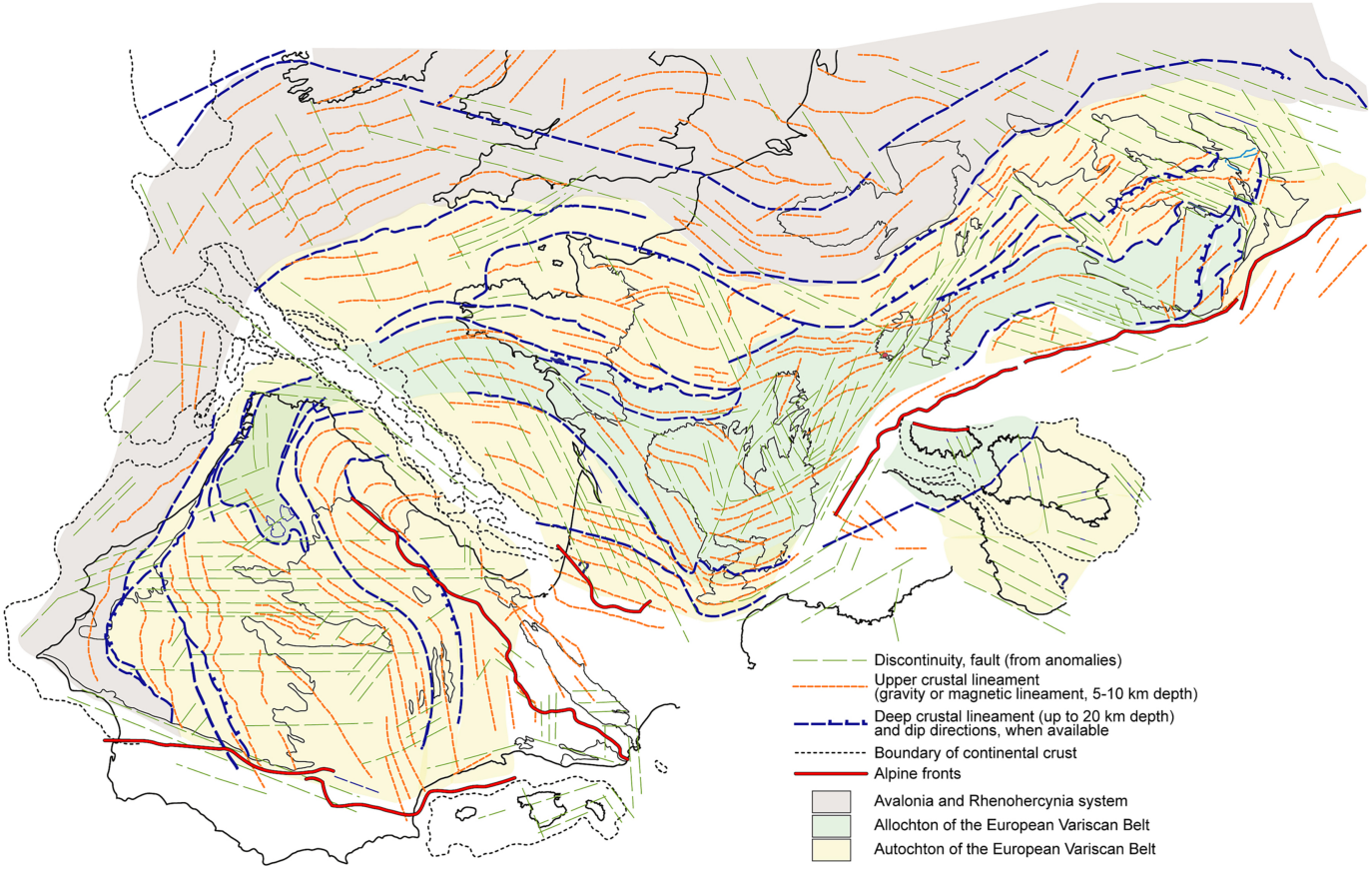
Discontinuity, fault (from anomalies)
Upper crustal lineament
(gravity or magnetic lineament, 5-10 km depth)
Deep crustal lineament (up to 20 km depth)
and dip directions, when available
Boundary of continental crust
Alpine fronts
Avalonia and Rhenohercynia system
Allochton of the European Variscan Belt
Autochton of the European Variscan Belt

Figure 13

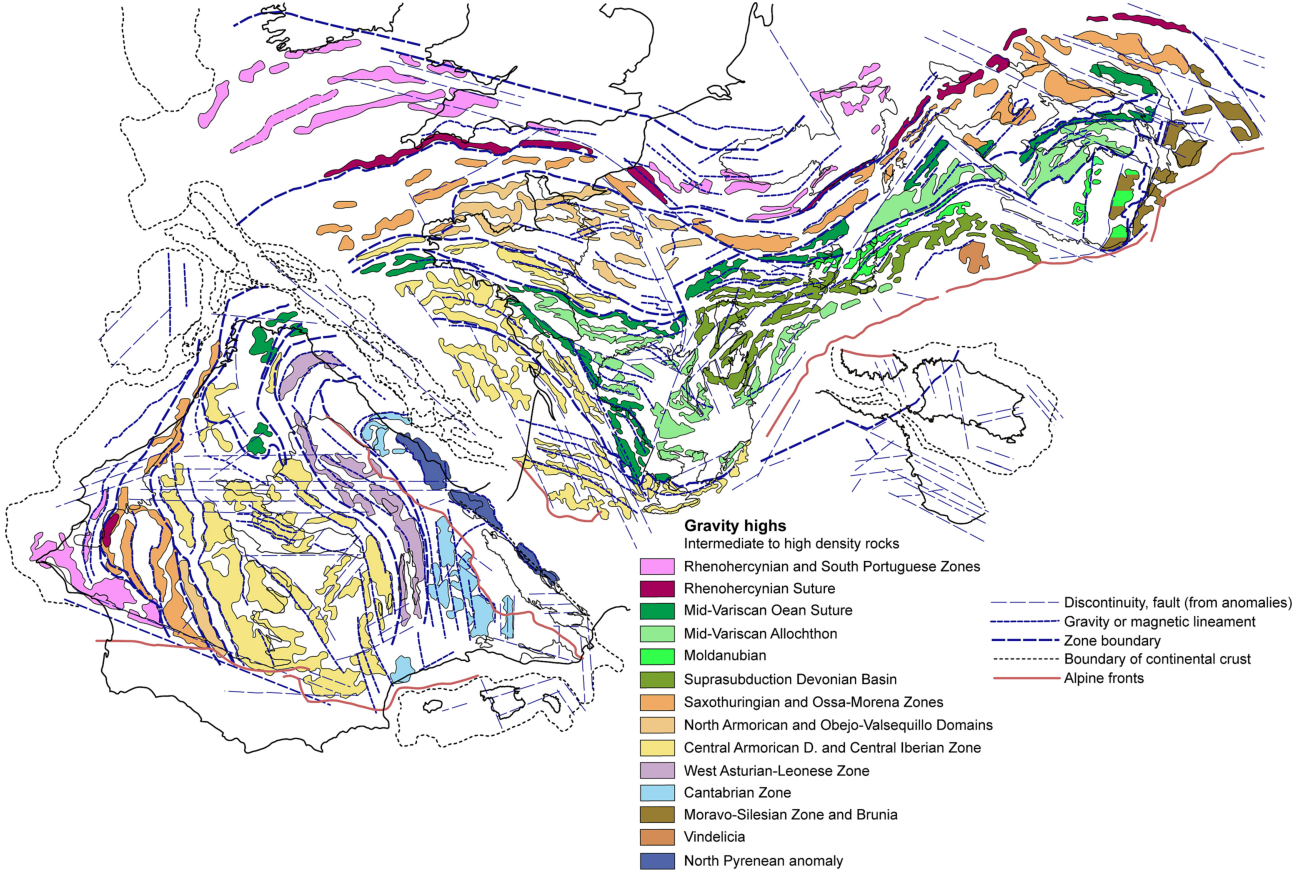
Gravity highs
Intermediate to high density rocks
Rhenohercynian and South Portuguese Zones
Rhenohercynian Suture
Mid-Variscan Oean Suture
Mid-Variscan Allochthon
Moldanubian
Suprasubduction Devonian Basin
Saxothuringian and Ossa-Morena Zones
North Armorican and Obejo-Valsequillo Domains
Central Armorican D. and Central Iberian Zone
West Asturian-Leonese Zone
Cantabrian Zone
Moravo-Silesian Zone and Brunia
Vindelicia
North Pyrenean anomaly
Discontinuity, fault (from anomalies)
Gravity or magnetic lineament
Zone boundary
Boundary of continental crust
Alpine fronts

Figure 14

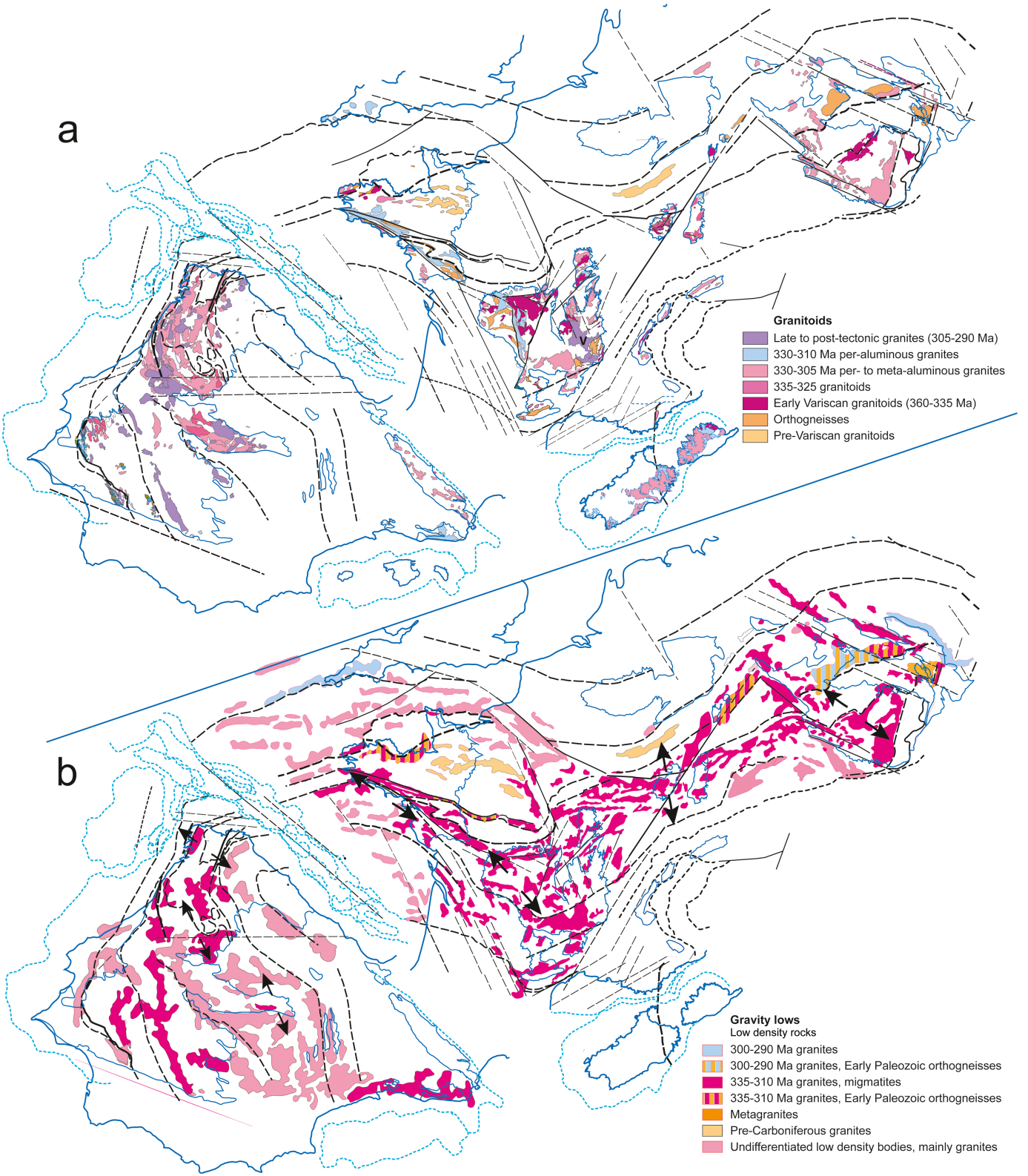
a
Granitoids
Late to post-tectonic granites (305-290 Ma)
330-310 Ma per-aluminous granites
330-305 Ma per- to meta-aluminous granites
335-325 granitoids
Early Variscan granitoids (360-335 Ma)
Orthogneisses
Pre-Variscan granitoids
b
Gravity lows
Low density rocks
300-290 Ma granites
300-290 Ma granites, Early Paleozoic orthogneisses
335-310 Ma granites, migmatites
335-310 Ma granites, Early Paleozoic orthogneisses
Metagranites
Pre-Carboniferous granites
Undifferentiated low density bodies, mainly granites

Figure 15

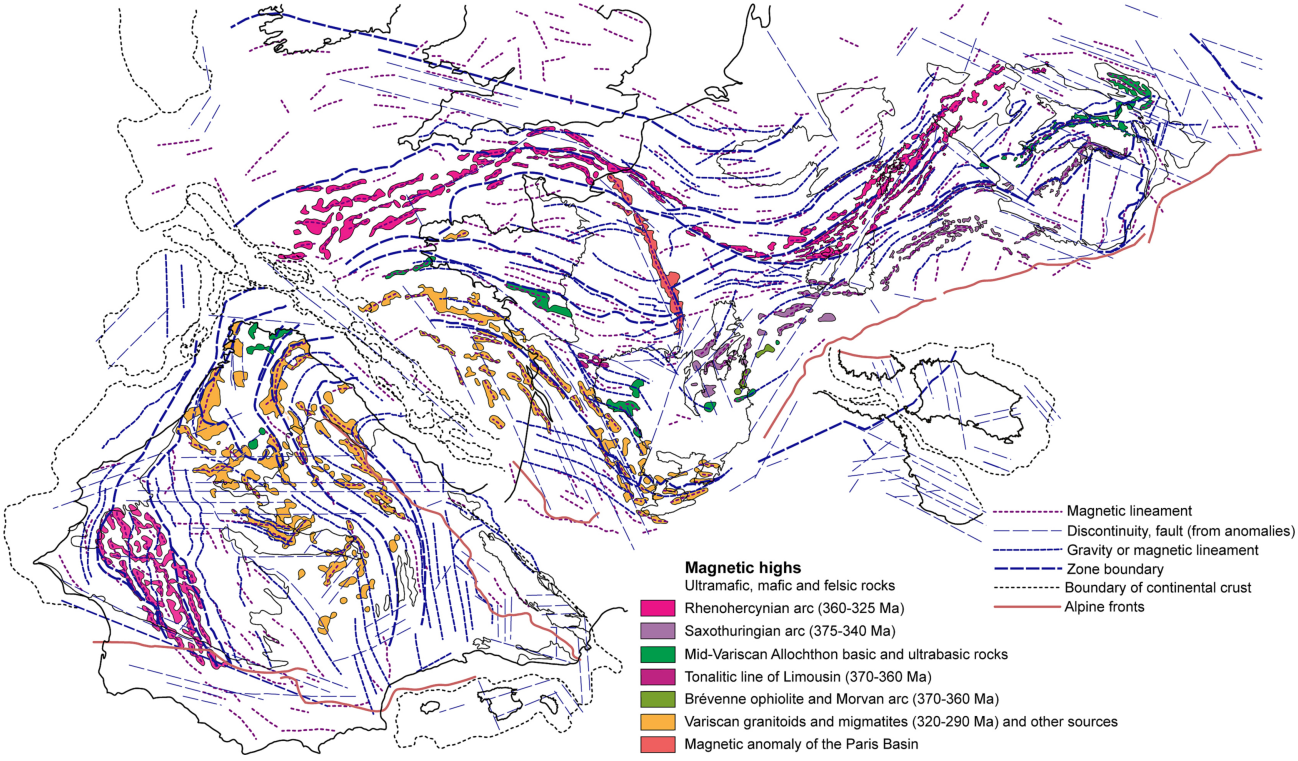
Magnetic lineament
Discontinuity, fault (from anomalies)
Gravity or magnetic lineament
Zone boundary
Boundary of continental crust
Alpine fronts
Magnetic highs
Ultramafic, mafic and felsic rocks
Rhenohercynian arc (360-325 Ma)
Saxothuringian arc (375-340 Ma)
Mid-Variscan Allochthon basic and ultrabasic rocks
Tonalitic line of Limousin (370-360 Ma)
Brévenne ophiolite and Morvan arc (370-360 Ma)
Variscan granitoids and migmatites (320-290 Ma) and other sources
Magnetic anomaly of the Paris Basin

Figure 16

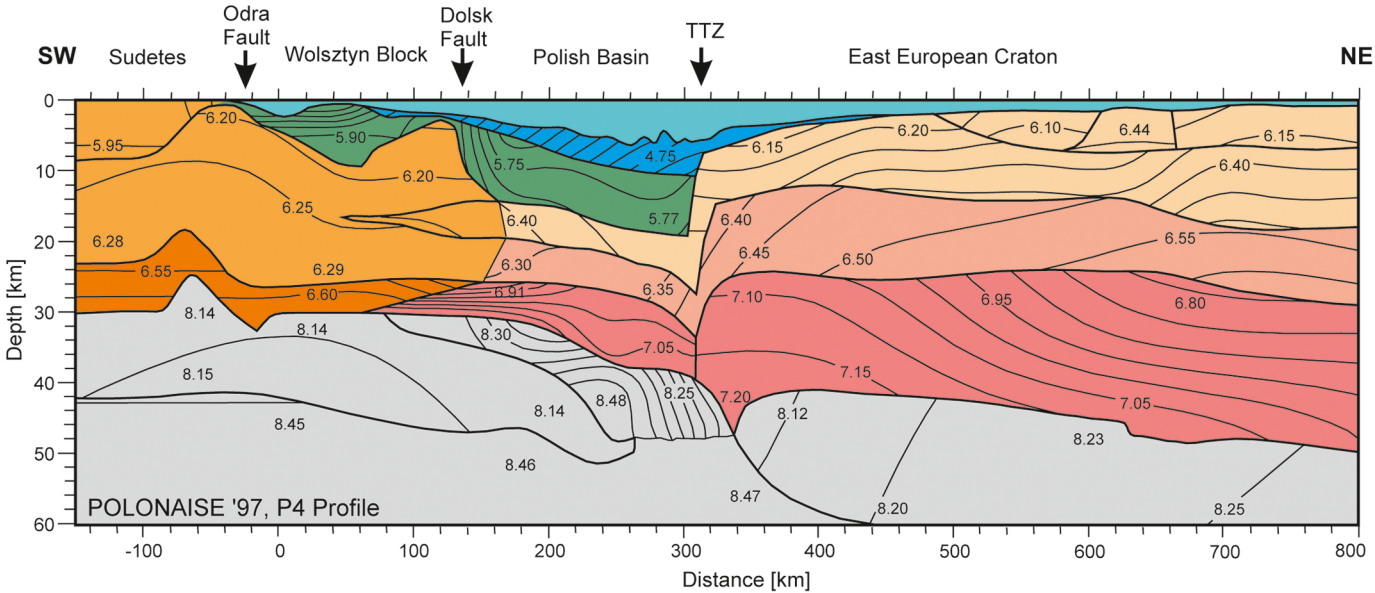
SW
Sudetes
Odra Fault
Wolsztyn Block
Dolsk Fault
Polish Basin
TTZ
East European Craton
NE
Depth [km]
Distance [km]
POLONAISE '97, P4 Profile
Variscides
Middle and upper crust
Lower crust
East European Craton
Upper crust
Middle crust
Lower crust
Sediments
Permian - Mesozoic (Polish Basin)
Ediacaran - Carboniferous
Upper mantle

Figure 17

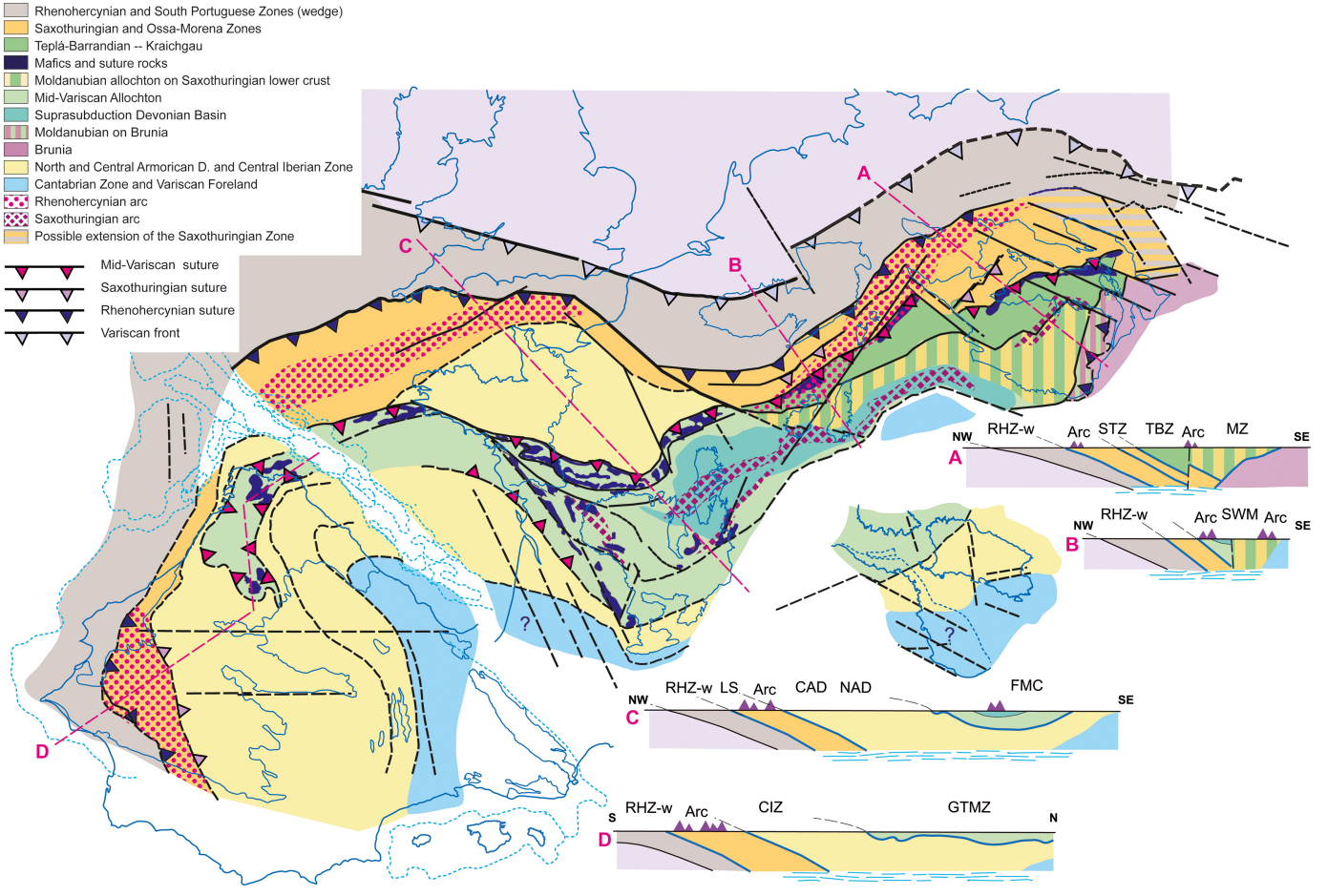
Rhenohercynian and South Portuguese Zones (wedge)
Saxothuringian and Ossa-Morena Zones
Teplá-Barrandian -- Kraichgau
Mafics and suture rocks
Moldanubian allochton on Saxothuringian lower crust
Mid-Variscan Allochton
Suprasubduction Devonian Basin
Moldanubian on Brunia
Brunia
North and Central Armorican D. and Central Iberian Zone
Cantabrian Zone and Variscan Foreland
Rhenohercynian arc
Saxothuringian arc
Possible extension of the Saxothuringian Zone
Mid-Variscan suture
Saxothuringian suture
Rhenohercynian suture
Variscan front
A
B
C
D
?
NW
SE
RHZ-w
Arc
STZ
TBZ
MZ
SWM
LS
CAD
NAD
FMC
S
N
CIZ
GTMZ

Figure 18

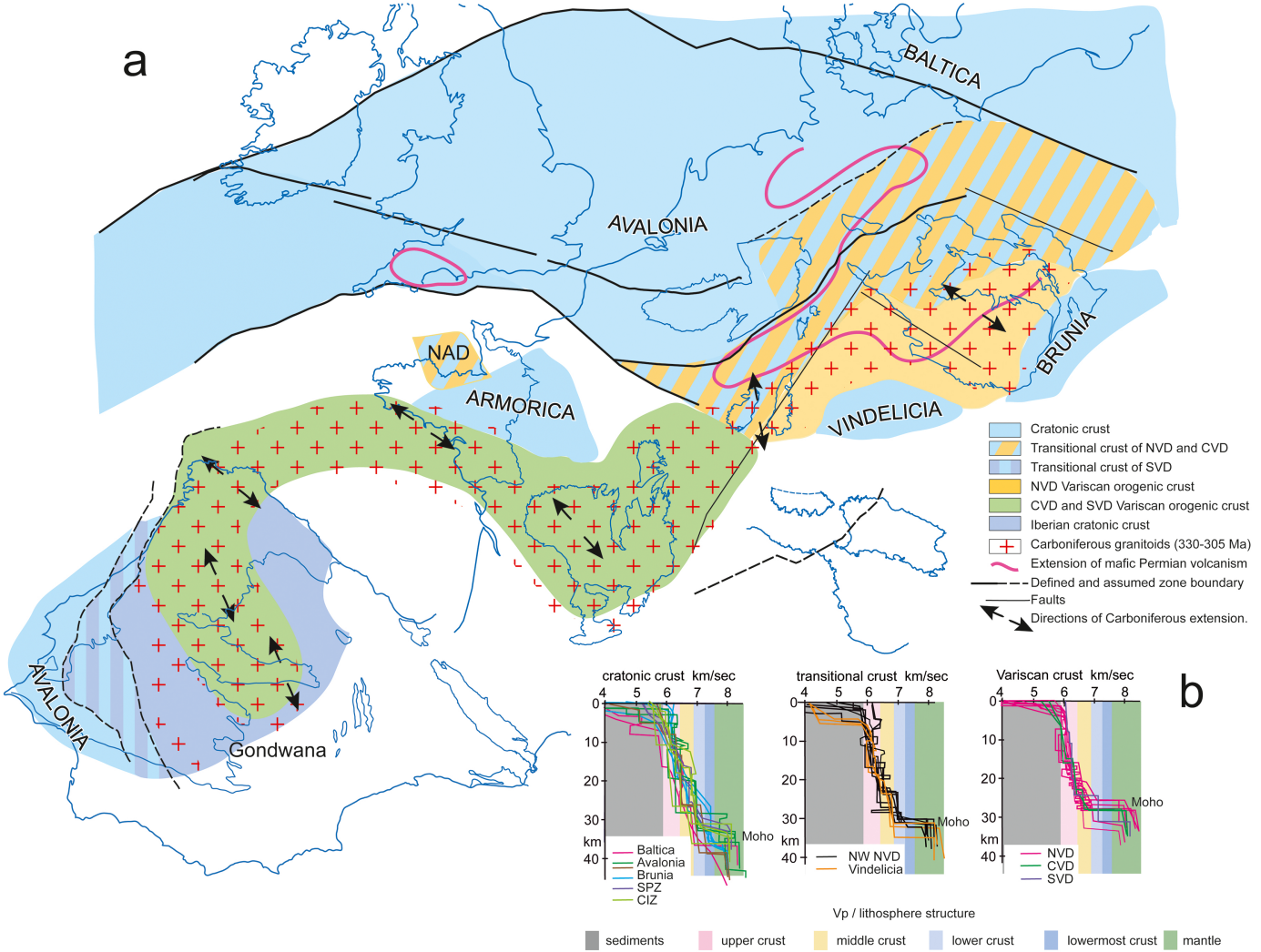
a
BALTICA
AVALONIA
NAD
ARMORICA
BRUNIA
VINDELICIA
AVALONIA
Gondwana
Cratonic crust
Transitional crust of NVD and CVD
Transitional crust of SVD
NVD Variscan orogenic crust
CVD and SVD Variscan orogenic crust
Iberian cratonic crust
Carboniferous granitoids (330-305 Ma)
Extension of mafic Permian volcanism
Defined and assumed zone boundary
Faults
Directions of Carboniferous extension.
b
cratonic crust km/sec
transitional crust km/sec
Variscan crust km/sec
4 5 6 7 8
0 10 20 30 km 40
Moho
Baltica
Avalonia
Brunia
SPZ
CIZ
NW NVD
Vindelicia
NVD
CVD
SVD
Vp / lithosphere structure
sediments
upper crust
middle crust
lower crust
lowermost crust
mantle

Figure 19